LBL-3384
c.2

A PROBABILISTIC APPROACH TO PLASTICITY IN POLYCRYSTALLINE MATERIALS USING DISLOCATION MECHANICS

Steven Jeffrey Sackett
(Ph. D. thesis)

November 8, 1974

Prepared for the U. S. Atomic Energy Commission
under Contract W-7405-ENG-48

TWO-WEEK LOAN COPY

This is a Library Circulating Copy which may be borrowed for two weeks. For a personal retention copy, call Tech. Info. Division, Ext. 5545

LAWRENCE BERKELEY LABORATORY
UNIVERSITY OF CALIFORNIA
BERKELEY

LBL-3384
c.2

DISCLAIMER

This document was prepared as an account of work sponsored by the United States Government. While this document is believed to contain correct information, neither the United States Government nor any agency thereof, nor the Regents of the University of California, nor any of their employees, makes any warranty, express or implied, or assumes any legal responsibility for the accuracy, completeness, or usefulness of any information, apparatus, product, or process disclosed, or represents that its use would not infringe privately owned rights. Reference herein to any specific commercial product, process, or service by its trade name, trademark, manufacturer, or otherwise, does not necessarily constitute or imply its endorsement, recommendation, or favoring by the United States Government or any agency thereof, or the Regents of the University of California. The views and opinions of authors expressed herein do not necessarily state or reflect those of the United States Government or any agency thereof or the Regents of the University of California.

LBL-3384

A PROBABILISTIC APPROACH TO PLASTICITY IN POLYCRYSTALLINE MATERIALS USING DISLOCATION MECHANICS

Steven Jeffrey Sackett

(Ph.D. Thesis)

November 8, 1974

AEC Contract No. W-7405-ENG-48

ABSTRACT

Using arguments based directly on the dislocation processes involved, we derive a set of constitutive equations for polycrystalline plasticity that is fully consistent with thermodynamic requirements. The idea of randomly distributed glide plane orientations and Burger's vector directions is introduced to facilitate handling of the polycrystalline structure. This yields equations involving probability distributions for variables which are directly related to measurable dislocation quantities.

When the motion of the dislocations is isochoric, the tensorial character of the plastic strain rate is shown to be entirely determined by a second rank symmetric tensor directly related to ordinary elements of crystallographic glide. This same tensor is also shown to determine to shear stress acting on a dislocation.

Characteristic yield conditions are calculated for several sample materials in which the dependence of the dislocation velocity on stress is given by an empirical power function. The shape of the yield surfaces for these materials is shown to vary from that of von Mises when the exponent is small to that of Tresca when the exponent is large. Additional examples illustrate the ability of the proposed theory to model such phenomena as the development of anisotropy during plastic deformation, material hardening and softening, the occurrence of upper and lower yield points, and Bauschinger effect.

ACKNOWLEDGEMENTS

The author wishes to express his sincere gratitude to Professor James M. Kelly for his guidance and encouragement through the course of this research and to Professor Karl S. Pister for his many helpful consultations. He also wishes to thank Professors Robert L. Taylor and Alexandre J. Chorin for reading the manuscript.

The author is deeply indebted to Mrs. Ardie Rutan for her careful typing of the manuscript on very short notice and expresses special thanks to her. The typing assistance of Mrs. Marty Morimoto is also gratefully acknowledged.

This work was supported by the U. S. Atomic Energy Commission through the Lawrence Berkeley Laboratory of the University of California.

TABLE OF CONTENTS

	Page
ABSTRACT	i
ACKNOWLEDGEMENT	ii
TABLE OF CONTENTS	iii
I. INTRODUCTION	
1.1 Historical Perspective	1
1.2 Basic Assumptions and Thermodynamic Results	2
II. DISLOCATION MECHANICS AND POLYCRYSTALLINE PLASTICITY	
2.1 Introduction	9
2.2 The Plastic Strain Rate Equation	11
2.3 Dislocation Production and Interaction	20
2.4 The Dislocation Velocity	25
2.5 Elastic Energy Due to Dislocations	28
2.6 Summary	29
III. BEHAVIOR OF THE CONSTITUTIVE EQUATIONS FOR POLYCRYSTALLINE PLASTICITY	
3.1 Introduction	32
3.2 Behavior of the Plastic Strain Rate for a Given Dislocation Distribution	35
3.3 Behavior of the Constitutive Model Under Uniaxial Loading	41
IV. CONCLUSIONS	46
REFERENCES	51
FIGURES	56

I. INTRODUCTION

1.1 Historical Perspective

In the past decade, the theory of plasticity in crystalline materials has undergone extensive development. Using the framework of modern continuum mechanics [1], very general three-dimensional theories have been proposed on the basis of thermodynamical arguments. By direct generalization of classical theory, Green and Naghdi [2, 3] developed a general theory of elastic-plastic materials of the rate independent type. A similar development was presented by Lee and Liu [4]. Pipkin and Rivlin [5] have developed the constitutive equations for rate independent materials with memory. They have shown that a general theory of elastic-plastic materials arises as a special case of the theory of rate-independent materials.

The formulation of the thermodynamic theory of rate-sensitive plastic material within the framework of thermodynamics of a material with internal state variables has been given by Perzyna and Wojno [6] and by Kratochvil and Dillon [7]. Similar work with particular attention to identifying the internal variables with dislocation quantities has been presented by Tseng [8], by Hahn and Jaunzemis [9], by Bhandari and Oden [10], and by Kelly and Gillis [11]. In addition, Bhandari and Oden have given a detailed comparison of the existing mathematical theories and have shown the equivalence of approaches using evolutionary equations and memory functionals.

In contrast to the mathematical theories just mentioned, physical theories of crystalline plasticity, that is, those in which the constitutive equations are derived by modeling the physical dis-

location processes directly, have been developed by Taylor [12], by Lin and Ito [13], by Lin [14], by Mura [15], and by Gilman [16]. Equations obtained in this manner have been identified with those obtained on the basis of thermodynamics by Kelly and Gillis [11].

In this work, we utilize results from both mathematical and physical theories. Our emphasis, however, is on direct physical arguments. We begin our discussion with a review of thermodynamic results obtained along the lines of Kelly and Gillis' [17] arguments. The constitutive equations for the plastic strain rate and the rate of change of the dislocation density are then derived using arguments based directly on the dislocation processes involved. Random variables and associated probability distributions are introduced to facilitate handling of the polycrystalline structure. The resulting equations are shown to be consistent with the forms obtained using thermodynamics. Finally, the behavior of the model is illustrated with several examples.

1.2 Basic Assumptions and Thermodynamic Results

It is our intention in this dissertation to construct a theory of plasticity for polycrystalline materials based on the use of internal variables. Following Coleman and Gurtin [18], the evolution of these internal variables is described by a set of differential equations which are of first order in time. In contrast to their work however, we develop our equations in the material rather than the spatial description and make use of a different set of state variables. In the derivation that follows we use symbolic notation for tensors and vectors, for example, $\underset{\sim}{\varepsilon}$, $\vec{x}$, where possible and use index notation, ε_{ij}, x_i, for manipulations.

We consider a body B acted on by a body force and a symmetric stress field. Although the presence of dislocations can, according to some geometric analyses, lead to body couples and couple stresses, these are assumed to be absent at the macroscopic level. Similarly, diffusion of mass in B is neglected as being of only microscopic importance. We refer the motion of B to a fixed system of rectangular cartesian axes and designate the position of a typical particle at time t by a column vector $\vec{x}$, where

$$\vec{x} = \vec{\chi}(\vec{X},t), \tag{1.1}$$

and $\vec{X}$ denotes a reference position of the particle, here taken to be the initial position. The vector mapping function $\vec{\chi}$ is assumed to be sufficiently smooth that its gradient,

$$\underset{\sim}{F} = \text{Grad } \vec{x} = \partial\vec{x}/\partial\vec{X}, \tag{1.2}$$

is continuous and such that $\det(\underset{\sim}{F}) > 0$ for all t.

In a plasticity theory, the initial annealed condition of the material has a special significance and it is convenient to develop the theory with respect to the initial configuration. A suitable measure of deformation under these circumstances is

$$\underset{\sim}{\varepsilon} = (1/2)(\underset{\sim}{C} - \underset{\sim}{I}) \tag{1.3}$$

and

$$\dot{\underset{\sim}{\varepsilon}} = \underset{\sim}{F}^T \underset{\sim}{D} \underset{\sim}{F}, \tag{1.4}$$

where $\underset{\sim}{I}$ is the identity tensor, $\underset{\sim}{C}$ is the right Cauchy-Green tensor

$$\underset{\sim}{C} = \underset{\sim}{F}^T \underset{\sim}{F} \tag{1.5}$$

and $\underset{\sim}{D}$ is the rate of deformation tensor,

$$\underset{\sim}{D} = (1/2)\ (\dot{\underset{\sim}{F}}\underset{\sim}{F}^{-1}) + (\dot{\underset{\sim}{F}}\underset{\sim}{F}^{-1})^T = (1/2)\left[\text{grad}\ \dot{\vec{x}} + (\text{grad}\ \dot{\vec{x}})^T\right]. \quad (1.6)$$

Here, as in what follows, a superposed dot denotes differentiation with respect to time holding $\vec{X}$ fixed and grad denotes the spatial gradient operator.

Let $\vec{h}$ denote the heat flux vector measured per unit tune and per unit area in the reference configuration, ρ_o the mass density in the reference configuration, and $\underset{\sim}{\sigma}$ the symmetric Piola-Kirchhoff stress tensor. From the integral form of the principle of balance of energy we can deduce the local rate of work equation:

$$\rho_o\dot{\varepsilon} = \text{tr}(\underset{\sim}{\sigma}\dot{\underset{\sim}{\varepsilon}}) - \text{Div}\ \vec{h} + \rho_o r, \quad (1.7)$$

where ε is the internal energy per unit mass, r is the heat supply per unit mass, and Div denotes the divergence operator with respect to $\vec{X}$. In a similar manner the integral form of the Clausius-Duhem inequality leads to the relation

$$\rho_o\dot{\eta} + \text{Div}(\vec{h}/T) - \rho_o(r/T) \geq 0, \quad (1.8)$$

where T is the temperature and η is the entropy per unit mass.

If we consider $\vec{h}/T$ as an entropy flux and r/T as an entropy supply, the inequality (1.8) defines a specific internal entropy production rate $\dot{\delta}$:

$$\rho_o T\dot{\delta} = \rho_o T\dot{\eta} + \text{Div}\ \vec{h} - \rho_o r - (1/T)\vec{h}\cdot\vec{g} \geq 0, \quad (1.9)$$

where $\vec{g}$ denotes the temperature gradient in the reference state, Grad T. Alternatively, equation (1.7) can be used to eliminate r and Div $\vec{h}$ yielding

$$\rho_o T\dot{\delta} = \rho_o T\dot{\eta} - \rho_o\dot{\varepsilon} + \text{tr}(\underset{\sim}{\sigma}\dot{\varepsilon}) - (1/T)\vec{h}\cdot\vec{g} \quad (1.10)$$

for the dissipation equation.

Following Kelly and Gillis [11], we introduce the Gibb's thermodynamic potential defined by

$$\rho_o \Phi = \rho_o(\eta T - \varepsilon) + \mathrm{tr}(\underset{\sim}{\sigma}\underset{\sim}{\varepsilon}). \tag{1.11}$$

Differentiating this expression with respect to time and substituting the result into (1.10) we have

$$\rho_o T\dot{\delta} = \rho_o \dot{\Phi} - \mathrm{tr}(\dot{\underset{\sim}{\sigma}}\underset{\sim}{\varepsilon}) - \rho_o \eta \dot{T} - (1/T)\vec{h} \cdot \vec{g}. \tag{1.12}$$

Assume that the Gibb's potential has the form

$$\Phi = \Phi(\underset{\sim}{\sigma}, T, \vec{\alpha}) \tag{1.13}$$

and the internal variables, $\vec{\alpha}$, are governed by the evolutionary equations

$$\dot{\vec{\alpha}} = \vec{q}(\underset{\sim}{\sigma}, T, \vec{g}, \vec{\alpha}). \tag{1.14}$$

The function Φ is taken to be continuously differentiable at least twice with respect to $\underset{\sim}{\sigma}$ and T and once with respect to $\vec{\alpha}$, while $\vec{q}$ is taken to be continuously differentiable at least once with respect to $\underset{\sim}{\sigma}$, T, $\vec{g}$, and $\vec{\alpha}$. With Φ defined as in equation (1.13), the dissipation equation becomes

$$\rho_o T\hat{\delta} = \mathrm{tr}\left[(\rho_o \Phi_{,\underset{\sim}{\sigma}} - \underset{\sim}{\varepsilon})\dot{\underset{\sim}{\sigma}}\right] + \rho_o(\Phi_{,T} - \eta)\dot{T} + \rho_o \Phi_{,\vec{\alpha}} \circ \dot{\vec{\alpha}} - (1/T)\vec{h} \cdot \vec{g}, \tag{1.15}$$

where we have used subscripts to indicate partial derivatives of the potential function with respect to the subscripted quantity, for example, $\Phi_{,T} = \partial\Phi/\partial T$.

The Clausius-Duhem inequality asserts that $\dot{\delta} \geq 0$ for every thermodynamic process in B. Since the values of $\dot{\underset{\sim}{\sigma}}$ and $\dot{T}$ can be prescribed arbitrarily for each time t, this inequality cannot be

satisfied independent of the signs of $\dot{\underset{\sim}{\sigma}}$ and $\dot{T}$ unless their coefficients in equation (1.15) vanish identically. Consequently, we obtain the relations

$$\underset{\sim}{\varepsilon} = \rho_o \Phi_{,\underset{\sim}{\sigma}} \tag{1.16}$$

and

$$\eta = \Phi_{,T} \tag{1.17}$$

and the dissipation equation reduces to

$$\rho_o T\dot{\delta} = \rho_o \Phi_{,\vec{\alpha}} \cdot \dot{\vec{\alpha}} - (1/T)\vec{h} \cdot \vec{g}. \tag{1.18}$$

This last result can then be combined with equation (1.9) to yield the form

$$\rho_o T\dot{\eta} = \rho_o r - \mathrm{Div}\, \vec{h} + \rho_o \Phi_{,\vec{\alpha}} \cdot \dot{\vec{\alpha}} \tag{1.19}$$

for the Gibb's equation.

Taking the time derivative of equation (1.16), we obtain the following expression for the rate of strain:

$$\dot{\underset{\sim}{\varepsilon}} = \rho_o \Phi_{,\underset{\sim}{\sigma}\underset{\sim}{\sigma}} \cdot \dot{\underset{\sim}{\sigma}} + \rho_o \Phi_{,\underset{\sim}{\sigma}T}\, T + \rho_o \Phi_{,\underset{\sim}{\sigma}\vec{\alpha}} \cdot \dot{\vec{\alpha}} \tag{1.20}$$

At normal temperatures, the most significant feature of plastic deformation in crystalline materials is that it alters the crystal positions without destroying the basic crystalline structure [19]. As a result, the thermoelastic response of crystalline solids is essentially unaffected by plastic deformation. This implies that the instantaneous thermoelastic compliances $\rho_o \Phi_{,\underset{\sim}{\sigma}\underset{\sim}{\sigma}}$ and $\rho_o \Phi_{,\underset{\sim}{\sigma}T}$ are independent of the internal state and hence independent of $\vec{\alpha}$.

The most general form for Φ that satisfies these restrictions is the following:

$$\Phi = \Phi^e(\underset{\sim}{\sigma},T) + (1/\rho_o)\mathrm{tr}(\underset{\sim}{\sigma}\underset{\sim}{H}) + G(T,\vec{\alpha}), \tag{1.21}$$

where $\underset{\sim}{H}$ must be a second order tensor function of $\vec{\alpha}$ only. Thus, equation (1.20) can be rewritten in the form

$$\dot{\underset{\sim}{\varepsilon}} = \rho_o \Phi^e_{,\underset{\sim}{\sigma}\underset{\sim}{\sigma}} \cdot \dot{\underset{\sim}{\sigma}} + \rho_o \Phi^e_{,\underset{\sim}{\sigma}T}\, \dot{T} + H_{,\vec{\alpha}} \cdot \dot{\vec{\alpha}} \tag{1.22}$$

and it appears reasonable to identify the elastic, thermal, and plastic strain rates as

$$\dot{\underset{\sim}{\varepsilon}}^e = \rho_o \Phi^e_{,\underset{\sim}{\sigma}\underset{\sim}{\sigma}} \cdot \dot{\underset{\sim}{\sigma}} \tag{1.23}$$

$$\dot{\underset{\sim}{\varepsilon}}^T = \rho_o \Phi^e_{,\underset{\sim}{\sigma}T}\, \dot{T}, \tag{1.24}$$

and

$$\dot{\underset{\sim}{\varepsilon}}^P = \underset{\sim}{H}_{,\vec{\alpha}} \cdot \dot{\vec{\alpha}} \tag{1.25}$$

respectively.

When crystalline solid is deformed plastically, not all of the plastic work is lost in heat. Some of this energy is stored in the crystal lattice, associated with the elastic strain field of newly created dislocations [20]. This energy is not released on unloading but can usually be recovered by annealing, a process which will remove dislocations. If we identify this stored energy with the function G as follows:

$$w^r = -\rho_o G_{,\vec{\alpha}} \cdot \dot{\vec{\alpha}} \tag{1.26}$$

then the equation for internal dissipation becomes

$$\rho_o T\dot{\delta} = (w^P - w^r) - (1/T)\vec{h} \cdot \vec{g}, \tag{1.27}$$

where w^P denotes the plastic work rate $\mathrm{tr}(\underset{\sim}{\sigma}\dot{\underset{\sim}{\varepsilon}}^P)$. In a similar manner we can combine this notation with equation (1.19) and the time

derivative of (1.17) to obtain

$$\rho_o T(\Phi^e_{,TT} + G_{,TT})\dot{T} = \rho_o r - \mathrm{Div}\,\vec{h} - \rho_o T\,\mathrm{tr}(\Phi^e_{,\underset{\sim}{\sigma}T}\dot{\underset{\sim}{\sigma}}) - \rho_o T\, G_{,T\vec{\alpha}} \cdot \dot{\vec{\alpha}} + (w^P - w^r) \tag{1.28}$$

for the equation governing changes in temperature.

Using the Gibb's potential in the form given in (1.21) has led to an expression relating the plastic strain rate to the rate of change of the internal variables. In addition, it gives the additivity of elastic and plastic strain rates as a consequence. This is in contrast to most other theories where it is an additional assumption. It only remains to identify $\vec{\alpha}$, $\underset{\sim}{H}(\vec{\alpha})$, and $G(T,\vec{\alpha})$ with known dislocation parameters in a manner consistent with equations (1.25) and (1.26). This will be investigated in the next section.

II. DISLOCATION MECHANICS AND POLYCRYSTALLINE PLASTICITY

2.1 Introduction

There are several known sources of irreversible or plastic defermation in solids. These include void growth, crack propagation, grain boundary sliding, twinning, diffusional processes, and the generation and motion of dislocations. In crystalline materials, however, it is well established that dislocation processes play the dominant role. Since the known properties of dislocations seem capable of explaining most features of polycrystalline plasticity, we base our constitutive development on dislocation mechanics.

Contemporary work in plasticity based on dislocation behavior extends across a broad range of mathematical sophistication. On one hand are general three-dimensional theories. These have been formulated based largely on either the theory of continuously distributed dislocations, as developed by Bilby [21] and Mura [22], or the use of statistical dislocation arrangement tensors, as advanced by Kröner [23] and Kratochvil and Dillon [7]. On the other hand, there are simple one-dimensional theories, such as those of Gilman [24], which seem to have had greater success in relating observed dislocation behavior to material properties. The chief disadvantage of the three-dimensional theories lies in their use of awkward variables that are difficult to relate directly to measurable dislocation quantities. We, therefore, attempt in our development to make use of the kinds of variables employed in the successful one-dimensional theories, generalized to three-dimensions.

Using direct physical arguments, we suggest a general three-

dimensional plastic strain rate equation relating this macroscopic quantity to microstructural parameters. Specializing this result to the case of pure glide, we show that the tensorial character of the plastic strain rate can be attributed to a second rank symmetric tensor directly related to ordinary elements of crystallographic glide.

To apply our results to arbitrary polycrystalline samples, we introduce the glide plane orientations and Burger's vector directions as continuously distributed random variables. This method follows the work of Johnson [25] and, more recently, Clough and Simmons [26]. In our derivation, however, we eliminate most of their assumptions and use a different set of transformations from local to global coordinates. Moreover, our theory is more general in that it allows for the possibility of a nonuniform distribution of dislocations and for their production and interaction.

We next formulate an evolutionary equation for the dislocation density. These results are based on the single and pair-wise dislocation processes of fixed source production, cross-glide multiplication, dislocation immobilization, and pair annihilation. Appropriate equations for the dislocation velocity are also discussed in the same context.

We complete our constitutive development by discussing the elastic energy stored in the crystal lattice as a result of the presence of dislocations.

2.2 The Plastic Strain Rate Equation

Consider a small segment of an arbitrary dislocation line. Associated with this segment are its velocity and its tangent, which define its local plane of motion, and its Burgers vector, which describes the crystallographic displacement it produces. We denote these vectors by $v\vec{y}_1$, $\vec{y}_2$, and $\vec{b}$ respectively, where $\vec{y}_1$ and $\vec{y}_2$ are unit vectors and v is the dislocation speed. The only dislocation motions that produce displacement changes are those for which the velocity is orthogonal to the line direction. We may therefore assume without loss of generality that $\vec{y}_1 \cdot \vec{y}_2 = 0$. These two vectors, taken with $\vec{y}_3 = \vec{y}_1 \times \vec{y}_2$, then form an orthonormal basis for a local dislocation coordinate system. In addition, the plane of motion and the Burgers vector provide us with a means for grouping dislocations which produce the same displacement changes. Among all dislocations in a specimen, we classify those characterized by the same $\vec{y}_3$ and the same $\vec{b}$ as one family.

If we now focus attention on a single family of dislocations identified by the plane of motion with normal $\vec{y}_3^k$ and by the Burgers vector $\vec{b}^k$ and construct a small rectangular volume element such that its edges are parallel to $\vec{y}_1^k$, $\vec{y}_2^k$, $\vec{y}_3^k$, we can compute the macroscopic plastic strain rate associated with the distortion of this family. It is assumed that the volume of this element is of the same order of magnitude as the core volume of a dislocation segment of length ℓ, where ℓ is the length of the element in the $\vec{y}_2^k$ direction.

Plastic deformation of this element is the result of dislocation flux through it. The passage of a single type k dislocation produces a relative displacement $\vec{b}^k$ of the element faces which are

parallel to the plane of motion. The relative velocity of these two faces is $\vec{b}^k/\Delta t$, where Δt is the mean time between dislocation arrivals (or departures) at the element. This is conveniently expressed in the $\vec{y}_1^k$, $\vec{y}_2^k$, $\vec{y}_3^k$ coordinate system as the two shear components,

$$(y)\dot{\varepsilon}_{13}^{Pk} = (y)\dot{\varepsilon}_{31}^{Pk} = \zeta^k(\vec{y}_1^k \cdot \vec{b}^k)/2w^k \, \Delta t, \tag{2.1a}$$

$$(y)\dot{\varepsilon}_{23}^{Pk} = (y)\dot{\varepsilon}_{32}^{Pk} = \zeta^k(\vec{y}_2^k \cdot \vec{b}^k)/2w^k \, \Delta t, \tag{2.1b}$$

and an extensional component,

$$(y)\dot{\varepsilon}_{33}^{Pk} = \zeta^k(\vec{y}_3^k \cdot \vec{b}^k)/w^k \, \Delta t, \tag{2.1c}$$

of a plastic strain rate tensor, all other components of which are zero. Here w^k is the separation between the element faces which are parallel to the plane of motion. Due to our assumption concerning the volume of the element, this can be taken to be the dislocation core width. The factor ζ^k is defined as follows:

$$\zeta^k = \mathrm{sgn}(\vec{f}^k \cdot \vec{y}_1^k), \tag{2.2}$$

where $\vec{f}^k$ is the force acting on the dislocation and sgn denotes the signum function (which ensures that the sign of $\dot{\underset{\sim}{\varepsilon}}^{Pk}$ is consistent with the convention that a positive force will produce a positive dislocation velocity).

The rate of change of the number of dislocations in our element is given by the formula

$$\dot{n}^k = \frac{D}{Dt}\left[\int_{Vk} N^k \, dV\right]/\int d\ell = \int_{Vk} \dot{N}^k dV/\int d\ell, \tag{2.3}$$

where N^k is the dislocation density (line length per unit volume)

for type k dislocations. We assume that during the time required for a unit change in n^k, the integrals in (2.3) can be approximated by their mean value. This yields the following relation between the mean dislocation arrival time and the rate of change of the dislocation density:

$$\Delta t = 1/(\dot{N}^k \, w^{k2}). \tag{2.4}$$

Substituting this result into (2.1), the componenets of the plastic strain rate tensor become

$$(y)\dot{\varepsilon}^{Pk}_{13} = (y)\dot{\varepsilon}^{PK}_{31} = \zeta^k(\vec{y}^k_1 \cdot \vec{b}^k) w^k \dot{N}^k/2, \tag{2.5a}$$

$$(y)\dot{\varepsilon}^{Pk}_{23} = (y)\dot{\varepsilon}^{Pk}_{32} = \zeta^k(\vec{y}^k_2 \cdot \vec{b}^k) w^k \dot{N}^k/2, \tag{2.5b}$$

$$(y)\dot{\varepsilon}^{Pk}_{33} = \zeta^k(\vec{y}^k_3 \cdot \vec{b}^k) w^k \dot{N}^k, \tag{2.5c}$$

$$(y)\dot{\varepsilon}^{Pk}_{11} = (y)\dot{\varepsilon}^{Pk}_{12} = (y)\dot{\varepsilon}^{Pk}_{21} = (y)\dot{\varepsilon}^{Pk}_{22} = 0, \tag{2.5d}$$

in terms of dislocation quantities.

Consider a global coordinate system with linearly independent base vectors $\vec{x}_1$, $\vec{x}_2$, $\vec{x}_3$. These vectors are related to the local base vectors $\vec{y}^k_1$, $\vec{y}^k_2$, $\vec{y}^k_3$ by the formula

$$\vec{x}_i = a^k_{ij} \, \vec{y}^k_j. \tag{2.6}$$

The components of the plastic strain rate tensor in the global coordinate system are given by the transformation

$$\dot{\varepsilon}^{Pk} = a^k_{im} \, a^k_{jn} \, (y)\dot{\varepsilon}^{Pk}_{mn}.$$

Applying this to (2.5), we obtain

$$\dot{\varepsilon}^{Pk}_{ij} = (\zeta^k/2)\left[a^k_{i3}(a^k_{j1}\vec{y}^k_1 \cdot \vec{b}^k + a^k_{j2}\vec{y}^k_2 \cdot \vec{b}^k + a^k_{j3}\vec{y}^k_3 \cdot \vec{b}^k)\right. \tag{2.8a}$$

$$\left. + a^k_{j3}(a^k_{i1}\vec{y}^k_1 \cdot \vec{b}^k + a^k_{i2}\vec{y}^k_2 \cdot \vec{b}^k + a^k_{i3}\vec{y}^k_3 \cdot \vec{b}^k)\right] w^k\dot{N}^k;$$

or equivalently,

$$\dot{\varepsilon}^{Pk}_{ij} = (\zeta^k/2)(y^k_{3i}b^k_j + y^k_{3j}b^k_i)w^k\dot{N}^k, \tag{2.8b}$$

where y^k_{3i} are the components of the vector $\vec{y}^k_3$ and b^k_i are the components of the vector $\vec{b}^k$ with respect to the global base vectors.

Equation (2.8) expresses the contribution of the motion of dislocations of type k to the plastic strain rate. If we consider other dislocation families, the same result applies but to materially different volume elements. All such elements, however, can be chosen so as to have a given point in common. The resultant plastic strain rate at this point can then be considered to be the summation of the contributions from each dislocation family:

$$\dot{\varepsilon}^{P}_{ij} = \sum^k(\zeta^k/2)(y^k_{3i}b^k_j + y^k_{3j}b^k_i)w^k\dot{N}^k. \tag{2.9}$$

This equation has exactly the form suggested by Kelly and Gillis [11] on the basis of thermodynamical arguments.

In the discussion that follows, we assume that $\vec{y}^k_3 \cdot \vec{b}^k = 0$ for all k. This corresponds to an assumption of pure glide. Since it is commonly observed that plastic deformation of crystalline materials is nearly isochoric, glide is the dominant process and this assumption will be a good approximation for most cases.

As a notational convenience, we now define the orientation tensors $\underset{\sim}{\mu}^k$:

$$\mu^k_{ij} = (y^k_{3i}b^k_j + y^k_{3j}b^k_i)/2b^k, \tag{2.10}$$

where $b^k = \sqrt{\vec{b}^k \cdot \vec{b}^k}$. These tensors, which describe the geometric properties of the dislocation families, have the following characteristics:

$$\underset{\sim}{\mu}^{kT} = \underset{\sim}{\mu}^k, \tag{2.11a}$$

$$\mathrm{tr}(\underset{\sim}{\mu}^k) = 0, \tag{2.11b}$$

$$\mathrm{tr}\left[(\underset{\sim}{\mu}^k)^2 \right] = 1/2, \tag{2.11c}$$

$$\mathrm{tr}\left[(\underset{\sim}{\mu}^k)^3\right] = 0, \tag{2.11d}$$

where T denotes transpose and tr the trace or sum of diagonal terms. Thus, there are only three independent values in each of these tensors.

Using (2.10), equation (2.9) can be rewritten in the form

$$\dot{\varepsilon}^P_{ij} = \sum^k \mu^k_{ij} \, \zeta^k \, b^k \, w^k \dot{N}^k. \tag{2.12}$$

It is clear from this expression that the orientation tensors entirely determine the tensorial character of $\underset{\sim}{\dot{\varepsilon}}^P$.

Equation (2.2) can also be recast in terms of $\underset{\sim}{\mu}^k$. The force exerted on a dislocation segment by a general stress field $\underset{\sim}{\sigma}$ is given by Weertman and Weertman [27] as

$$\vec{f}^k = \vec{y}^k_2 \times (\underset{\sim}{\sigma} \, \vec{b}^k). \tag{2.13}$$

Taking the scalar product of this with $\vec{y}^k_1$, we obtain

$$\vec{f}^k \cdot \vec{y}^k_1 = (\vec{y}^k_1 \times \vec{y}^k_2)^T \, \underset{\sim}{\sigma} \, \vec{b}^k = \vec{y}^{kT}_3 \, \underset{\sim}{\sigma} \, b^k \tag{2.14}$$

for the component of this force in the direction of dislocation motion. The stress tensor, however, is symmetric. Equation (2.14) is therefore equivalent to

$$\vec{f}^k \cdot \vec{y}^k_1 = (1/2)(\vec{y}^{kT}_3 \, \underset{\sim}{\sigma} \, \vec{b}^k + \vec{b}^{kT} \, \underset{\sim}{\sigma} \, \vec{y}^k_3) = b^k \, \mathrm{tr}(\underset{\sim}{\mu}^k \underset{\sim}{\sigma}). \tag{2.15}$$

Let $\underset{\sim}{s}$ denote the stress deviator:

$$\underset{\sim}{s} = \underset{\sim}{\sigma} - (1/3)\mathrm{tr}(\underset{\sim}{\sigma})\underset{\sim}{I}, \tag{2.16}$$

where $\underset{\sim}{I}$ is the unit tensor. Since $\mathrm{tr}(\underset{\sim}{\mu}) = 0$, we may replace $\underset{\sim}{\sigma}$ by $\underset{\sim}{s}$ in (2.15). We thus obtain

$$\vec{f}^k \cdot \vec{y}_1^k = b^k \, \mathrm{tr}(\underset{\sim}{\mu}^k \underset{\sim}{s}) \tag{2.17}$$

for the force producing dislocation motion, and

$$\zeta^k = \mathrm{sgn}\left[\, \mathrm{tr}(\underset{\sim}{\mu}^k \underset{\sim}{s}) \,\right] \tag{2.18}$$

for the sense term in the plastic strain rate equation.

Choose a global coordinate system such that the base vectors $\vec{x}_1$, $\vec{x}_2$, $\vec{x}_3$ are orthonormal. In this case, the transformation from local to global coordinates can be constructed from a sequence of rotations. Using the sequence shown in Figure 1, the components of the resulting transformation matrix are as follows:

$$a_{11}^k = \cos\phi^k \cos\psi^k - \cos\theta^k \sin\phi^k \sin\psi^k, \tag{2.19a}$$

$$a_{12}^k = -\cos\phi^k \sin\psi^k - \cos\theta^k \sin\phi^k \cos\psi^k, \tag{2.19b}$$

$$a_{13}^k = \sin\theta^k \sin\phi^k, \tag{2.19c}$$

$$a_{21}^k = \sin\phi^k \cos\psi^k + \cos\theta^k \cos\phi^k \sin\psi^k, \tag{2.19d}$$

$$a_{22}^k = \sin\phi^k \sin\psi^k + \cos\theta^k \cos\phi^k \cos\psi^k, \tag{2.19e}$$

$$a_{23}^k = -\cos\phi^k \sin\theta^k, \tag{2.19f}$$

$$a_{31}^k = \sin\theta^k \sin\psi^k, \tag{2.19g}$$

$$a_{32}^k = \sin\theta^k \cos\psi^k, \tag{2.19h}$$

$$a_{33}^k = \cos\theta^k. \tag{2.19i}$$

Equation (2.10), the expression defining the orientation tensors,

can be written in the form

$$\mu_{ij}^k = (1/2)\left[(a_{i1}a_{j3} + a_{j1}a_{i3})\cos\omega^k + (a_{i2}a_{j3} + a_{j2}a_{i3})\sin\omega^k\right], \tag{2.20}$$

where ω^k is the angle between the local base vector $\vec{y}_1^k$ and the Burgers vector $\vec{b}^k$. Substituting into this from (2.19), the components of $\underset{\sim}{\mu}^k$ in the global coordinate system are

$$\mu_{11}^k = (\tfrac{1}{2})\left[\cos(\psi^k + \omega^k)\sin 2\phi^k \sin 2\theta^k - \sin(\psi^k + \omega^k)\sin^2\phi^k \sin 2\theta^k\right], \tag{2.21a}$$

$$\mu_{12}^k = (\tfrac{1}{2})\left[(\tfrac{1}{2})\sin(\psi^k + \omega^k)\sin 2\phi^k \sin 2\theta^k - \cos(\psi^k + \omega^k)\cos 2\phi^k \sin\theta^k\right], \tag{2.21b}$$

$$\mu_{13}^k = (\tfrac{1}{2})\left[\cos(\psi^k + \omega^k)\cos\phi^k \cos\theta^k - \sin(\psi^k + \omega^k)\sin\phi^k \cos 2\theta^k\right], \tag{2.21c}$$

$$\mu_{22}^k = (\tfrac{1}{2})\left[-\cos(\psi^k + \omega^k)\sin 2\phi^k \sin\theta^k - \sin(\psi^k + \omega^k)\sin\phi^k \cos 2\theta^k\right], \tag{2.21d}$$

$$\mu_{23}^k = (\tfrac{1}{2})\left[\cos(\psi^k + \omega^k)\sin\phi^k \cos\theta^k + \sin(\psi^k + \omega^k)\cos\phi^k \cos 2\theta^k\right], \tag{2.21e}$$

$$\mu_{33}^k = (\tfrac{1}{2})\left[\sin(\psi^k + \omega^k) \sin 2\theta^k\right]. \tag{2.21f}$$

Note that the angles ψ^k and ω^k appear only in the linear combination $\psi^k + \omega^k$. We may therefore replace these two angles by the single angle $\chi^k = \psi^k + \omega^k$:

$$\mu_{11}^k = (\tfrac{1}{2})\left[\cos\chi^k \sin 2\phi^k \sin\theta^k - \sin\chi^k \sin^2\phi^k \sin 2\theta^k\right], \tag{2.22a}$$

$$\mu_{12}^k = (\tfrac{1}{2})\left[(\tfrac{1}{2})\sin\chi^k \sin 2\phi^k \sin 2\theta^k - \cos\chi^k \cos 2\phi^k \sin\theta^k\right], \tag{2.22b}$$

$$\mu_{13}^k = (\tfrac{1}{2}) \left[\cos \chi^k \cos\phi^k \cos\theta^k - \sin\chi^k \sin\phi^k \cos 2\theta^k \right], \tag{2.22c}$$

$$\mu_{22}^k = (\tfrac{1}{2}) \left[-\cos\chi^k \sin 2\phi^k \sin\theta^k - \sin\chi^k \cos^2\phi^k \sin 2\theta^k \right], \tag{2.22d}$$

$$\mu_{23}^k = (\tfrac{1}{2}) \left[\cos\chi^k \sin\phi^k \cos\theta^k + \sin\chi^k \cos\phi^k \cos 2\theta^k \right], \tag{2.22e}$$

$$\mu_{33}^k = (\tfrac{1}{2}) \left[\sin\chi^k \sin 2\theta^k \right]. \tag{2.22f}$$

Thus, the tensor $\underset{\sim}{\mu}^k$ depends on only three independent angles. Moreover it is evident from this result that $\underset{\sim}{\dot{\varepsilon}}^p$ is independent of the screw or edge character of the dislocations.

For single crystal specimens, the possible glide systems are usually well-defined. In a polycrystalline sample, however, this is not the case. The principal axes of the grains will in general vary throughout the solid making it impossible to specify the set of orientation angles $\{\chi^k, \phi^k, \theta^k\}$ a priori. It, therefore, appears reasonable and advantageous to replace this discrete set by a set of three continuous random variables $\{\chi, \phi, \theta\}$. This allows us to replace the summation in equation (2.12) by an integral and write the plastic strain rate equations as follows:

$$\dot{\varepsilon}_{ij}^p = \int \mu_{ij}(\chi, \phi, \theta)\, \zeta(\chi, \phi, \theta)\, b(\chi, \phi, \theta)\, w(\chi, \phi, \theta)\, \dot{N}(\chi, \phi, \theta) dk, \tag{2.23}$$

where dk is the fractional number of dislocation families having coordinates between (χ, ϕ, θ) and $(\chi + d\chi, \phi + d\phi, \theta + d\theta)$.

The function ζ and the tensor $\underset{\sim}{\mu}$ are defined by the continuous equivalents of equations (2.18) and (2.22). This yields

$$\zeta = \mathrm{sgn}\left[\mathrm{tr}(\underset{\sim}{\mu}\underset{\sim}{s}) \right], \tag{2.24}$$

for the sense function, and

$$\mu_{11} = (\tfrac{1}{2}) \left[\cos\chi \sin 2\phi \ \sin\theta - \sin\chi \sin^2\phi \sin 2\theta \right] \tag{2.25a}$$

$$\mu_{12} = (\tfrac{1}{2}) \left[(\tfrac{1}{2}) \sin\chi \sin 2\phi \sin 2\theta - \cos\chi \cos 2\phi \sin\theta \right], \tag{2.25b}$$

$$\mu_{13} = (\tfrac{1}{2}) \left[\cos\chi \cos\phi \cos\theta - \sin\chi \sin\phi \cos 2\theta \right] \tag{2.25c}$$

$$\mu_{22} = (\tfrac{1}{2}) \left[-\cos\chi \sin 2\phi \sin\theta - \sin\chi \cos^2\phi \sin 2\theta \right], \tag{2.25d}$$

$$\mu_{23} = (\tfrac{1}{2}) \left[\cos\chi \sin\phi \cos\theta + \sin\chi \cos\phi \cos 2\theta \right] \tag{2.25e}$$

$$\mu_{33} = (\tfrac{1}{2}) \left[\sin\chi \sin 2\theta \right], \tag{2.25f}$$

for the components of the orientation tensor.

Consider a single glide plane with unit normal $\vec{y}_3$. The probability that this vector lies between (ϕ, θ) and $(\phi + d\phi, \theta + d\theta)$ is identical to the probability that its endpoint lies within an element of area $dS = \sin\theta \, d\theta \, d\phi$ on the surface of the unit sphere. This geometric analogy yields

$$dP_{\vec{y}_3} = f_{\vec{y}_3}(\phi, \theta) \sin\theta \, d\theta \, d\phi, \tag{2.26}$$

where $f_{\vec{y}_3}$ is the probability density function of $\vec{y}_3$; that is, it describes how the endpoints of the glide plane normals are distributed over the surface of the unit sphere.

In a similar manner, the probability that the Burgers vector in a given glide plane will lie between χ and $\chi + d\chi$ is identical to the probability that the endpoing of the vector $\vec{b}/\sqrt{\vec{b} \cdot \vec{b}}$ lies within an element of arc length $ds = d\chi$ on the unit circle. This yields

$$dP_{\vec{b}} = f_{\vec{b}}(\chi, \phi, \theta) d\chi \tag{2.27}$$

where $f_{\vec{b}}$ is the probability density function for the direction of the Burgers vector. It is a function of ϕ and θ as well as χ because

the distribution of possible directions for $\vec{b}$ will, in general, depend on the glide plane under consideration.

The probability given by (2.26) is equivalent to the fractional number of glide planes between (ϕ, θ) and $(\phi + d\phi, \theta + d\theta)$, while that given by (2.27) is equivalent to the fractional number of Burger vector directions between χ and $\chi + d\chi$ on the glide plane with coordinates (ϕ, θ). The fractional number of dislocation families, dk, is just the product of these two numbers:

$$dk = f_{\vec{b}}(\chi,\phi,\theta)\ f_{\vec{y}_3}(\phi,\theta)\sin\theta\ d\theta\ d\phi\ d\chi. \tag{2.28}$$

Thus, the macroscopic plastic strain rate in a polycrystalline material is given by

$$\dot{\varepsilon}^P_{ij} = \int_{-\pi}^{+\pi}\int_{-\pi}^{+\pi}\int_{0}^{\pi/2} \mu_{ij}\ \zeta\ bw\ f_{\vec{b}}\ f_{\vec{y}_3}\ \dot{N}\ \sin\theta\ d\theta\ d\phi\ d\chi, \tag{2.29}$$

where, to avoid double counting of dislocations, the integration is taken over the unit hemisphere.

2.3 Dislocation Production and Interaction

In this section we consider processes which result in changes in dislocation density. Neglecting interactions between more than two dislocations, these are production by fixed sources (Frank-Read sources), breeding by multiple cross-glide, and pair annihilation. For dislocations of type k, this can be expressed by the equation

$$\dot{N}^k = a_o^k + a_1^k N^k - a_2^k N^{k2}, \tag{2.30}$$

where a_o^k is the net rate at which fixed sources create dislocations of type k, a_1^k is a breeding coefficient, and a_2^k is an attrition coefficient [16]. These coefficients will, in general, depend

on the dislocation densities for all families, the applied stress, the temperature distribution, and the distribution of such things as grain boundaries, precipitate particles, and free surfaces.

For the case of a single dislocation family, theoretical [28] and experimental [29] investigations have shown that the breeding rate due to cross-glide multiplication is proportional to the mean dislocation speed. By considering multiplication and blocking interactions when several dislocation types are present, Kelly and Gillis [17] have generalized this result according to the formula

$$a_1^k = \lambda^k \langle v^k \rangle = \lambda^k \beta^k v^k, \tag{2.31}$$

where λ^k is the reciprocal mean free path between multiplication interactions for type k dislocations and v^k is the mean speed of the mobile type k dislocations. The variable β^k, which we call the mobile fraction, is the ratio of the mobile density to the total density of type k dislocations. It has been introduced because experimental measurements of dislocation density invariably relate to total density while measurements of dislocation speed relate to the mobile density.

The probability of pair-wise annihilation depends on the presence of two dislocations of the same family in a given neighborhood of each other. The average time between such encounters will be inversely proportional to the mean dislocation speed and, since only mobile dislocations can move into the neighborhood of other dislocations, directly proportional to the mobile fraction. An appropriate expression for the attrition coefficient is therefore

$$a_2^k = \kappa^k \beta^k v^k, \tag{2.32}$$

where κ^k is the mean radius of the interaction neighborhood for annihilation events for type k dislocations. Substituting this result and that given by (2.31) into equation (2.30), the evolutionary equation for the dislocation density becomes

$$\dot{N}^k = a_o^k + \lambda^k v^k \beta^k N^k - \kappa^k v^k \beta^k N^{k2}. \tag{2.33}$$

We now assume that all dislocations produced by fixed sources and by multiplication events are initially mobile. By analogy with equation (2.33), this leads to the following expression for the rate of change of the mobile density:

$$\dot{N}^{k(m)} = a_o^k + (\lambda^k - \lambda_o^k) v^k N^{k(m)} - \kappa_o^k v^k N^{k(m)^2}. \tag{2.34}$$

Here λ_o^k is the reciprocal mean free path for the immobilization of type k dislocations by inclusions and by other dislocation families. The quantity κ_o^k represents the resultant mean interaction distance for the removal of mobile type k dislocations by type k dislocations (this includes both annihilation and immobilization events). It follows from these last two equations and the definition of the mobile fraction that

$$\begin{aligned}\dot{\beta}^k = {} & a_o^k(1 - \beta^k)/N^k + \lambda^k(1 - \beta^k) - \lambda_o^k v^k \beta^k \\ & + (\kappa^k - \kappa_o^k) v^k N^k \beta^{k2}.\end{aligned} \tag{2.35}$$

The elements of dislocation production and interaction essential to the present theory are given by the continuous equivalents, in terms of glide system orientation, of equations (2.33) and (2.35). These equations are

$$\begin{aligned}\dot{N} = {} & a_o(\chi,\phi,\theta) + \lambda(\chi,\phi,\theta) v(\chi,\phi,\theta)\beta N \\ & - \kappa(\chi,\phi,\theta) v(\chi,\phi,\theta)\beta N^2,\end{aligned} \tag{2.36}$$

and $$\dot{\beta} = a_o(\chi,\phi,\theta)(1 - \beta)/N + \left[\lambda(\chi,\phi,\theta)(1 - \beta) - \lambda_o(\chi,\phi,\theta)\right] v(\chi,\phi,\theta,)\beta + \left[\kappa(\chi,\phi,\theta) - \kappa_o(\chi,\phi,\theta)\right] v(\chi,\phi,\theta,)N\beta^2, \tag{2.37}$$

where, as in the discrete formulation, the coefficient may depend on stress, temperature, and the variables β and N.

In many cases the above expressions are more general than necessary. Production by fixed sources, while sometimes important to the initiation of plastic deformation, is quickly eclipsed by production due to cross-glide multiplication once flow has started [16]. In addition, experimental evidence suggests that the mobile fraction is small compared to unity most of the time [30]. Under these conditions equation (2.36) can be approximated by

$$\dot{N} = \lambda(\chi,\phi,\theta)\left[1 - N/N^*(\chi,\phi,\theta)\right] \; v(\chi,\phi,\theta)\beta N \tag{2.38}$$

and equation (2.37) by

$$\dot{\beta} = \left[\kappa_o(\chi,\phi,\theta) - \kappa(\chi,\phi,\theta)\right]\left[N^{\dagger}(\chi,\phi,\theta)/N - \beta\right] v(\chi,\phi,\theta)N\beta. \tag{2.39}$$

Here $N^* = \lambda/\kappa$ and $N^{\dagger} = (\lambda - \lambda_o)/(\kappa_o - \kappa)$. The first of these parameters, N^*, can be thought of as a saturation value for the dislocation density. When N approaches N^*, the rate of annihilation becomes equal to the rate of production and the dislocation density remains constant. Assuming $\lambda \geq \lambda_o$ and $\kappa_o > \kappa$, $N^{\dagger}$ defines a similar limiting value for the mobile density. In this case, however, it is a lower rather than an upper limit.

If the parameters λ, λ_o, κ, and κ_o do not depend explicitly on time, equations (2.38) and (2.39) can be combined to yield an equation for β in terms of dislocation density. Dividing (2.38) by (2.39) we have

$$d\beta/dN + \left[(\kappa_o-\kappa)/\lambda\right]\beta/(1-N/N^*) = (1-\lambda_o/\lambda)/\left[N(1-N/N^*)\right]. \qquad (2.40)$$

Provided the bracketed terms above are independent of β, this differential equation is linear. As such, it has the general solution

$$\beta = \exp(-P)\ \{C + \int (1-\lambda_o/\lambda)\ \exp(P)\ dN/\left[N(1-N/N^*)\right]\} \qquad (2.41)$$

where P is an integrating factor,

$$P = \int \left[(\kappa_o-\kappa)/\lambda\right] dN/(1-N/N^*), \qquad (2.42)$$

and C is the constant of integration. Since this result gives β explicitly in terms of N, it is possible to eliminate the mobile fraction from equation (2.38). Thus, in this particular case we are able to reduce the required number of constitutive equations by one.

We conclude this section by noting that when the parameters λ, κ, and κ_o are independent of N as well as β, the integral in (2.42) can be evaluated analytically. Using the definition of N* this yields

$$P = (1-\kappa_o/\kappa)\ln(1-\kappa N/\lambda) \qquad (2.43)$$

for the integrating factor. If we take the limit of this expression as $\kappa \to 0$, that is, the case of an infinite saturation density, we obtain

$$P = (\kappa_o/\lambda)N. \qquad (2.44)$$

Taking $\lambda_o = \lambda$ and substituting (2.44) into (2.41) then yields the result

$$\beta = C\ \exp\left[-(\kappa_o/\lambda)N\right]. \qquad (2.45)$$

We thus obtain the form suggested by Gilman [16] on the basis of creep behavior as a limiting case of equations (2.38) and (2.39).

2.4 The Dislocation Velocity

The importance of the dislocation velocity in modern theories of crystalline plasticity has led to considerable effort being devoted to the study of dislocation mobilities. It is generally accepted that these mobilities depend primarily on the applied stress and the resistance of the lattice. Direct measurements of the stress dependence of v at various temperatures have been obtained by dividing the displacement of specially introduced mobile dislocations by the duration of an applied stress pulse [31]. The dislocation displacements are determined by either selective etch-pitting [31], or by x-ray topography [32]. This method relies on the fact that the inertia of dislocations is extremely small, a situation that has been verified experimentally since the velocities obtained have proven to be largely independent of the pulse duration. The stress and temperature dependence of the dislocation velocity can also be obtained by interpretive analysis of ultrasonic attenuation measurements [33]. Data obtained in this manner, however, may be valid only over a limited stress range. The model on which it is based assumes that the force normal to each unit length of a moving dislocation is linearly related to its velocity.

Theoretical models for the experimentally observed stress and temperature dependence of v have been developed by several authors [34, 35]. Klahn [36], for example, considers the effects of thermally activated, athermal, and viscous drag dislocation mechanisms on v, both individually and in combination. Diffusion controlled creep mechanisms are also discussed. These processes, however, are significant only at very low stresses and at temperatures

above about one-half the melting temperature.

Here we take the thermally activated mechanisms to be dominated by the cutting of simple rectangular obstacles in a homogeneous array and the athermal mechanisms by a sinusoidally varying long range back stress. Assuming an independent time sequence for thermally activated and for viscous drag mechanisms, we have the following expression for the dislocation velocity:

$$v = \left\{ \frac{B}{\tau^* b} + \left(\frac{2\,\Gamma\,L^2}{\nu_o^3\,\tau^*\,b^7} \right)^{1/3} \exp\left[\frac{u\,\Gamma\,d - d(2\Gamma L^2\,\tau^{*2}\,b^2)^{1/3}}{kT} \right] \right\}^{-1} . \tag{2.46}$$

Here B is the viscous damping coefficient, Γ is the average dislocation energy per unit length, L is the spacing between obstacles, ν_o is the Debye frequency, d is the barrier width, u is the relative barrier strength ($0 \le u \le 2$), and k is the Boltzman constant. To account for relativistic effects when v approaches the shear wave velocity, c, we assume that B is of the form [37]

$$B = B_o/(1 - v^2/c^2), \tag{2.47}$$

and that Γ is of the form

$$\Gamma = \Gamma_o/\sqrt{1 - v^2/c^2} . \tag{2.48}$$

The quantity τ^* represents the effective stress acting on the dislocation. Averaging stresses over one wave length for the back stress, it is given by the formula

$$\tau^* = \sqrt{tr^2(\underset{\sim}{\mu s}) - \delta^2\,b^2\,\mu_e^2\,N} , \tag{2.49}$$

where δ is an experimentally determined factor (~1/5) [38], and μ_e is the elastic shear modulus. The first term in this formula is the shear stress driving the dislocation motion and is obtained

from the result (2.17); the second term represents the effect of the long range back stresses assuming the dislocations are imbedded in an isotropic elastic lattice.

A model similar to that leading to equation (2.46) has recently been proposed by Gillis, Gilman, and Taylor [39]. In their characterization, the mechanism for motion through the obstacle array is taken to be tunneling [35] rather than thermal activation. Assuming an independent time sequence for tunneling and for viscous glide, this results in the following stress-velocity relation:

$$v = \left\{ (2\ b\ \tau^*/c^2B_o)/ \left[\sqrt{1 + (2b\tau^*/cB_o)^2} - 1 \right] + \exp(D/\tau)/\nu_o L \right\}^{-1}, \tag{2.50}$$

where τ is the applied shear stress, tr($\underset{\sim}{\mu s}$), D is a characteristic drag stress, and ν_o is the frequency with which the dislocations attempt to surmount obstacles.

As can be seen in Figure 2, the dislocation speeds predicted by (2.46) and (2.50) can be made nearly identical by an appropriate choice of parameter values. In most cases both thermal activation and tunneling will probably be operative over some range of stress and a combination of these two forms will be required to fit the observed behavior.

Both of the velocity equations just presented are quite complicated and, hence, difficult to use in studies of the behavior of our constitutive model. Two simple forms which have been successfully used in approximating experimental curves are an empirically determined power law [31],

$$v = v_o(\tau/\tau_o)^n, \tag{2.51}$$

where v_o is a characteristic velocity and τ_o the effective stress at that velocity, and the Gilman relation [40],

$$v = v^* \exp(-D/\tau), \tag{2.52}$$

where v^* is a characteristic limiting velocity. These equations will be used in lieu of (2.46) or (2.50) for the behavioral studies given in Section III.

2.5 Elastic Energy Due to Dislocations

The presence of dislocations in a polycrystalline material produces an elastic distortion of the crystal lattice. As such, the energy of the resulting strain field is stored in the material, being recoverable upon removal of the dislocations. The energy per unit length of a dislocation in an isotropic material has been calculated by several authors [41, 42]. For type k dislocations, it is given by the formula

$$\xi^k = (\mu_e/4\pi)\left[(\vec{b}^k \cdot \vec{y}_1^k)^2/(1-\nu) + (\vec{b}^k \cdot \vec{y}_2^k)^2\right] \left[\ln(w_e^k/w^k) + a^k\right], \tag{2.53}$$

where μ_e is the shear modulus of the material, ν is its Poissons ratio, and w_e^k is the radius of the extent of influence of the dislocation. The quantity a, which is of order unity, represents the contribution of the core energy to the total dislocation energy.

Using equation (2.53), we obtain the following expression for the total stored energy per unit volume due to dislocations:

$$\varepsilon^d = (\mu_e/4\pi) \sum^k N^k \left[(b^k \cdot y_1^k)^2/(1-\nu) + (b^k \cdot y_2^k)^2\right] \left[\ln(w_e^k/w^k) + a^k\right]. \tag{2.54}$$

It is clear that this expression requires the stored energy to increase with increasing dislocation density; that is, with increasing plastic deformation. This result is consistent with available data for polycrystalline [20] and monocrystalline [43] metals.

Equation (2.54) is adequate as long as we know which glide systems are available. For a random distribution of systems as in a polycrystalline sample, however, it is convenient to reformulate this equation in terms of the random variables introduced in section 2.2. We thus obtain

$$\varepsilon^d = (\mu_e/4\pi)\int_{-\pi}^{+\pi}\int_{-\pi}^{+\pi}\int_{0}^{\pi/2} N\, b^2 \left[\ln(w_e/w) + a\right] f_{\vec{b}}\, f_{\vec{y}_3}\, \sin\theta\, d\theta\, d\phi\, d\chi \int_{-\pi}^{+\pi} \left[\cos^2\omega/(1-\nu) + \sin^2\omega\right] d\omega, \tag{2.55}$$

where ω is a new random variable define as shown in Figure 1 and we have assumed that the dislocations are uniformly distributed between edge and screw types. After evaluating the last integral in (2.55), we have

$$\varepsilon^d = (\mu_e/4)\left[(2-\nu)/(1-\nu)\right]\int_{-\pi}^{+\pi}\int_{-\pi}^{+\pi}\int_{0}^{\pi/2} N\, b^2 \left[\ln(w_e/w) + a\right] f_{\vec{b}}\, f_{\vec{y}_3}\, \sin\theta\, d\theta\, d\phi\, d\chi \tag{2.56}$$

for the total internal energy density due to dislocations in an isotropic (elastic) material.

2.6 Summary

The visco-plastic behavior of polycrystalline materials has been shown to be characterized by three rate equations:

$$\dot{\underset{\sim}{\varepsilon}}^P = \int_{\pi}^{+\pi}\int_{\pi}^{+\pi}\int_{0}^{\pi/2} \underset{\sim}{\mu}\, \zeta\, bw\, f_{\vec{b}}\, f_{\vec{y}_3}\, \dot{N}\, \sin\theta\, d\theta\, d\phi\, d\chi, \tag{2.29}$$

$$\dot{N} = a_o(\chi,\phi,\theta) + \lambda(\chi,\phi,\theta)\ v(\chi,\phi,\theta)\beta N - \kappa(\chi,\phi,\theta)\ v(\chi,\phi,\theta)\ \beta N^2, \tag{2.33}$$

$$\dot{\beta} = a_o(\chi,\phi,\theta)(1-\beta)/N + \left[\lambda(\chi,\phi,\theta)(1-\beta) - \lambda_o(\chi,\phi,\theta)\right] v(\chi,\phi,\theta)\beta + \left[\kappa(\chi,\phi,\theta)-\kappa_o(\chi,\phi,\theta)\right] v(\chi,\phi,\theta)\beta^2 N. \tag{2.35}$$

These equations relate the microscopic phenomenon of dislocation production and interaction to the macroscopic plastic strain rate. Although these equations were obtained by restricting the dislocations to glide motions only, they are general enough to reproduce a wide range of observed material behavior. This includes strain hardening and softening, Bauschinger effect, and the development of plastic anisotropy. These aspects of the model are illustrated in the next section by several examples.

In conclusion, we note that if we identify the vector of internal variables, $\vec{\alpha}$, with the discrete dislocation densities, N^k, the functions G and $\underset{\sim}{H}$ from the thermodynamic development of Section 1.2 can be identified with dislocation expressions. In the limit of an infinite number of dislocation families; that is, $N^k \to N(\chi,\phi,\theta)$, the dimension of the vector space for $\vec{\alpha}$ becomes infinite and the inner products in equations (1.25) and (1.26) can be defined using integrals. This yields

$$\dot{\underset{\sim}{\varepsilon}}^P = (1/4\pi^2) \int_{-\pi}^{+\pi}\int_{-\pi}^{+\pi}\int_{o}^{\pi/2} \underset{\sim}{H}_{,\vec{\alpha}}\ \dot{N} \sin\theta\ \ d\theta\ d\phi\ d\chi \tag{2.57}$$

and

$$w^r = (-\rho_o/4\pi^2) \int_{-\pi}^{+\pi}\int_{-\pi}^{+\pi}\int_{o}^{\pi/2} G_{,\vec{\alpha}}\ \dot{N} \sin\theta\ d\theta\ d\phi\ d\chi. \tag{2.58}$$

Comparing (2.57) with (2.29), it is clear that

$$\underset{\sim}{H}_{,\vec{\alpha}} = 4\pi^2 \underset{\sim}{\mu} \zeta b w \vec{f}_b \vec{f}_{y_3} . \tag{2.59}$$

To obtain a similar relation for G we require the time derivative of equation (2.56). Assuming that w_e is a function of N only and that all other parameters in (2.56) are independent of N and time, we have

$$w^r = \dot{\varepsilon}^d = (\mu_e/4) \quad (2-\nu)/(1-\nu) \int_{-\pi}^{+\pi} \int_{-\pi}^{+\pi} \int_{0}^{\pi/2} \tag{2.60}$$

$$b^2 \left[\ln(w_e/w) + (1/w_e)(dw_e/dN) + a \right] \dot{N} \vec{f}_b \vec{f}_{y_3} \sin\theta \, d\theta \, d\phi \, d\chi .$$

Comparing this result with (2.58) then yields the identification

$$-\rho_o G_{,\vec{\alpha}} = \pi^2 \mu_e \left[(2-\nu)/(1-\nu)\right] b^2 \left[\ln(w_e/w) + (1/w_e)(dw_e/dN) + a\right] \vec{f}_b \vec{f}_{y_3} . \tag{2.61}$$

Thus, we see that the constitutive equations we have developed using dislocation mechanics are consistent with thermodynamics as presented in Section 1.2.

III. BEHAVIOR OF THE CONSTITUTIVE EQUATIONS FOR POLYCRYSTALLINE PLASTICITY

3.1 Introduction

To illustrate the utility of the constitutive theory just presented, we now consider several examples chosen for simplicity and the range of behavior obtainable. In keeping with the idea of simplicity, we neglect thermal effects and assume that the dislocation parameters b, w, λ, λ_o, κ, and κ_o are all constant. In addition, we assume that the elastic response of the sample materials is isotropic and linear and that dislocation production by fixed sources is negligible. With these restrictions in mind, the constitutive equations characterizing our samples are as follows:

$$\dot{\varepsilon}^P_{ij} = \lambda\, bw \int_{-\pi}^{+\pi}\int_{-\pi}^{+\pi}\int_{o}^{\pi/2} \mu_{ij}\, \zeta\, v\, \beta\, N(1-N/N^*)\, f_{\vec{b}}\, f_{\vec{y}_3} \sin\theta\, d\theta\, d\phi\, d\chi, \tag{3.1}$$

$$\dot{N} = \lambda\, v\, \beta\, N(1 - N/N^*), \tag{3.2}$$

$$\dot{\beta} = v\, \beta[\lambda^* - \beta(\lambda + \kappa^* N)], \tag{3.3}$$

$$\dot{\varepsilon}_{ij} = \dot{\varepsilon}^P_{ij} + (1/E)\, [(1+\nu)\dot{\sigma}_{ij} - \nu\dot{\sigma}_{kk}\, \delta_{ij}], \tag{3.4}$$

$$v = v(\mu_{ij}\, s_{ij}) \geq 0, \tag{3.5}$$

where $\lambda^* = \lambda - \lambda_o$, $\kappa^* = \kappa_o - \kappa$, E is Young's modulus, δ_{ij} is the Kronecker delta ($\delta_{ij} = 0$ if $i \neq j$, $\delta_{ij} = 1$ if $i = j$), and all other quantities are as previously defined. Here also we have made use of summation notation; that is, a repeated index implies summation on that index, and have used equation (2.38) to obtain (3.1).

For comparison of results, it is convenient to non-dimensionalize the variables involved. We, therefore, define a normalized strain tensor and a normalized plastic strain tensor,

$$\bar{\varepsilon}_{ij} = (E/\tau_o)\varepsilon_{ij} \quad , \quad \bar{\varepsilon}^P_{ij} = (E/\tau_o)\varepsilon^P_{ij}, \tag{3.6}$$

a normalized stress tensor and a normalized stress deviator,

$$\bar{\sigma}_{ij} = \sigma_{ij}/\tau_o \quad , \quad \bar{s}_{ij} = s_{ij}/\tau_o, \tag{3.7}$$

a normalized dislocation density,

$$\bar{N} = N/N^*, \tag{3.8}$$

and a normalized dislocation speed,

$$\bar{v} = v/v_o. \tag{3.9}$$

Making the required change of variables in our constitutive equations, we have:

$$\dot{\bar{\varepsilon}}^P_{ij} = v_o \lambda b w N^*(E/\tau_o) \int_{-\pi}^{+\pi}\int_{-\pi}^{+\pi}\int_{0}^{\pi/2} \mu_{ij} \zeta \bar{v} \beta \bar{N}(1-\bar{N}) f_{\vec{b}} f_{\vec{y}3} \sin\theta \, d\theta \, d\phi \, d\chi, \tag{3.10}$$

$$\dot{\bar{N}} = v_o \lambda \bar{v} \beta \bar{N}(1 - \bar{N}), \tag{3.11}$$

$$\dot{\beta} = v_o \lambda \bar{v} \beta [\beta^* - \beta(1 + B^* \bar{N})], \tag{3.12}$$

$$\dot{\bar{\varepsilon}}_{ij} = \dot{\bar{\varepsilon}}^P_{ij} + (1 + \nu) \dot{\bar{\sigma}}_{ij} - \nu\dot{\bar{\sigma}}_{kk} \delta_{ij} \tag{3.13}$$

$$\bar{v} = (1/v_o) v(\tau_o \mu_{ij} \bar{s}_{ij}), \tag{3.14}$$

where $\beta^* = \lambda^*/\lambda$ and $B^* = (\kappa^*/\lambda)N^*$. The quantity $v_o\lambda b \, w \, N^*(E/\tau_o)$ has the dimensions of reciprocal time and hence defines a characteristic material rate, $\dot{\varepsilon}^*$. Using this to normalize t, we have the following form for our fully non-dimensional constitutive equations:

$$\frac{d\bar{\varepsilon}^P_{ij}}{d\bar{t}} = \int_{-\pi}^{+\pi}\int_{-\pi}^{+\pi}\int_{0}^{\pi/2} \mu_{ij} \zeta \bar{v} \beta \bar{N}(1-\bar{N}) f_{\vec{b}} f_{\vec{y}3} \sin\theta \, d\theta \, d\phi \, d\chi, \tag{3.15}$$

$$\frac{d\bar{N}}{d\bar{t}} = A \beta \bar{N}(1 - \bar{N}) \bar{v}, \tag{3.16}$$

$$\frac{d\beta}{d\bar{t}} = A\ \beta\ [\beta^* - \beta(1 + B^*\bar{N})]\ \bar{v}, \tag{3.17}$$

$$\frac{d\bar{\varepsilon}_{ij}}{d\bar{t}} = \frac{d\bar{\varepsilon}^P_{ij}}{d\bar{t}} + (1 + \nu)\ \frac{d\bar{\sigma}_{ij}}{d\bar{t}} - \nu\ \frac{d\bar{\sigma}_{kk}}{d\bar{t}}\ \delta_{ij}, \tag{3.18}$$

where $\bar{t} = \dot{\varepsilon}^*\ t$, and $A = v_o\lambda/\dot{\varepsilon}^* = [b\ w\ N^*(E/\tau_o)]^{-1}$.

Due to the complicated nature of the integrand in (3.15), it is unlikely that the required integration can be performed analytically. In addition, since the dependence of $\bar{N}$ and β on χ, ϕ, and θ changes with time through equations (3.16) and (3.17), the angular dependence of the integrand changes with time. It is, therefore, necessary to have some numerical means of approximating the required integration.

To obtain a suitable quadrature scheme we define three new variables as follows:

$$z_1 = \sin[2(\theta - \pi/4)], \tag{3.19a}$$

$$z_2 = \sin(2\phi), \tag{3.19b}$$

$$z_3 = \sin(2\chi). \tag{3.19c}$$

Making a change of variables in (3.15) from χ, ϕ, θ to z_3, z_2, z_1, we have

$$\frac{d\bar{\varepsilon}^P_{ij}}{d\bar{t}} = 2 \int_{-1}^{+1}\int_{-1}^{+1}\int_{-1}^{+1} \mu_{ij}\ \zeta\ \bar{v}\ \beta\ \bar{N}(1-\bar{N})\ f_{\vec{b}}\ f_{\vec{y}3}$$
$$\sin\theta[(1-z_1^2)(1-z_2^2)(1-z_3^2)]^{-1/2}\ dz_1\ dz_2\ dz_3. \tag{3.20}$$

These integrals are in a form suitable for approximation by the Chebyshev-Gauss formula [44]

$$\int_{-1}^{+1} f(z)(1 - z^2)^{-1/2}\ dz \simeq (\pi/m) \sum_{i=1}^{m} f(z_i), \tag{3.21}$$

where $z_i = \cos[(2i - 1)\pi/2m]$ and m is the number of abscissa values (this formula has the advantage of having precision of order 2m - 1 with equal weights). Thus we obtain

$$\frac{d\bar{\varepsilon}^P}{d\bar{t}}_{ij} \simeq (2\pi^3/n_1 n_2 n_3) \sum_{k=\ell}^{n_3} \sum_{\ell=1}^{n_2} \sum_{m=1}^{n_1} \mu_{ij}(\chi_k,\phi_\ell,\theta_m)\ \zeta(\chi_k,\phi_\ell,\theta_m)$$

$$\bar{v}(\chi_k,\phi_\ell,\theta_m)\ \beta(\chi_k,\phi_\ell,\theta_m)$$

$$\cdot\ \bar{N}(\chi_k,\phi_\ell\ ,\theta_m)[1-\bar{N}(\chi_k,\phi_\ell,\theta_m)]\ f_{\vec{b}}(\chi_k,\phi_\ell,\theta_m) \tag{3.22}$$

$$f_{\vec{y}_3}(\chi_k,\phi_\ell,\theta_m)\ \sin\theta_m,$$

where $\theta_m = (\pi/2)[1 - (2m - 1)/2n_1]$, $\phi_\ell = \pi[1-(2\ell - 1)/n_2]$, $\chi_k = \pi[1 - (2k - 1)/n_3]$. (3.23)

This result completes the preliminary mathematical manipulations necessary for our subsequent behavioral analysis.

3.2 Behavior of the Plastic Strain Rate for a Given Dislocation Distribution

The behavior of the plastic strain rate for multiaxial states of stress can be explored most easily by choosing a distribution for the dislocations. We can then evaluate the right-hand side of equation (3.15) without the necessity of solving (3.16) - (3.18). For simplicity, we assume that $\bar{N} << 1$. In this case (3.15) reduces to the form

$$\frac{d\bar{\varepsilon}^P}{d\bar{t}}_{ij} = \beta\ \bar{N} \int_{-\pi}^{+\pi}\int_{-\pi}^{+\pi}\int_{0}^{\pi/2} \mu_{ij}\ \zeta\ \bar{v}\ f_{\underset{\sim}{\varepsilon}}\ \sin\theta\ d\theta\ d\phi\ d\chi, \tag{3.24}$$

where $f_{\underset{\sim}{\varepsilon}}$ denotes the product of the probability density distributions for $\bar{N}$ and β with the distributions $f_{\vec{b}}$ and $f_{\vec{y}_3}$ for the available Burger's vector and glide plane orientations.

In the examples that follow we consider three different functional forms for $f_{\underset{\sim}{\varepsilon}}$

$$f_{\underset{\sim}{\varepsilon}} = 1/4\ \pi^2 \tag{3.25a}$$

which corresponds to a uniform distribution in all variables with respect to Burger's vector and glide plane orientation, and

$$f_{\underset{\sim}{\varepsilon}} = (5/4\ \pi^2)\ \sin^4(\phi)\ \sin^4(\theta), \tag{3.25b}$$

$$f_{\underset{\sim}{\varepsilon}} = (3/4\ \pi^2)\ \sin^2(\phi/2)\ \sin^2(\theta), \tag{3.25c}$$

which corresponds to a uniform distribution in all variables with respect to Burger's vector orientation and a nonuniform distribution with respect to glide plane orientation. It will be shown that (3.25a) leads to isotropic behavior, (3.25b) leads to orthotropic behavior (due to symmetries in the distribution function), and (3.25c) leads to fully anisotropic behavior. Thus we can conclude that changes in the distribution of $\bar{N}$ and β with respect to glide plane orientation can result in the development of plastic anisotropy as flow progresses. This phenomena is often observed experimentally but is not readily explained by other theories.

For simplicity we assume that the dislocation speed is given by the power law (2.51). Using equation (3.14), this yields the relation

$$\bar{v} = |\mu_{ij}\ \bar{s}_{ij}|^n, \tag{3.26}$$

where we have neglected the back stress. For the case of a linear dependence of $\bar{v}$ on $\mu_{ij}\ \bar{s}_{ij}$; that is, n = 1,

$$\zeta\ \bar{v} = \mu_{ij}\ \bar{s}_{ij} \tag{3.27}$$

and the integrals (3.24) can be evaluated analytically for all three

forms chosen for the probability density, $f_{\underset{\sim}{\varepsilon}}$. Omitting the algebraic details, the results are as follows:

$$\frac{d\bar{\varepsilon}^P}{d\bar{t}}\,11 = (\beta\,\bar{N}/15)\,[\bar{s}_{11} - (1/2)\,\bar{s}_{22} - (1/2)\,\bar{s}_{33}], \tag{3.28a}$$

$$\frac{d\bar{\varepsilon}^P}{d\bar{t}}\,12 = (\beta\,\bar{N}/10)\,\bar{s}_{12}, \tag{3.28b}$$

$$\frac{d\bar{\varepsilon}^P}{d\bar{t}}\,13 = (\beta\,\bar{N}/10)\,\bar{s}_{13}, \tag{3.28c}$$

$$\frac{d\bar{\varepsilon}^P}{d\bar{t}}\,22 = (\beta\,\bar{N}/15)\,[\bar{s}_{22} - (1/2)\,\bar{s}_{33} - (1/2)\,\bar{s}_{11}], \tag{3.28d}$$

$$\frac{d\bar{\varepsilon}^P}{d\bar{t}}\,23 = (\beta\,\bar{N}/10)\,\bar{s}_{23}, \tag{3.28e}$$

$$\frac{d\bar{\varepsilon}^P}{d\bar{t}}\,33 = (\beta\,\bar{N}/15)\,[\bar{s}_{33} - (1/2)\,\bar{s}_{11} - (1/2)\,\bar{s}_{22}], \tag{3.28f}$$

for $f_{\underset{\sim}{\varepsilon}}$ given by (3.25a),

$$\frac{d\bar{\varepsilon}^P}{d\bar{t}}\,11 = \beta\,\bar{N}(5/63)\,[\bar{s}_{11} - (1/2)\,\bar{s}_{22} - (1/2)\bar{s}_{33}], \tag{3.29a}$$

$$\frac{d\bar{\varepsilon}^P}{d\bar{t}}\,12 = \beta\,\bar{N}(17/126)\,\bar{s}_{12}, \tag{3.29b}$$

$$\frac{d\bar{\varepsilon}^P}{d\bar{t}}\,13 = \beta\,\bar{N}(17/126)\,\bar{s}_{13}, \tag{3.29c}$$

$$\frac{d\bar{\varepsilon}^P}{d\bar{t}}\,22 = \beta\,\bar{N}(1/21)\,[\bar{s}_{22} - (1/6)\,\bar{s}_{33} - (5/6)\,\bar{s}_{11}], \tag{3.29d}$$

$$\frac{d\bar{\varepsilon}^P}{d\bar{t}}\,23 = \beta\,\bar{N}(7/126)\,\bar{s}_{23}, \tag{3.29e}$$

$$\frac{d\bar{\varepsilon}^P}{d\bar{t}}\,33 = \beta\,\bar{N}(1/21)\,[\bar{s}_{33} - (5/6)\,\bar{s}_{11} - (1/6)\,\bar{s}_{22}], \tag{3.29f}$$

for $f_{\underset{\sim}{\varepsilon}}$ given by (3.25b), and

$$\frac{d\bar{\varepsilon}^P}{d\bar{t}}\,11 = \beta\,N[(1/14)\bar{s}_{11} - (3/70)\bar{s}_{22} - (1/35)\bar{s}_{33} - (3/112)\bar{s}_{23}], \tag{3.30a}$$

$$\frac{d\bar{\varepsilon}^P}{d\bar{t}}\,12 = \beta\,\bar{N}[(4/35)\,\bar{s}_{12} - (39/2240)\,\bar{s}_{13}], \tag{3.30b}$$

$$\frac{d\bar{\varepsilon}^P}{d\bar{t}}\,13 = \beta\,\bar{N}[(13/140)\,\bar{s}_{13} - (39/2240)\,\bar{s}_{12}], \tag{3.30c}$$

$$\frac{d\bar{\varepsilon}^P}{d\bar{t}}\,22 = \beta\,\bar{N}[(1/14)\,\bar{s}_{22}-(1/35)\,\bar{s}_{33}-(3/70)\,\bar{s}_{11}-(3/560)\,\bar{s}_{23}], \tag{3.30d}$$

$$\frac{d\bar{\varepsilon}^P}{d\bar{t}}\,23 = \beta\,\bar{N}[(13/140)\,\bar{s}_{23}-(3/224)\,\bar{s}_{11}-(3/1120)\,\bar{s}_{22}-(9/560)\,\bar{s}_{33}], \tag{3.30e}$$

$$\frac{d\bar{\varepsilon}^P}{d\bar{t}}\,33 = \beta\,\bar{N}[(2/35)\,\bar{s}_{33}-(1/35)\,\bar{s}_{11}-(1/35)\,\bar{s}_{22} + (9/280)\,\bar{s}_{23}], \tag{3.30f}$$

for $f_{\underset{\sim}{\varepsilon}}$ given by (3.25c).

Equations (3.28) clearly indicate that the plastic strain rate is isotropic in this case. This is just the behavior that would be expected for a polycrystalline sample in which the dislocations are uniformly distributed over all glide systems and all glide systems are equally probable. The form of equations (3.29), on the other hand, can be seen to be consistent with the definition of orthotropic behavior. As in the isotropic case, the principal axes of stress coincide with those of the plastic strain rate. The dependence of the principal plastic strain rates on the principal stresses, however, does not exhibit the symmetry characteristic of isotropy. Finally, although equations (3.30) do possess some symmetry, the presence of tensile stress terms in the expression for $d\bar{\varepsilon}^P_{23}/d\bar{t}$ clearly implies that the plastic strain rate exhibits anisotropic behavior in this case.

For other than the linear stress-speed relation just considered, the integrals in (3.24) cannot be easily evaluated except by numerical means. We therefore make use of the results expressed in (3.22) to

compute the plastic strain rate for more complicated stress-speed relations. As examples we have chosen the power function (3.26) with n = 3, 5, 11, 21, and 51. Odd integer powers have been chosen for computational economy while illustraing the behavior as n becomes large (since using (2.51) with $n \simeq 10 - 50$ seems to fit the data for many metals well). If n is an odd integer greater than zero,

$$\zeta\, \bar{v} = (\mu_{ij}\, \bar{s}_{ij})^n = [(\mu_{11} - \mu_{33})\, \bar{s}_1 + (\mu_{22} - \mu_{33})\, \bar{s}_2]^n, \tag{3.31}$$

where $\bar{s}_1$ and $\bar{s}_2$ are the principal components of the normalized stress deviator. This result can be expanded by using the binomial theorem. Thus

$$\zeta\, \bar{v} = \sum_{r=o}^{n} \binom{n}{r} (\mu_{11} - \mu_{33})^{n-r} (\mu_{22} - \mu_{33})^r\, \bar{s}_1^{\,n-r}\, \bar{s}_2^{\,r}, \tag{3.32}$$

and we can write

$$\frac{d\bar{\varepsilon}^P}{d\bar{t}}{}_{ij} = \beta\, \bar{N} \sum_{r=o}^{n} C_{ij}^{nr}\, \bar{s}_1^{\,n-r}\, \bar{s}_2^{\,r}, \tag{3.33}$$

where the coefficients C_{ij}^{nr} are defined by the formula

$$C_{ij}^{nr} = (2\pi^3/n_1 n_2 n_3) \binom{n}{r} \sum_{k=1}^{n_3} \sum_{\ell=1}^{n_2} \sum_{m=1}^{n_1} \mu_{ij}(\chi_k, \phi_\ell, \theta_m)$$

$$[\mu_{11}(\chi_k, \phi_\ell, \theta_m) - \mu_{33}(\chi_k, \phi_\ell, \theta_m)]^{n-r} \cdot$$

$$\cdot\, [\mu_{22}(\chi_k, \phi_\ell, \theta_m) - \mu_{33}(\chi_k, \phi_\ell, \theta_m)]^r$$

$$f_{\underset{\sim}{\varepsilon}}(\chi_k, \phi_\ell, \theta_m) \sin\theta_m. \tag{3.34}$$

These coefficients need to be calculated only once. Equation (3.33) can then be used to compute $d\bar{\underset{\sim}{\varepsilon}}^P/d\bar{t}$ for arbitrary $\bar{s}_1$, $\bar{s}_2$, resulting in a considerable savings in computational effort.

A convenient means for comparing the plastic strain rates obtained with various stress-speed relations and dislocation system

distributions is the rate of plastic work, $w^P = tr(\underset{\sim}{\sigma}\,\dot{\underset{\sim}{\varepsilon}}^P)$. Equivalently, we can define a normalized rate of plastic work, $\bar{w}^P = tr(\bar{\underset{\sim}{\sigma}}\,\dot{\bar{\underset{\sim}{\varepsilon}}}^P)$, or, in terms of principal stresses,

$$\bar{w}^P = (\bar{\sigma}_1 - \bar{\sigma}_3)\dot{\bar{\varepsilon}}^P_{11} + (\bar{\sigma}_2 - \bar{\sigma}_3)\dot{\bar{\varepsilon}}^P_{22}. \tag{3.35}$$

Using equations (3.33) and (3.34) to calculate the plastic strain rate, we have computed $\bar{w}^P$ in a square in $(\bar{\sigma}_1-\bar{\sigma}_3),(\bar{\sigma}_2-\bar{\sigma}_3)$ space for $\bar{n}$ = 1, 3, 5, 11, 21, and 51, and for $f_{\underset{\sim}{\varepsilon}}$ given by (3.25a), (3.25b), and (3.25c). The results are shown in Figures 3 - 25, where we have plotted contours of constant plastic power dissipation (rate of plastic work). To faciliate comparison, the same contour values were used in all plots for a given $f_{\underset{\sim}{\varepsilon}}$.

Consider first the results for a uniform distribution of dislocations and glide systems (Figures 3 - 14). For small n, the contours closely approximate the von Mises yield surface in shape and, in fact, are identical to it for n = 1. As the value of n is increased, the contours move closer together and approach the yield surface of Tresca in shape. If we define the yield stress to be that state of stress at which the plastic power dissipation reaches a prescribed critical value, these contours correspond to possible yield surfaces.

The appearance of Tresca type surfaces as n is increased is due to the fact that for large values of n there is a signficant difference in dislocation speed between glide planes on which the shear stress is maximum and all other glide planes. Plastic flow is therefore dominated by the motion of dislocations on such planes resulting in Tresca type yielding. For small values of n, the dislocation speed is not so strongly dependent on glide plane orientation

and dislocation motion on a large number of glide planes will contribute significantly to the flow, thus resulting in von Mises type yielding. Behavior similar to this was also noted by Lin and Ito [13] based on a simpler model.

The large spacing of the contours for small n suggests a gradual increase in plastic strain rate with stress. This behavior is typical of such materials as artificial graphite [45]. The concentration of contours for large n, on the other hand, implies that there is a sharp increase in the plastic strain rate after yielding as is observed in tests on mild steels. To more clearly illustrate this behavior and its dependence on n, we have plotted the plastic power dissipation in perspective (Figures 9 - 14). Note that in all cases there is a flat area of essentially zero dissipation before yielding. This is followed by a rapid increase in $\bar{w}^p$ as the stress is increased. The rate of this increase, as well as the shape of the surface is seen to depend on n in the manner just discussed. The flat portion of the surface at the top is the result of putting limits on the plotting space and has no real significance.

The results for the cases when $f_{\underset{\sim}{\varepsilon}}$ is given by (3.25b) and (3.25c) shown in Figures 15 - 20 and 21 - 26, exhibit essentially the same behavior with respect to increasing n as was observed when $f_{\underset{\sim}{\varepsilon}}$ was given by (3.25a). The contours are somewhat distorted from these obtained for the previous cases, however, due to the anisotropic behavior pointed out in our analytic solutions for n = 1.

3.3 Behavior of the Constitutive Model Under Uniaxial Loading

In order to illustrate the type of material behavior our theory is capable of modeling, we consider three examples using uniaxial

stress deformation under the assumption of homogeneous strain. They are (i) a constant strain rate test, (ii) a stress relaxation test, and (iii) cyclic loading at constant strain rate magnitude. These examples have the advantage of demonstrating the essential features of the model while maintaining a reasonable degree of computational simplicity.

For uniaxial loading under homogeneous strain, equations (3.15) and (3.18) reduce to

$$\frac{d\bar{\varepsilon}^P}{d\bar{t}} = \frac{1}{4\pi^2} \int_{-\pi}^{+\pi} \int_{-\pi}^{+\pi} \int_{0}^{\pi/2} \mu_{11}\ \zeta\ \bar{v}\ \beta\ \bar{N}(1-\bar{N}) \sin\theta\ d\theta\ d\phi\ d\chi \tag{3.36}$$

and

$$\frac{d\bar{\sigma}}{d\bar{t}} = \frac{d\bar{\varepsilon}}{d\bar{t}} - \frac{d\bar{\varepsilon}^P}{d\bar{t}} \tag{3.37}$$

respectively, where we have assumed that all glide planes and all Burger's vector orientations are equally probable. In addition, the dislocation speed relation for our sample material, which we again take to be the empirical power law, simplifies to

$$\bar{v} = |\mu_{11}\ \bar{\sigma}|^n. \tag{3.38}$$

In order to maintain a uniaxial state of stress during isochoric plastic deformation, the distribution of dislocation systems must possess certain symmetries throughout the deformation. This implies that we can take N and β to be independent of the orientation angles χ, ϕ, and θ. One way to ensure this independence and the required symmetry is to let $\bar{N}$ and β be initially uniformly distributed and replace $\bar{v}$ in equations (3.16) and (3.17) by its average value,

$$\langle \bar{v} \rangle = (1/4\ \pi^2) \int_{-\pi}^{+\pi} \int_{-\pi}^{+\pi} \int_{0}^{\pi/2} \bar{v}\ \sin\theta\ d\theta\ d\phi\ d\chi. \tag{3.39}$$

This yields the following set of nonlinear ordinary differential equations characterizing uniaxial plastic deformation:

$$\frac{d\bar{\varepsilon}^P}{d\bar{t}} = C_\varepsilon \; \beta \; \bar{N}(1-\bar{N}) \; \bar{\sigma}|\bar{\sigma}^{n-1}|, \tag{3.40}$$

$$\frac{d\bar{N}}{d\bar{t}} = A \; C_v \; \beta \; \bar{N}(1-\bar{N})|\bar{\sigma}^n|, \tag{3.41}$$

$$\frac{d\beta}{d\bar{t}} = A \; C_v \; \beta[\beta^* - \beta(1 + B^* \; \bar{N})]|\bar{\sigma}^n|, \tag{3.42}$$

$$\frac{d\bar{\sigma}}{d\bar{t}} = \frac{d\bar{\varepsilon}}{d\bar{t}} = \frac{d\bar{\varepsilon}^P}{d\bar{t}}, \tag{3.37}$$

where we have substituted (3.38) for $\bar{v}$ and the coefficients C_ε and C_v are defined by

$$C_\varepsilon = (1/4 \; \pi^2) \int_{-\pi}^{+\pi} \int_{-\pi}^{+\pi} \int_{0}^{\pi/2} |\mu_{11}^{n+1}| \; \sin\theta \; d\theta \; d\phi \; d\chi \tag{3.43}$$

and $$C_v = (1/4 \; \pi^2) \int_{-\pi}^{+\pi} \int_{-\pi}^{+\pi} \int_{0}^{\pi/2} |\mu_{11}^{n}| \; \sin\theta \; d\theta \; d\phi \; d\chi \tag{3.44}$$

respectively. For our examples, the integrals in these expressions were evaluated using the quadrature scheme given in Section 3.1 and the differential equations were solved numerically using a routine based on Gear's method [46, 47].

Figures 27 - 29 show typical results for constant strain rate tests. In Figure 27 we have plotted the normalized stress, $\bar{\sigma}$, versus the normalized strain, $\bar{\varepsilon}$, for various values of normalized strain rate, $d\bar{\varepsilon}/d\bar{t}$. These results clearly show a rate sensitivity with higher stresses prevailing for a given value of strain at higher strain rates. A yield drop is also observed with the magnitude of the drop increasing with increasing strain rate. In Figure 28

curves for the same strain rate values are plotted for a material with the same parameters as those used in Figure 27 but a higher initial dislocation density. Comparison of these curves with the previous ones shows that the yield drop has decreased but the rest of the curve has remained unchanged. This indicates that the yield drop is due mainly to the magnitude of the initial dislocation density, N_o, relative to N^*. When N_o/N^* is small the dislocation density initially increases much faster than the plastic strain. This produces a cascade effect which results in the yield drop. Finally, in Figure 29 we show the variation in results that can be obtained by changing some of the parameter in equations (3.40)-(3.42). Among other things we note that the yield drop is also affected by the value of B^*, which controls the rate of hardening, and the exponent in the dislocation speed relation.

In a stress relaxation experiment, the material is subjected to an instantaneously applied strain, ε_o, which is maintained constant. The initial stress is given by the elastic response of the material and relaxes by relief of elastic strain as plastic strain accumulates. In Figure 30, we have plotted curves of normalized stress, $\bar{\sigma}$, versus normalized time, $\bar{t}$, for several values of normalized strain, $\bar{\varepsilon}_o$. For values of $\bar{\varepsilon}_o$ below approximately 3 the stress initially decays very slowly. At the smaller values of $\bar{\varepsilon}_o$ the dislocation density increases rather slowly. If the initial dislocation density is small, as it is in this case, it takes a certain amount of time for it to build up to a value at which the plastic strain rate becomes significant. Thus we observe an initial slow decay followed by a rapid quasi-exponential decay when the dislocation density builds up. Figure 31

shows the same curves for a material with a larger initial dislocation density. In this case, however, all curves have the expected behavior in that the stress decays exponentially with time.

For the case of cyclic loading, we take the total strain rate to be given by the equation

$$d\bar{\varepsilon}/d\bar{t} = r_1 \operatorname{sgn}[\cos(\pi r_1 \bar{t}/2r_2)], \tag{3.45}$$

where sgn denotes the signum function, which is plus or minus unity according to the sign of its argument. This expression yields a constant magnitude of r_1 for the applied strain rate and a constant amplitude of r_2 for the applied strain cycle. In Figures 32 - 34 we have plotted normalized stress versus normalized strain for three cycles with $r_1 = 10$ and $r_2 = 20$. The first plot is for a material with a small initial dislocation density. It exhibits a yield drop followed by softening and finally by hardening. When the initial dislocation density is increased, as shown in Figure 33, the yield drop is eliminated along with the initial softening. This behavior is similar to that observed by Kelly and Gillis [48] in their recent work on cyclic loading. Figure 34 demonstrates the behavior obtained when a fraction of the immobile dislocations become mobile at each strain rate reversal. As can be seen, the stress decreases sharply when this occurs. This behavior is consistent with recently reported experimental work on single crystals [49].

IV. CONCLUSIONS

Using arguments based directly on the dislocation processes involved, we have derived a set of constitutive equations for polycrystalline plasticity that is fully consistent with thermodynamic requirements. The idea of randomly distributed glide plane orientations and Burger's vector directions has been introduced to facilitate handling of the polycrystalline structure. This avoids the awkward dislocation arrangement tensors associated with the statistical dislocation theory proposed by Kröner [23] as well as the necessity of knowing a priori the available glide systems at each material point for all times of interest. Instead we obtain equations involving probability distributions for variables which are directly related to measurable dislocation quantities.

In our initial derivation of the plastic strain rate equation we consider both conservative and non-conservative motions of arbitrary dislocations (i.e., they can be edge, screw, or mixed). Non-conservative motions however, are rare at normal temperatures. Hence we restrict our final analysis to conservative motions only, i.e. pure glide. For this case it is shown that the tensorial character of the macroscopic plastic strain rate can be attributed entirely to a second rank symmetric tensor, $\underset{\sim}{\mu}$, directly related to the ordinary elements of crystallographic glide and independent of the edge or screw character of the dislocations.

The evolutionary equations for the dislocation density and the mobile fraction are based on single and pair-wise dislocation processes. These include production by fixed sources (such as

Frank-Read sources), breeding by cross-glide multiplication, immobilization of dislocations by inclusions and other dislocations, and pair annihilation. As a result of the inclusion of annihilation events, the equations obtained allow for the occurrence of such phenomena as saturation of the dislocation density. In other theories, e.g. Kelly and Gillis [11], this has been included only by using additional assumptions.

Simplified forms of these evolutionary equations have been developed for the case when production by fixed sources is unimportant and the mobile fraction is small. As this is the usual situation, these simplified equations are probably adequate for most cases. Moreover, it has been shown that an analytic expression for the mobile fraction in terms of the dislocation density can be obtained in this case, provided that the equation coefficients are independent of β and time. If these coefficients are also independent of N, this expression has been shown to reduce to the exponential form suggested by Gilman [16] in the limit of zero probability for annihilation events.

Because of the importance of the dislocation velocity to the evolutionary equations for N and β, we have included a brief discussion of the stress and temperature dependence of this quantity. Resistance to dislocation motion is assumed to be controlled by activation past fixed obstacles and viscous glide through a clear lattice. Two different activation models have been considered, (1) thermal activation, and (2) tunneling. After modification to account for relativistic effects, the thermal activation model with an athermal back stress is shown to

yield essentially the same results as the tunneling model.

In order to further correlate our theory with results obtained from thermodynamics, we have developed an expression for the energy stored in the crystal lattice as a result of the presence of dislocations. This represents the fraction of the total plastic work that could ultimately be recovered if the dislocations were removed. The expression obtained assumes that the dislocations are uniformly distributed between edge and screw types and that the crystal matrix is isotropic and linearly elastic. It requires that the stored energy increase with increasing plastic deformation, but at a slower rate, as is observed experimentally.

Using our plastic strain rate equation, characteristic yield conditions have been computed for three sample dislocation probability density functions. For simplicity, the dislocation speed was assumed to be given by the empircal power law and thermal effects were ignored. When the stress-speed relationship is linear, we have been able to evaluate the integrals in the plastic strain rate equation analytically. The solutions obtained clearly show the ability of our theory to model the development of plastic anisotropy. For higher powers in the stress-speed relation we must resort to numerical methods to evaluate the integrals involved and we have suggested a particularly efficient quadrature formula for this purpose. It has Gaussian precision but uses equal weights and equally spaced abscissas in the random variables χ, ϕ, and θ. Plots of the calculated yield surfaces show that the shape varies from that of von Mises at small exponent values to that of Tresca at large exponent values. This be-

havior has been attributed to the fact that at large exponent values the stress-speed relation has a strong orientation dependence. This makes the dislocation speed very large on glide planes close to those with maximum shear stress and negligible on all others. Hence only a few glide planes contribute to the plastic flow in this case giving a Tresca type surface. This variation in the shape of the surfaces with exponent value has also been shown to be relatively independent of the isotropy of the dislocation probability distribution.

To demonstrate the utility of our theory we have examined several examples of uniaxial stress deformation. These examples, which consist of constant strain rate, stress relaxation, and cyclic loading tests, show that our theory can qualitatively model most observed one-dimensional results. These include the occurrence of upper and lower yield points, material hardening and softening, Bauschinger effect, and strain rate sensitivity. Among other things, it has been shown that the occurrence of a yield drop in the constant strain rate test and a delay time in the stress relaxation test are particularly sensitive to the initial dislocation density relative to the saturation density.

With regard to further developments of this theory, we believe that identification of the probability density functions involved is probably the most important. To do this properly non-uniform three-dimensional experiments would have to be performed. A numerical identification scheme such as that proposed by Iding [50] could then be used to obtain parameter values. In lieu of this, a simple tension-torsion test could possibly provide an iden-

tification for some of the structure of the distributions.

REFERENCES

1. C. Truesdell and W. Noll, The Nonlinear Field Theories of Mechanics, in: S. Flugge (ed.), Encyclopedia of Physics, Vol. III, Pt. 3 (Springer-Verlag DHG, Berlin) 1965.
2. A. E. Green and P. M. Naghdi, A General Theory of an Elastic-Plastic Continuum, Arch. Ration. Mech. Anal. 18 (1965) 251-281.
3. A. E. Green and P. M. Naghdi, A Thermodynamic Development of Elastic-Plastic Continua, in: H. Parkus and L. I. Sedov (eds.), IUTAM Symposia on Irreversible Aspects of Continuum Mechanics and Transfer of Physical Characteristics in Moving Fluids, Vienna (Springer-Verlag) 1966, 117-131.
4. E. H. Lee and D. T. Liu, Finite Strain Elastic-Plastic Theory with Applications to Plane-Wave Analysis, J. Appl. Phys. 38 (1967) 19-27.
5. A. C. Pipkin and R. S. Rivlin, Mechanics of Rate-Independent Materials, Z. Angew. Math. Phys. 16 (1965) 313-327.
6. P. Perzyna and W. Wojno, Thermodynamics of Rate Sensitive Plastic Material, Arch. Mech. Stos. 20 (1968) 499-511.
7. J. Kratochvil and O. W. Dillon, Jr., Thermodynamics of Elastic-Plastic Materials as a Theory with Internal State Variables, J. Appl. Phys. 40 (1968) 3207-3218.
8. W. S. Tseng, A Constitutive Theory for Elastic-Plastic Crystalline Simple Solids, Ph.D. Dissertation, Graduate Division, Univ. of Calif. (Berkeley) 1971.
9. H. T. Hahn and W. Jaunzemis, A Dislocation Theory of Plasticity, Int. J. Eng. Sci. 11 (1973) 1065-1078.

10. D. R. Bhandari and J. T. Oden, A Unified Theory of Thermoviscoplasticity of Crystalline Solids, Int. J. Non-Linear Mech. 8 (1973) 261-277.

11. J. M. Kelly and P. P. Gillis, Thermodynamics and Dislocation Mechanics, J. Franklin Inst. 297 (1974) 59-73.

12. G. I. Taylor, Strains of Crystalline Aggregates, Proc. Colloq. on Deformation and Flow in Solids (1956) 3-12.

13. T. H. Lin and Y. M. Ito, Theoretical Plastic Stress-Strain Relationship of a Polycrystal and Comparison with von Mises' and Tresca's Plasticity Theories, Int. J. Eng. Sci. 4 (1966) 543-561.

14. T. H. Lin, Physical Theory of Plasticity, in: Chia-Shun Yih (ed.), Advances in Applied Mechanics, Vol. 11 (Academic Press, New York) 1971, 255-311.

15. T. Mura, Generalized Stress-Strain Laws Developed by Dislocation Theory, Proc. Metallurgical Society of AIME, Work Hardening, Vol. 46 (Gordon and Breach) 1968, 141-149.

16. J. J. Gilman, Micro Mechanics of Flow in Solids (McGraw-Hill, New York) 1969, 157-242.

17. J. M. Kelly and P. P. Gillis, On a Thermodynamic Basis of Viscoplasticity Using Dislocation Mechanics, unpublished research, 1970.

18. B. D. Coleman and M. E. Gurtin, Thermodynamics with Internal State Variables, J. Chem. Phys. 47 (1967) 597-613.

19. J. J. Gilman, Physical Nature of Plastic Flow and Fracture, in: E. H. Lee and P. S. Symonds (eds.), Proc. Second Sym. Naval Struc. Mech., Plasticity (Pergammom Press) 1960, 43-99.

20. A. L. Tichener and M. B. Bever, The Stored Energy of Cold Work, Prog. Metal Phys. 7 (1958) 247-338.

21. B. A. Bilby, Continuous Distributions of Dislocations, in: I. N. Sneddon and R. Hill (eds.), Progress in Solid Mechanics, Vol. 1 (North Holland, Amsterdam) 1960.

22. T. Mura, On Dynamic Problems of Continuous Distribution of Dislocations, Int. J. Eng. Sci. 1 (1963) 371-381.

23. E. Kröner, Initial Studies of a Plasticity Theory Based Upon Statistical Mechanics, Colloq. on Inelastic Behavior of Solids, Battelle Memorial Inst., Columbus, Ohio, Sept. 1968.

24. J. J. Gilman, Progress in the Microdynamical Theory of Plasticity, Proc. Fifth U. S. Cong. Appl. Mech., ASME, New York (1966) 385-403.

25. J. N. Johnson, Constitutive Relation for Rate-Dependent Plastic Flow in Polycrystalline Metals, J. Appl. Phys. 40 (1969) 2287-2293.

26. R. B. Clough and J. A. Simmons, A Theory of Multiaxial Plasticity Based on Integral Dislocation Dynamics, Acta Met. 22 (1974) 513-521.

27. J. Weertman and J. R. Weertman, Elementary Dislocation Theory (Macmillan, New York) 1964, 15.

28. J. C. M. Li, Cross Slip and Cross Climb of Dislocations Induced by a Locked Dislocation, J. Appl. Phys. 32 (1961) 593-599.

29. W. G. Johnston and J. J. Gilman, Dislocation Multiplication in Lithium Flouride Crystals, J. Appl. Phys. 31 (1960) 632-643.

30. A. R. Rosenfield, G. T. Hahn, A. L. Bement, and R. L. Jaffee,

Dislocation Dynamics (McGraw-Hill, New York) 1968.

31. W. G. Johnston and J. J. Gilman, Dislocation Velocities, Dislocation Densities, and Plastic Flow in Lithium Flouride Crystals, J. Appl. Phys. 30 (1959) 129-144.

32. J. A. Gorman, D. S. Wood, and T. Vreeland, Jr., Mobility of Dislocations in Aluminum, J. Appl. Phys. 40 (1969) 833-841.

33. A. V. Granato and K. Lucke, Application of Dislocation Theory to Internal Friction Phenomenon at High Frequencies, J. Appl. Phys. 27 (1956) 789-805.

34. J. S. Koehler, Imperfections in Nearly Perfect Crystals (Wiley, New York) 1952.

35. J. J. Gilman, Escape of Dislocations from Bound States by Tunneling, J. Appl. Phys. 39 (1968) 6086-6090.

36. D. H. Klahn, Dislocation Modeling of Strain Rate Phenomena, Report no. LBL-800, Lawrence Berkeley Laboratory, University of Calif., Berkeley, 1972.

37. J. W. Taylor, Hypervelocity Impact Phenomena (Academic Press, New York) 1968.

38. A. Foreman and M. Makin, Dislocation Movement Through Random Arrays of Obstacles, Phil. Mag. 14 (1966) 911-924.

39. P. P. Gillis, J. J. Gilman, and J. W. Taylor, Stress Dependences of Dislocation Velocities, Phil. Mag. 20 (1969) 279-289.

40. J. J. Gilman, Dislocation Mobility in Crystals, J. Appl. Phys. 36 (1965) 3195-3206.

41. J. D. Campbell and K. J. Marsh, The Effect of Grain Size on the Delayed Yielding of Mild Steel, Phil. Mag. 7 (1962) 933.

42. J. P. Hirth and J. Lothe, Theory of Dislocations (McGraw-Hill, New York) 1968, 87.

43. A. Wolfender, The Energy Relations in Room Temperature Deformation of Aluminum Single Crystals, Scripta Metallurgica 3 (1969) 709.

44. C. Froberg, Introduction to Numerical Analysis (Addison-Wesley) 1969, 213-216.

45. W. L. Greenstreet and A. Phillips, A Theory of an Elastic-Plastic Continuum with Special Emphasis to Artificial Graphite, Acta Mechanica 16 (1973) 143-156.

46. A. C. Hindmarsh, Linear Miltistep Methods for Ordinary Differential Equations: Method Formulations, Stability, and the Methods of Nordsieck and Gear, Report no. UCRL-51186, Rev. 1, Lawrence Livermore Laboratory, Univ. of Calif., Livermore,1972.

47. A. C. Hindmarsh, GEAR: Ordinary Differential Equation System Solver, Report no. UCID-30001, Rev. 1, Lawrence Livermore Laboratory, Univ. of Calif., Livermore, 1972.

48. J. M. Kelly and P. P. Gillis, Continuum Descriptions of Dislocations Under Stress Reversals, J. Appl. Phys. 45 (1974) 1091-1096.

49. R. Stevenson and J. B. Vander Sande, The Cyclic Deformation of Magnesium Single Crystals, Acta Metallurgica, 22 (1974) 1079-1086.

50. R. H. Iding, Identifiction of Nonlinear Materials by Finite Element Methods, Ph.D. Dissertation, Graduate Division, Univ. of Calif. (Berkeley) 1973.

Transformation from global coordinates (x_1, x_2, x_3) to local coordinates (y_1, y_2, y_3) can be accomplished by a sequence of three rotations:

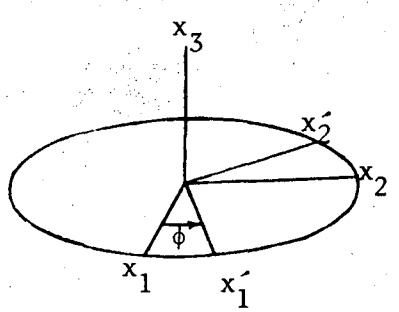

$$\underset{\sim}{D} = \begin{bmatrix} \cos\phi & \sin\phi & 0 \\ -\sin\phi & \cos\phi & 0 \\ 0 & 0 & 1 \end{bmatrix}$$

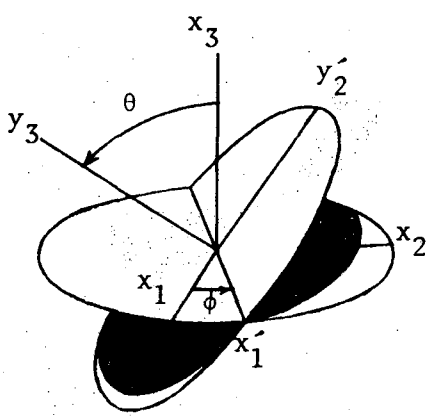

$$\underset{\sim}{C} = \begin{bmatrix} 1 & 0 & 0 \\ 0 & \cos\theta & \sin\theta \\ 0 & -\sin\theta & \cos\theta \end{bmatrix}$$

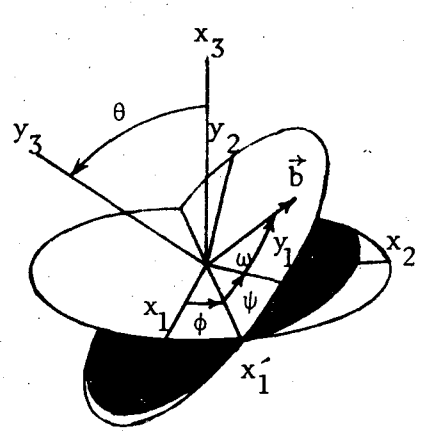

$$\underset{\sim}{B} = \begin{bmatrix} \cos\psi & \sin\psi & 0 \\ -\sin\psi & \cos\psi & 0 \\ 0 & 0 & 1 \end{bmatrix}$$

$$\underset{\sim}{A} = \underset{\sim}{B}\,\underset{\sim}{C}\,\underset{\sim}{D}$$

Since rotations are orthogonal transformation, the inverse transformation, from local to global coordinates, is $\underset{\sim}{a} = \underset{\sim}{A}^{-1} = \underset{\sim}{A}^{T}$.

Fig. 1

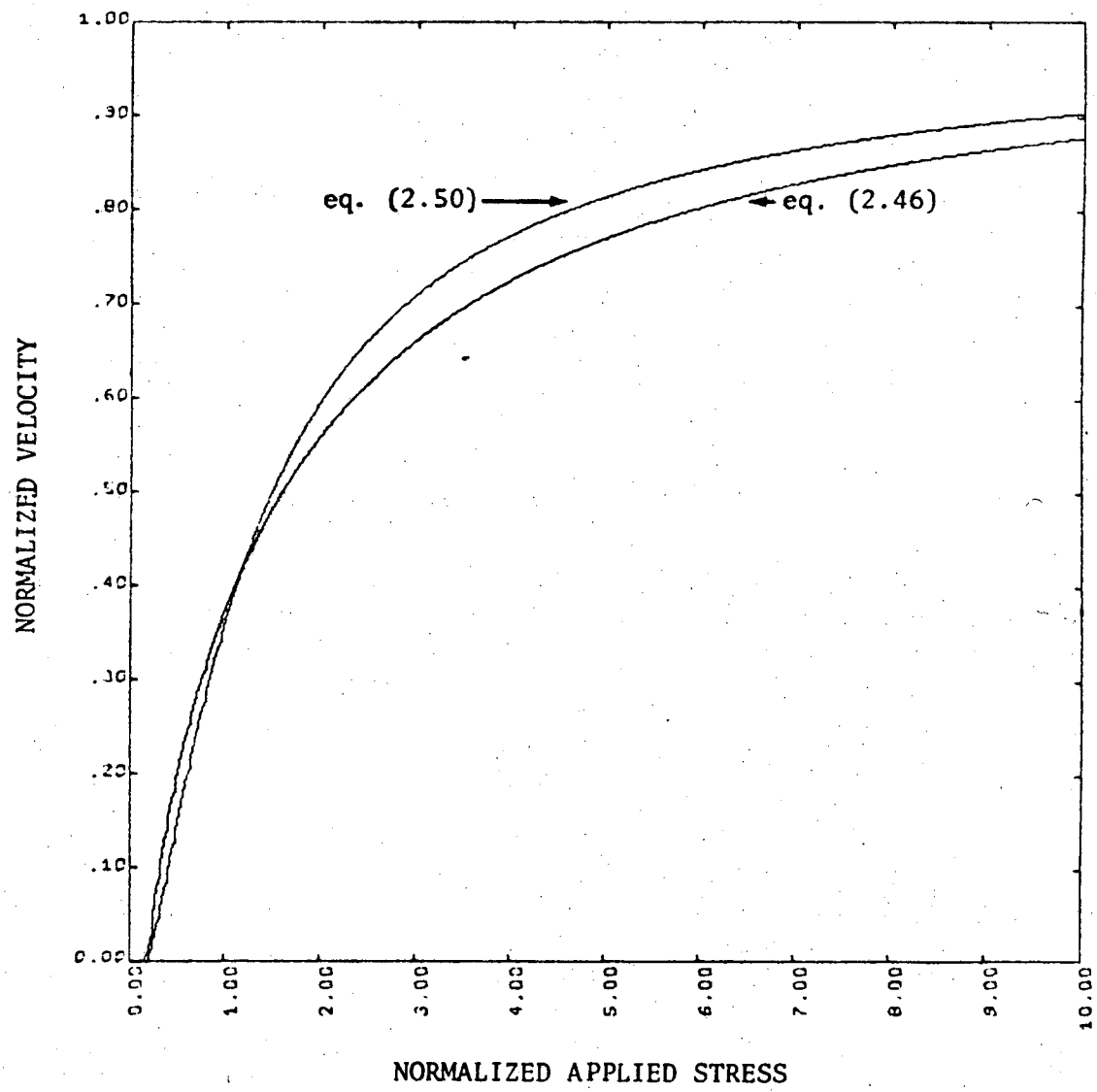
1.00
.90
.80
.70
.60
.50
.40
.30
.20
.10
0.00
NORMALIZED VELOCITY
eq. (2.50)
eq. (2.46)
0.00
1.00
2.00
3.00
4.00
5.00
6.00
7.00
8.00
9.00
10.00
NORMALIZED APPLIED STRESS

Fig. 2

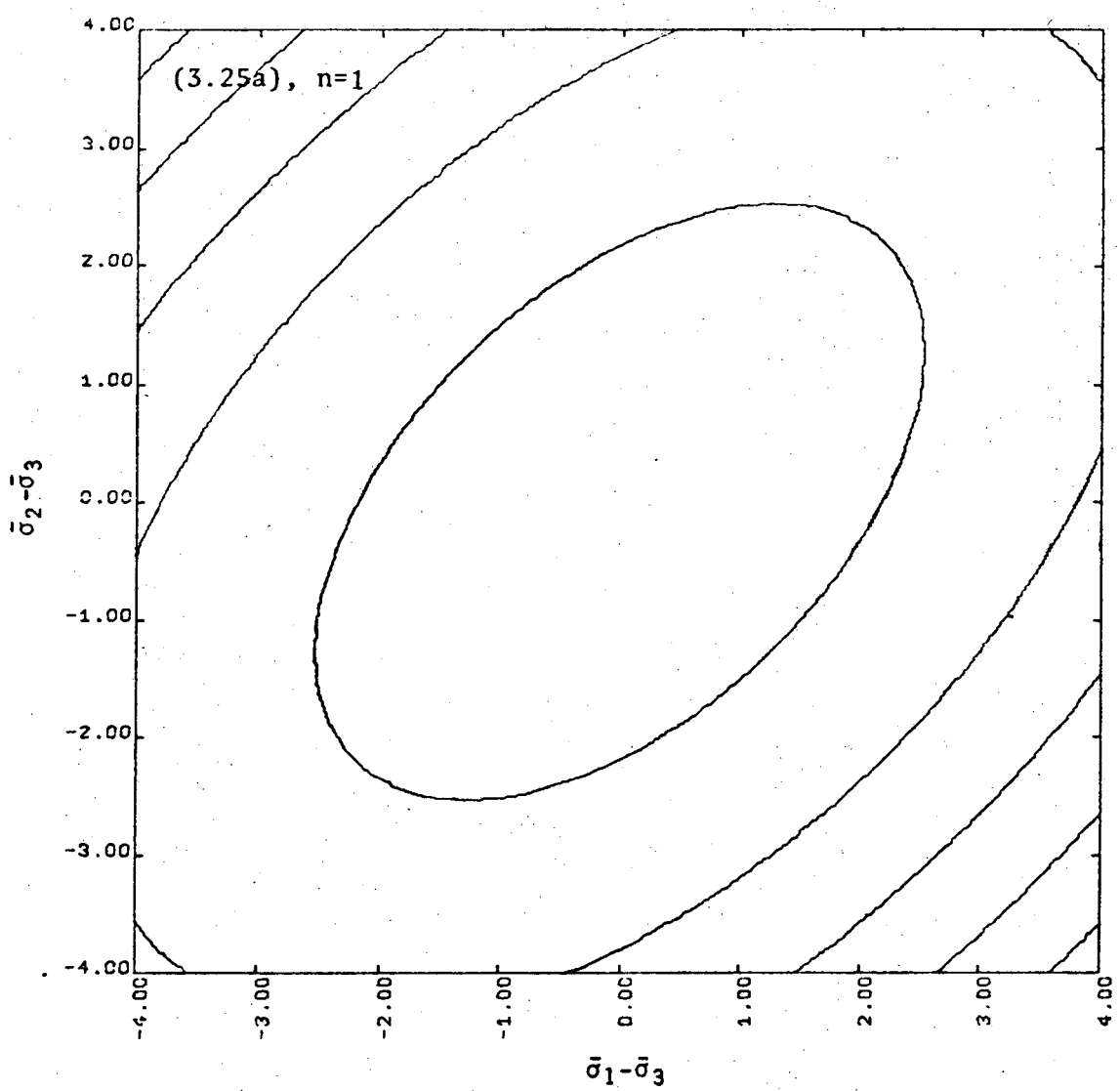
(3.25a), n=1
4.00
3.00
2.00
1.00
0.00
-1.00
-2.00
-3.00
-4.00
$\bar{\sigma}_2-\bar{\sigma}_3$
-4.00
-3.00
-2.00
-1.00
0.00
1.00
2.00
3.00
4.00
$\bar{\sigma}_1-\bar{\sigma}_3$

Fig. 3

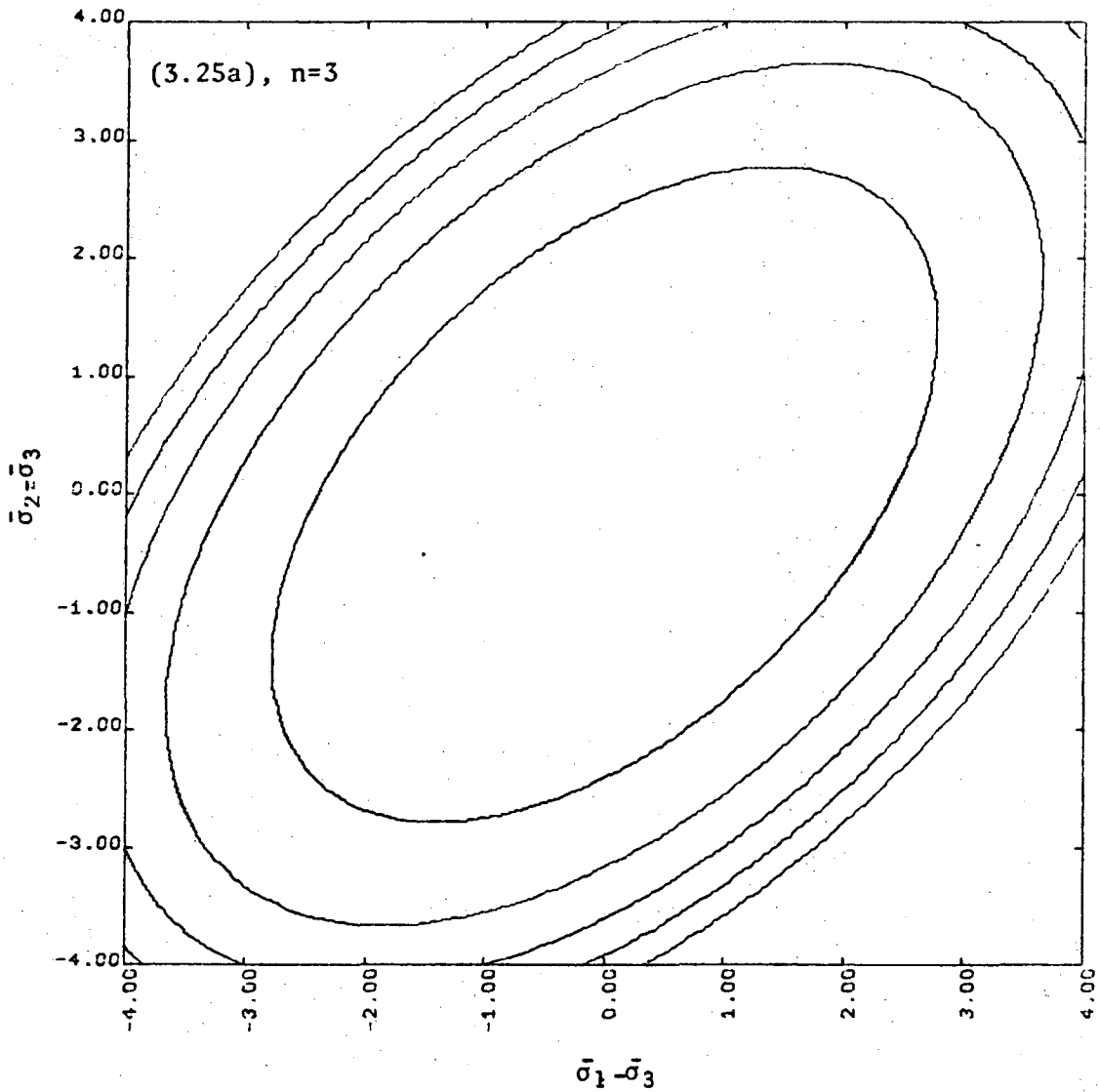
(3.25a), n=3
4.00
3.00
2.00
1.00
0.00
-1.00
-2.00
-3.00
-4.00
$\bar{\sigma}_2 = \bar{\sigma}_3$
-4.00
-3.00
-2.00
-1.00
0.00
1.00
2.00
3.00
4.00
$\bar{\sigma}_1 - \bar{\sigma}_3$

Fig. 4

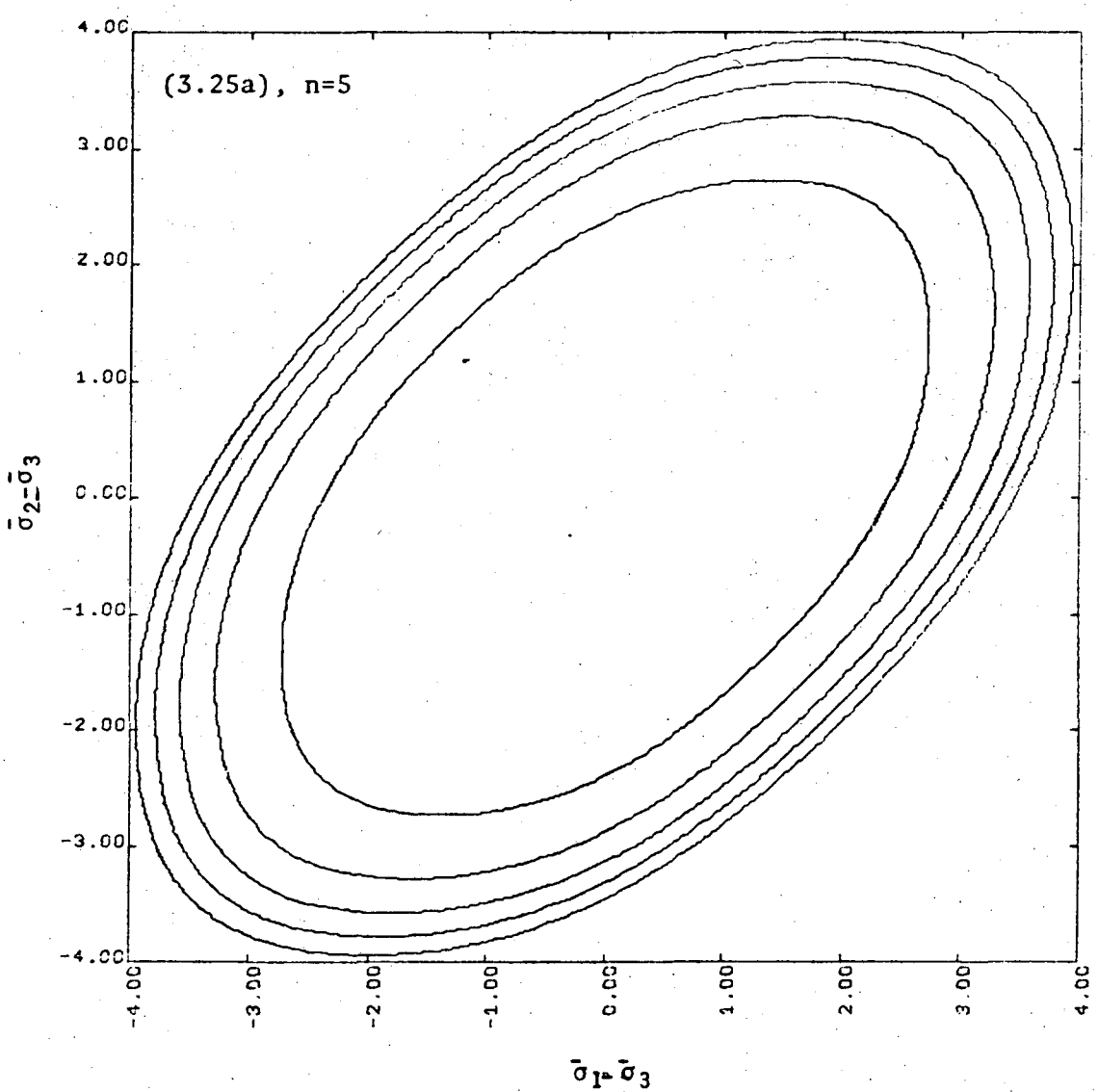
(3.25a), n=5
4.00
3.00
2.00
1.00
0.00
-1.00
-2.00
-3.00
-4.00
$\bar{\sigma}_2-\bar{\sigma}_3$
-4.00
-3.00
-2.00
-1.00
0.00
1.00
2.00
3.00
4.00
$\bar{\sigma}_1-\bar{\sigma}_3$

Fig. 5

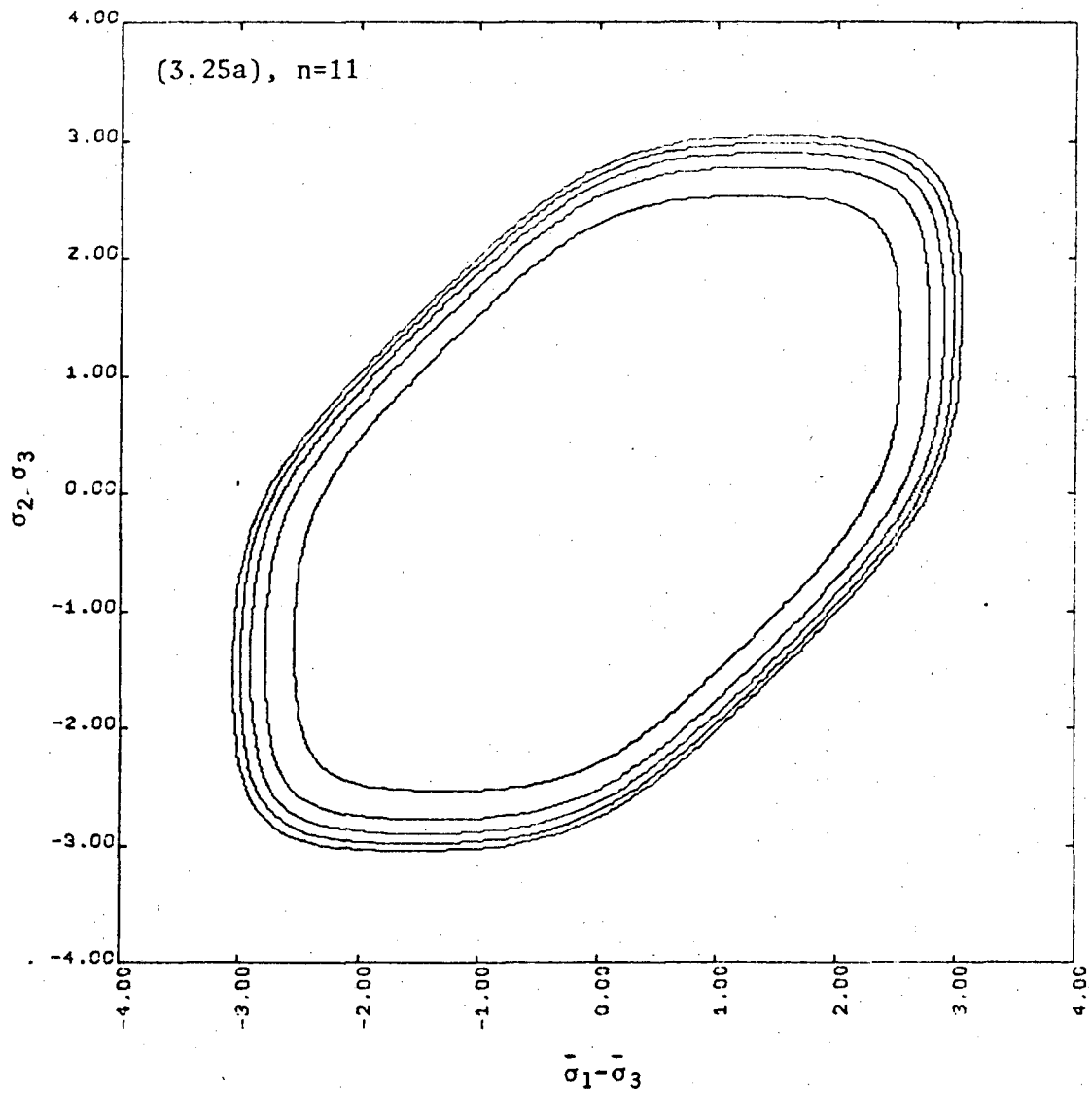
(3.25a), n=11
4.00
3.00
2.00
1.00
0.00
-1.00
-2.00
-3.00
-4.00
$\sigma_2 - \sigma_3$
-4.00
-3.00
-2.00
-1.00
0.00
1.00
2.00
3.00
4.00
$\bar{\sigma}_1 - \bar{\sigma}_3$

Fig. 6

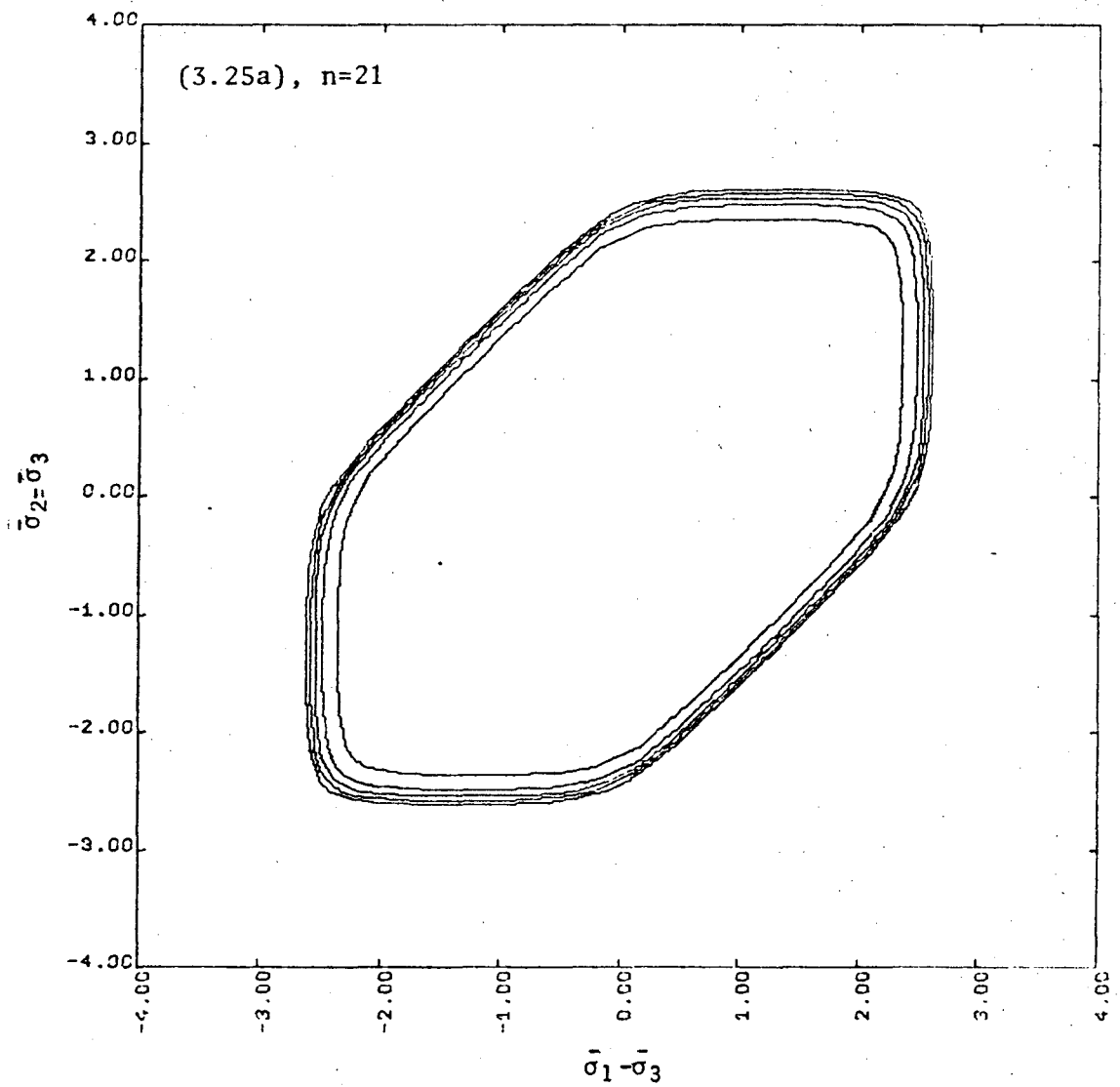
(3.25a), n=21
4.00
3.00
2.00
1.00
0.00
-1.00
-2.00
-3.00
-4.00
-4.00
-3.00
-2.00
-1.00
0.00
1.00
2.00
3.00
4.00
$\bar{\sigma}_2 = \bar{\sigma}_3$
$\bar{\sigma}_1 - \bar{\sigma}_3$

Fig. 7

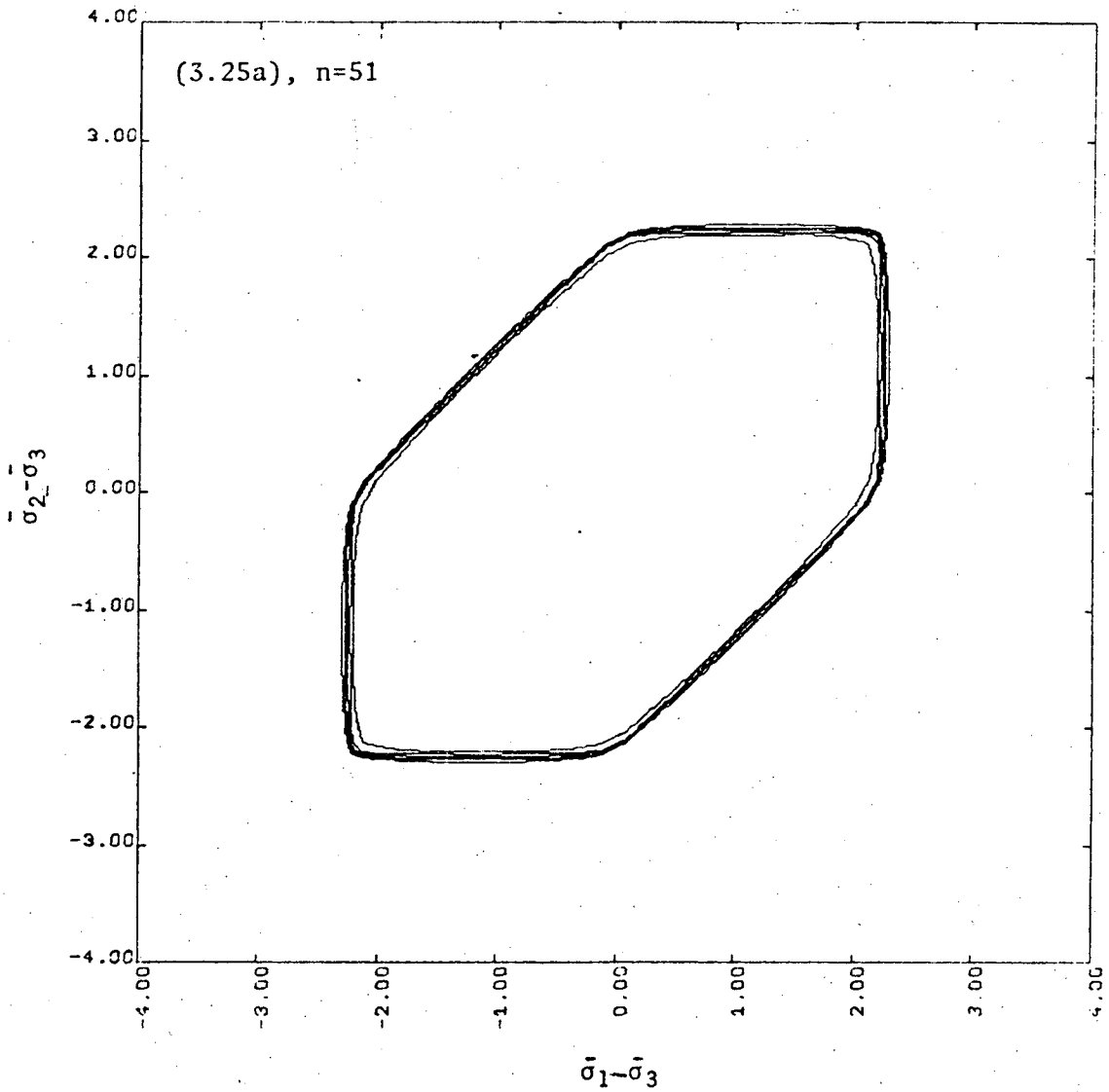
(3.25a), n=51
4.00
3.00
2.00
1.00
0.00
-1.00
-2.00
-3.00
-4.00
-4.00
-3.00
-2.00
-1.00
0.00
1.00
2.00
3.00
4.00
$\bar{\sigma}_2-\bar{\sigma}_3$
$\bar{\sigma}_1-\bar{\sigma}_3$

Fig. 8

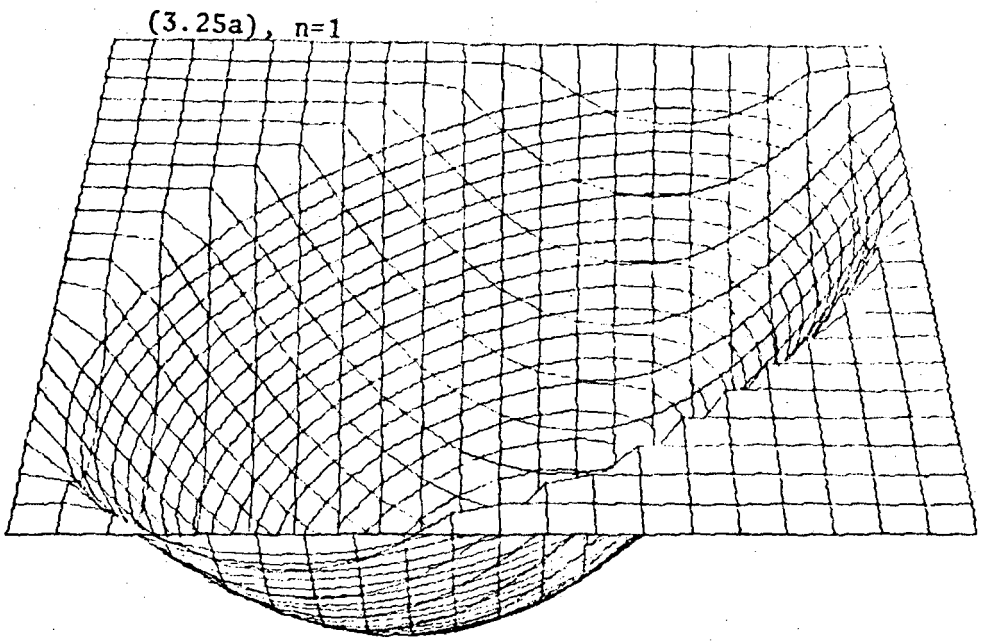

Fig. 9

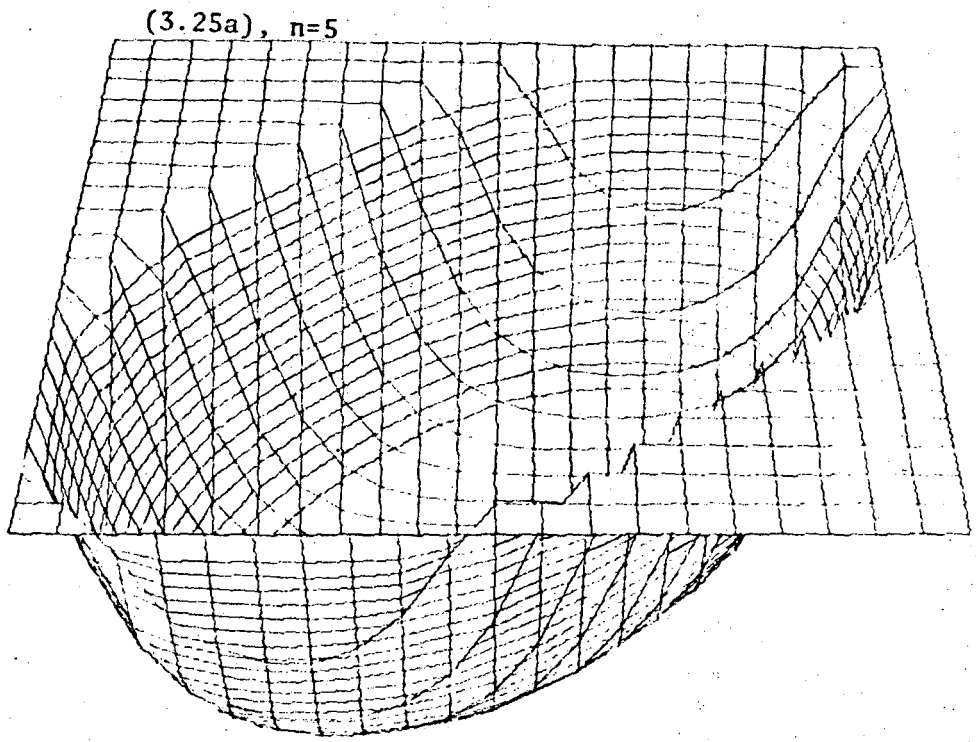

Fig. 11

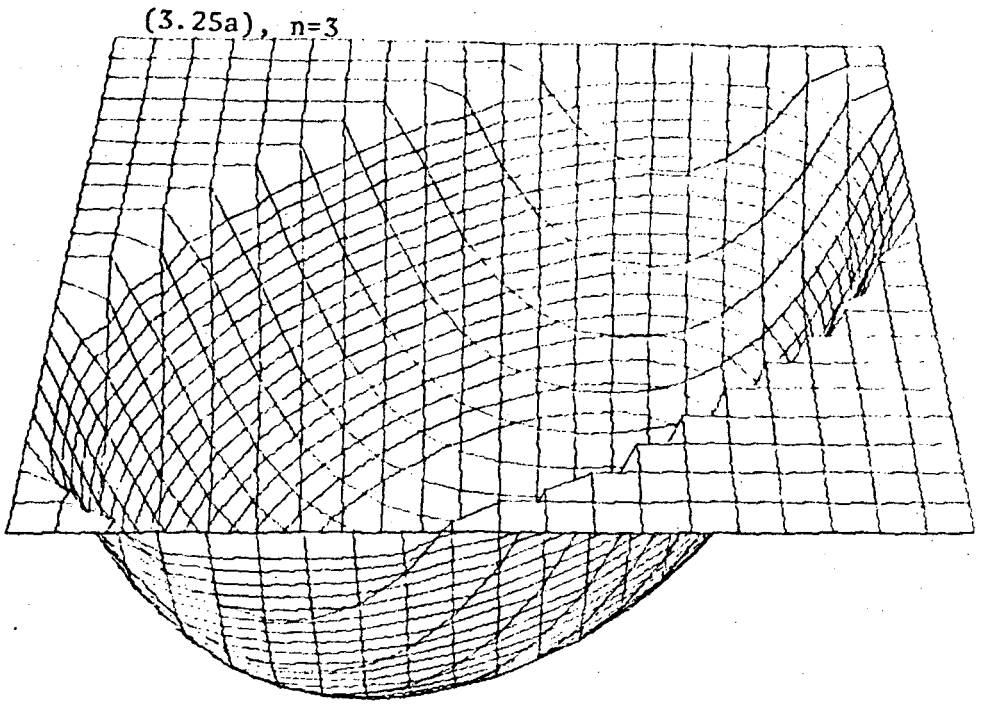

Fig. 10

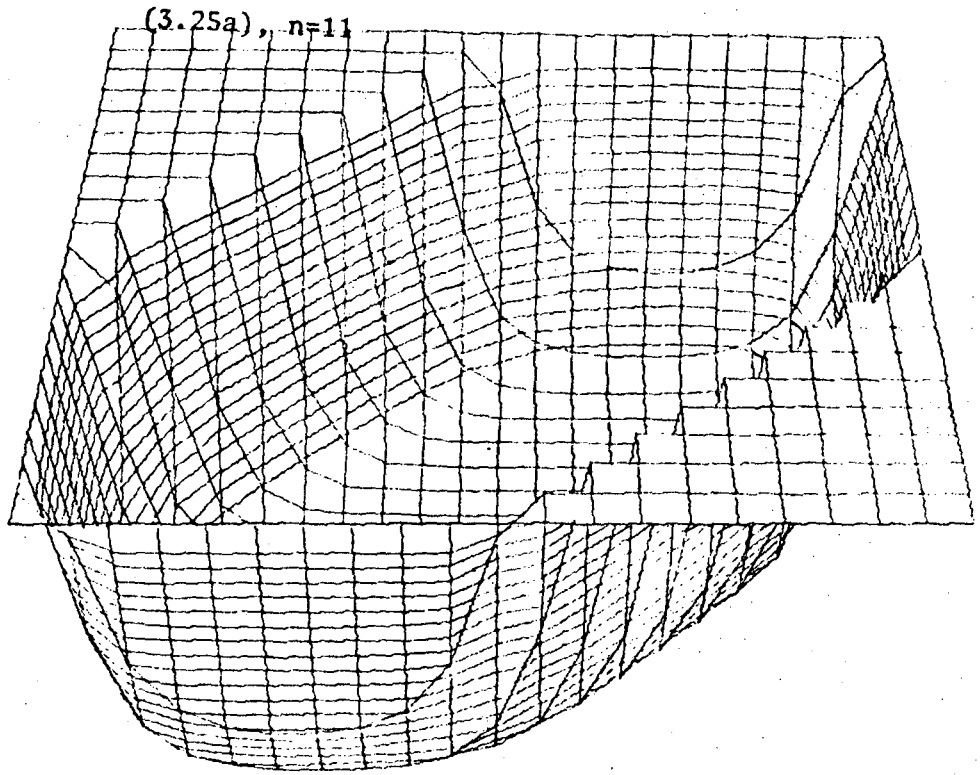

Fig. 12

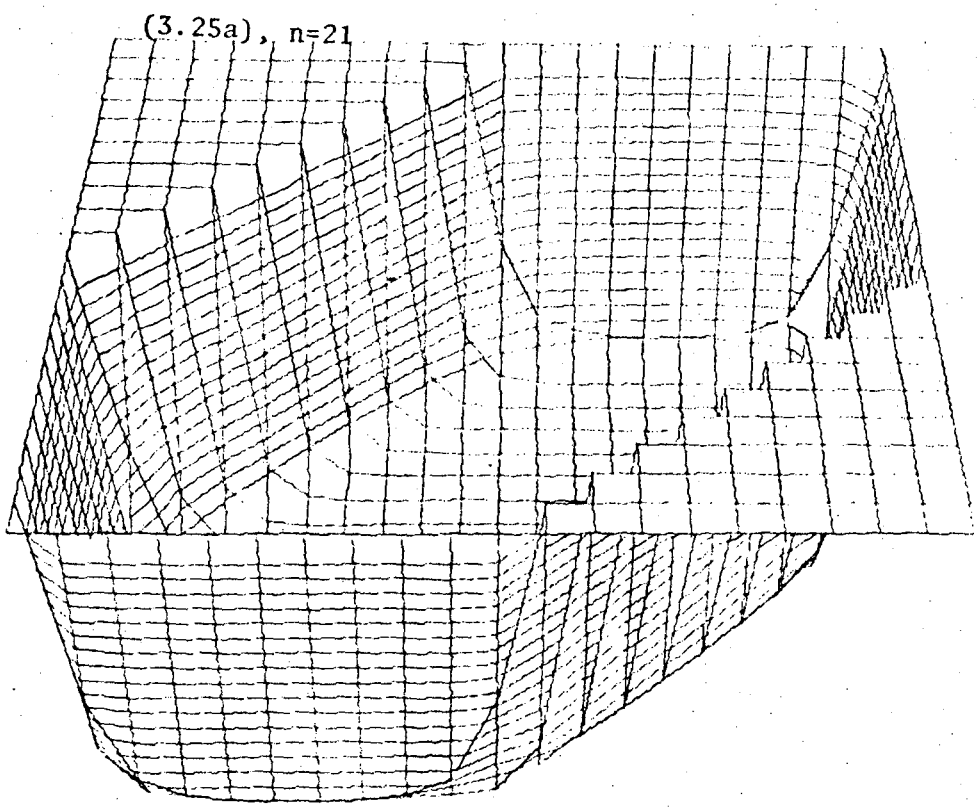

Fig. 13

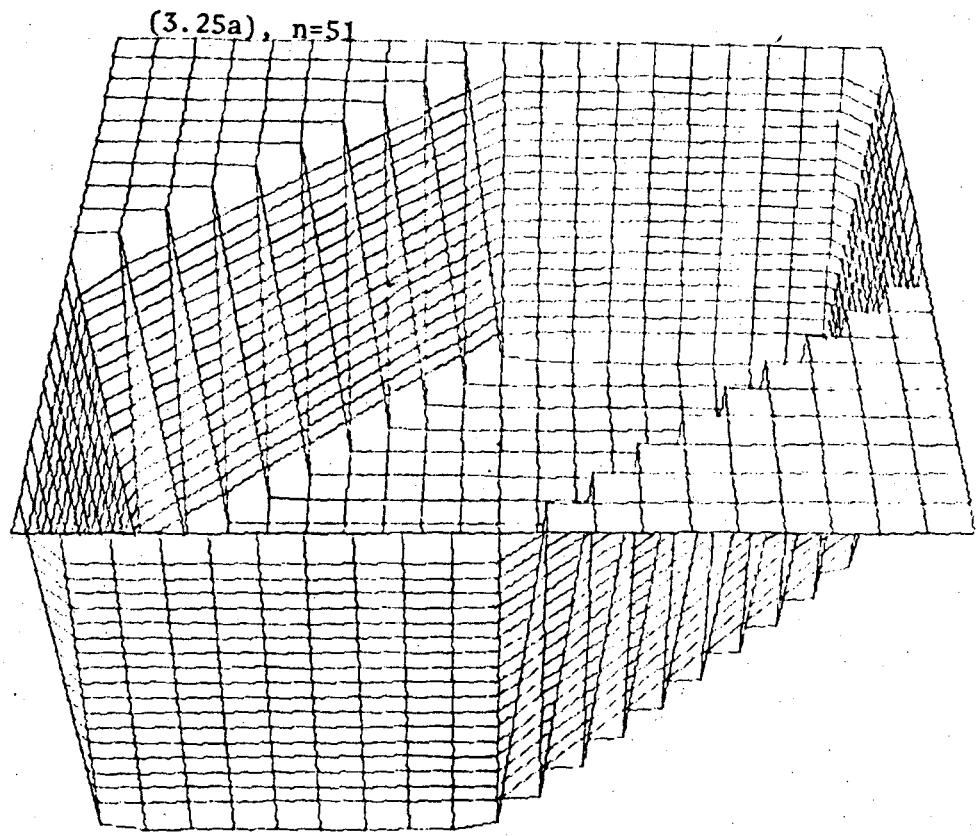

Fig. 14

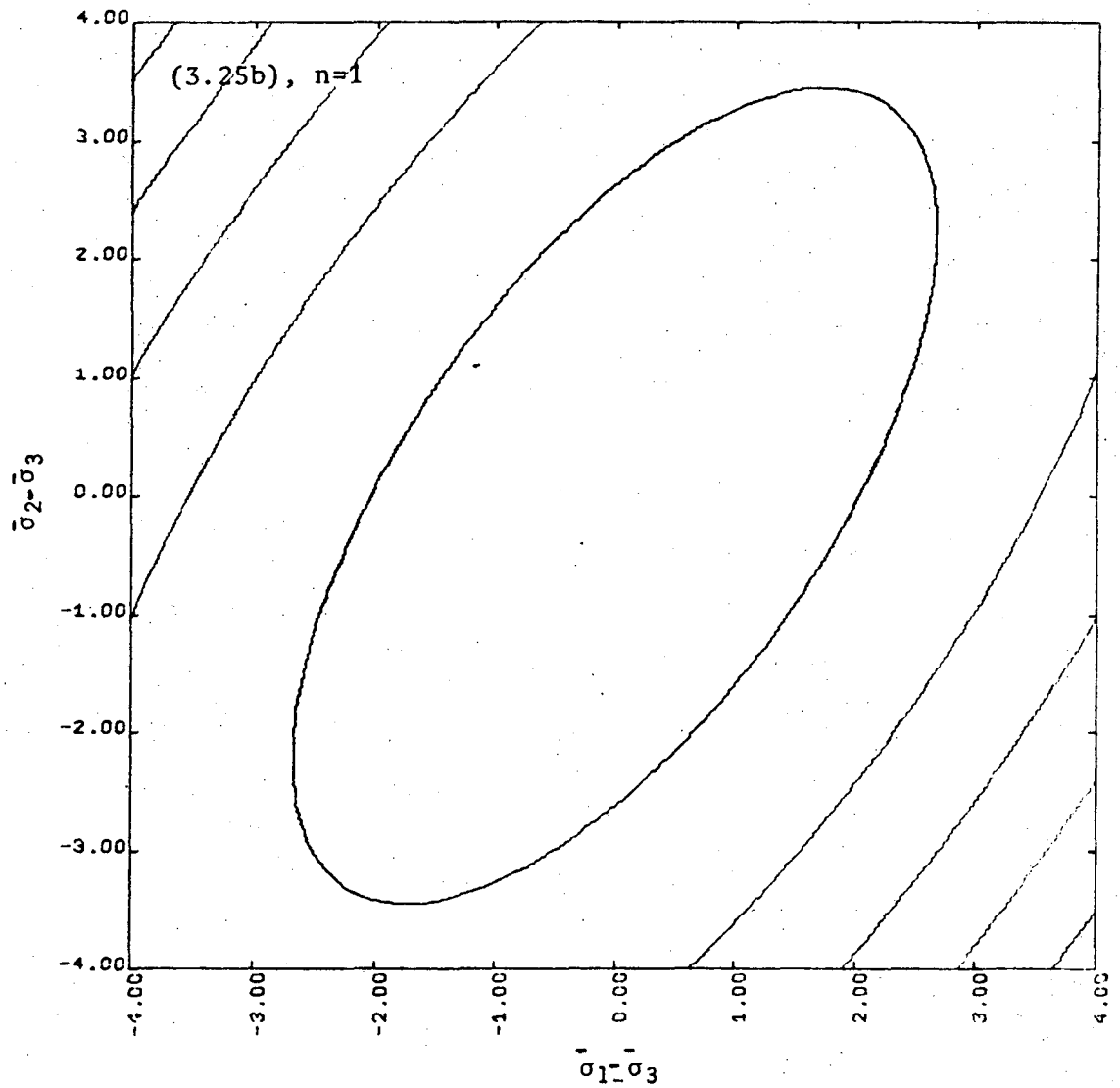
(3.25b), n=1
4.00
3.00
2.00
1.00
0.00
-1.00
-2.00
-3.00
-4.00
$\bar{\sigma}_2-\bar{\sigma}_3$
-4.00
-3.00
-2.00
-1.00
0.00
1.00
2.00
3.00
4.00
$\bar{\sigma}_1-\bar{\sigma}_3$

Fig. 15

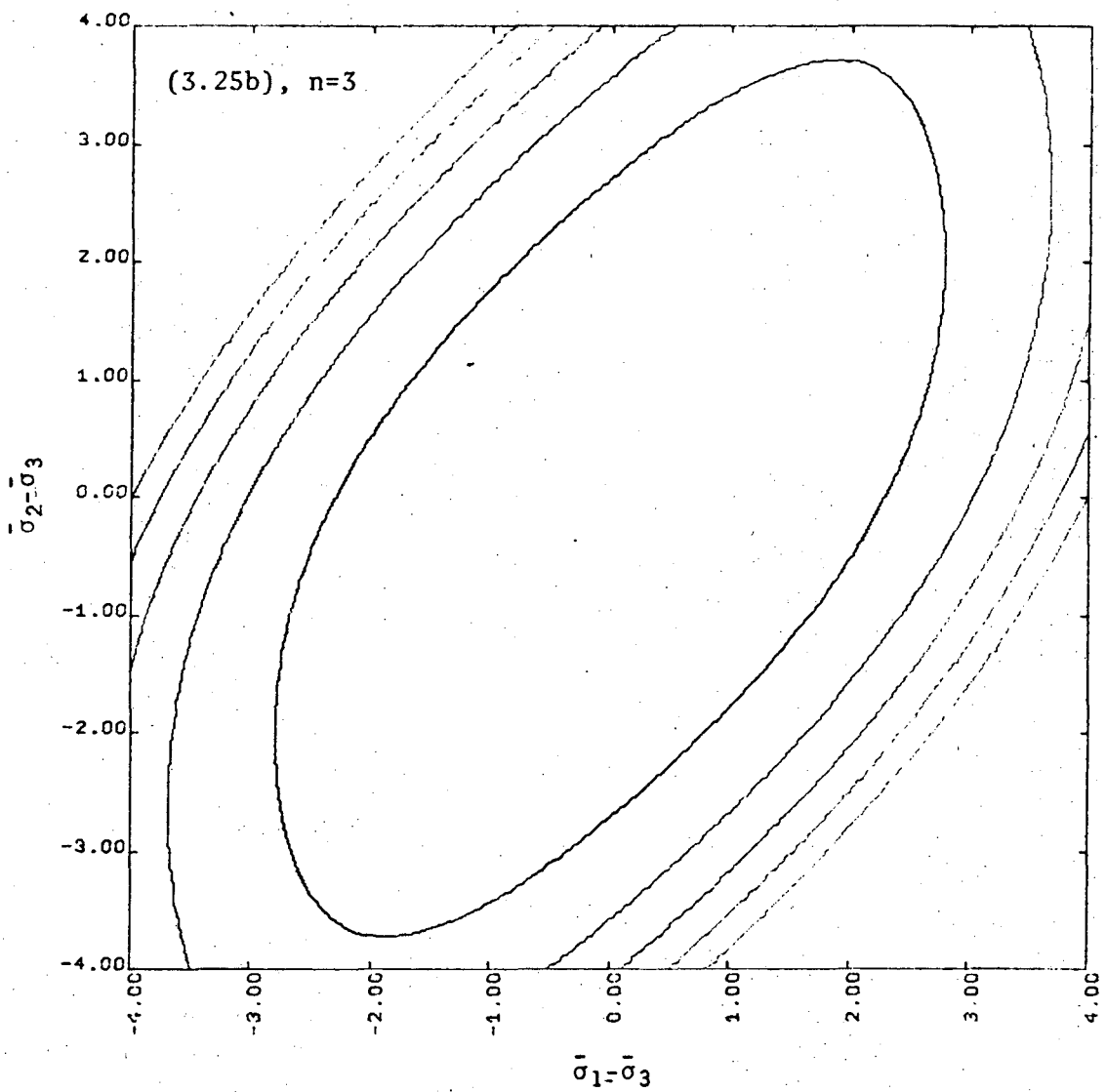
(3.25b), n=3
4.00
3.00
2.00
1.00
0.00
-1.00
-2.00
-3.00
-4.00
$\bar{\sigma}_2-\bar{\sigma}_3$
-4.00
-3.00
-2.00
-1.00
0.00
1.00
2.00
3.00
4.00
$\bar{\sigma}_1-\bar{\sigma}_3$

Fig. 16

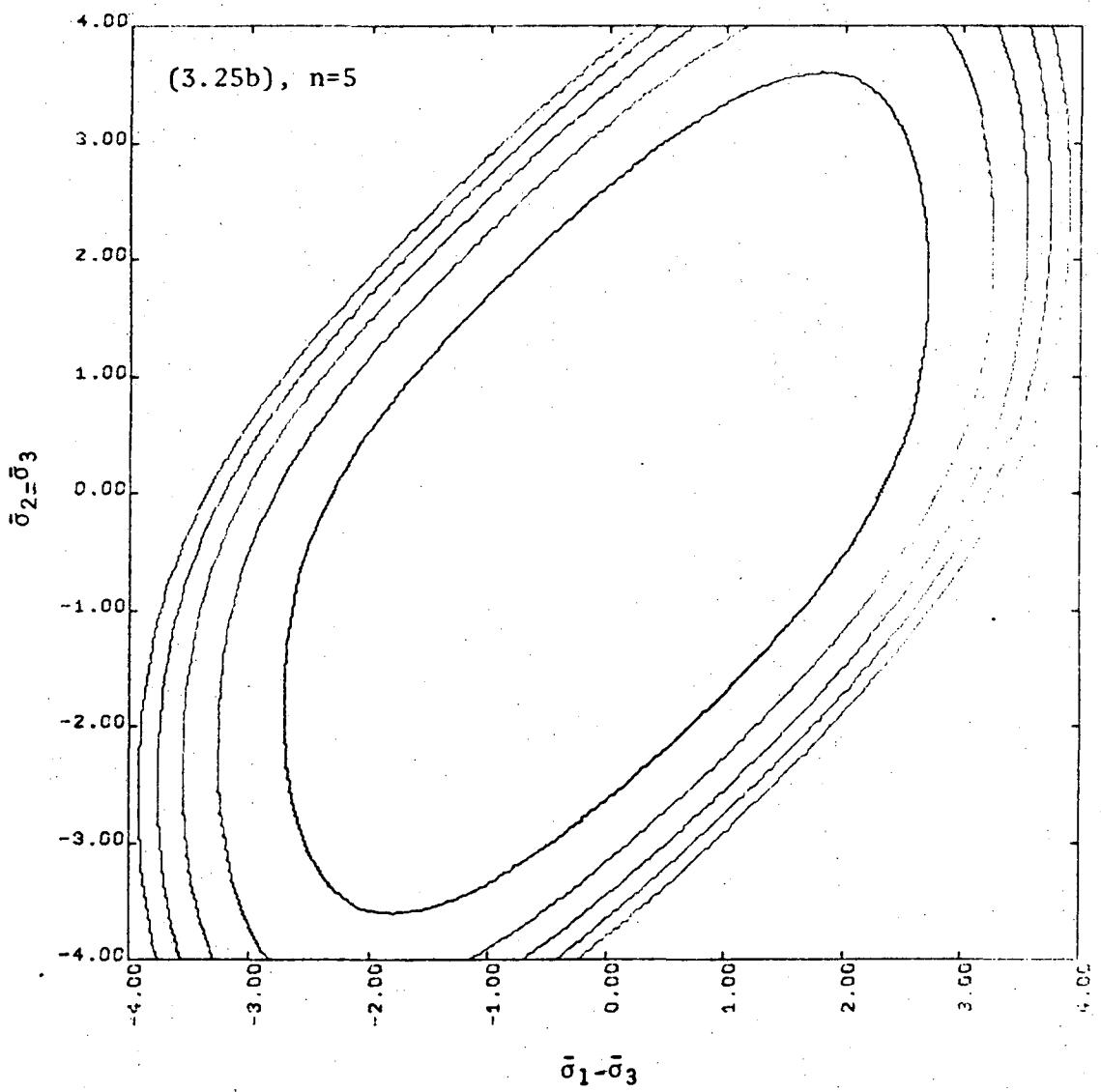
(3.25b), n=5
4.00
3.00
2.00
1.00
0.00
-1.00
-2.00
-3.00
-4.00
$\bar{\sigma}_2-\bar{\sigma}_3$
-4.00
-3.00
-2.00
-1.00
0.00
1.00
2.00
3.00
4.00
$\bar{\sigma}_1-\bar{\sigma}_3$

Fig. 17

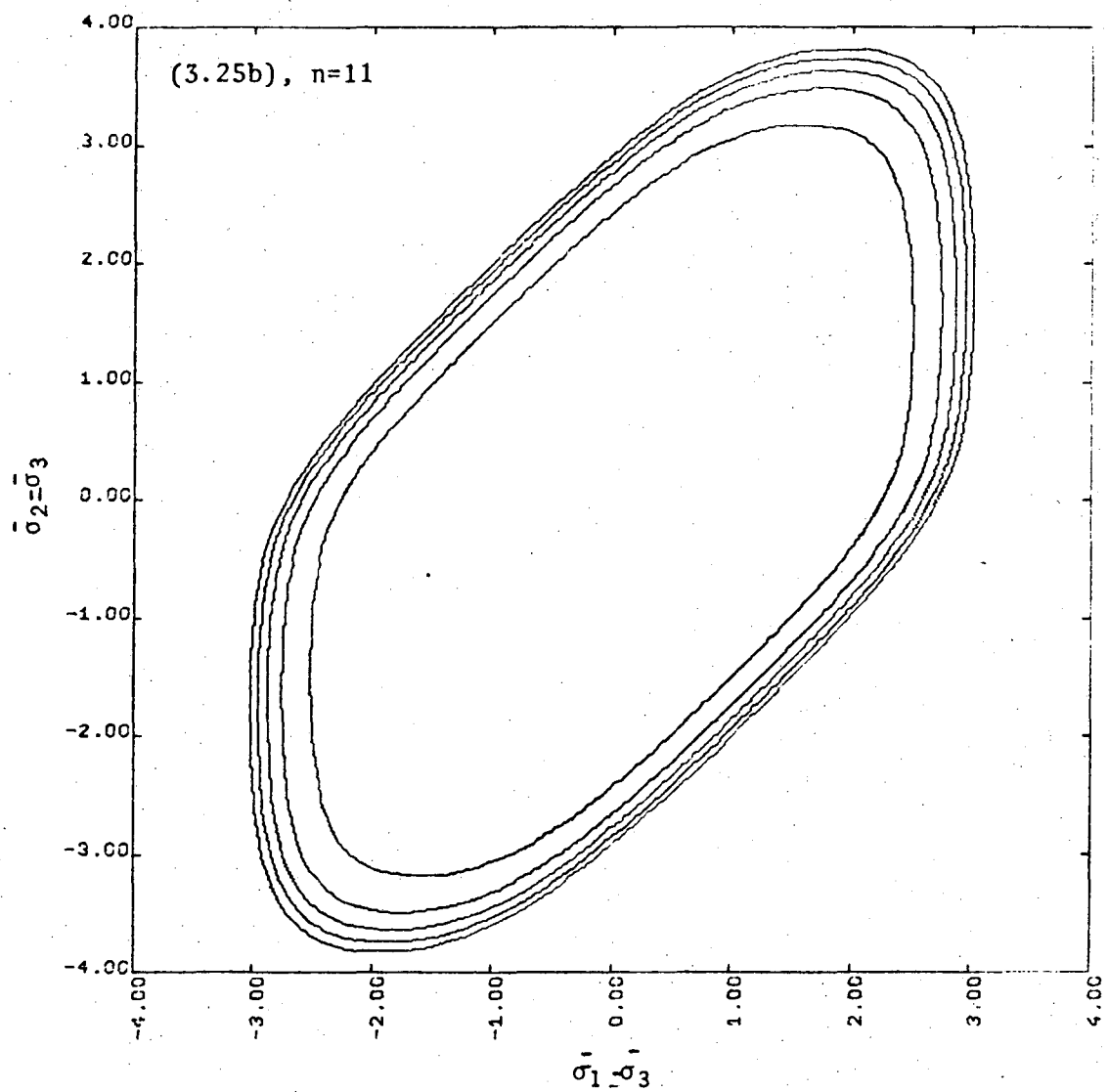
(3.25b), n=11
4.00
3.00
2.00
1.00
0.00
-1.00
-2.00
-3.00
-4.00
-4.00
-3.00
-2.00
-1.00
0.00
1.00
2.00
3.00
4.00
$\bar{\sigma}_2=\bar{\sigma}_3$
$\bar{\sigma}_1-\bar{\sigma}_3$

Fig. 18

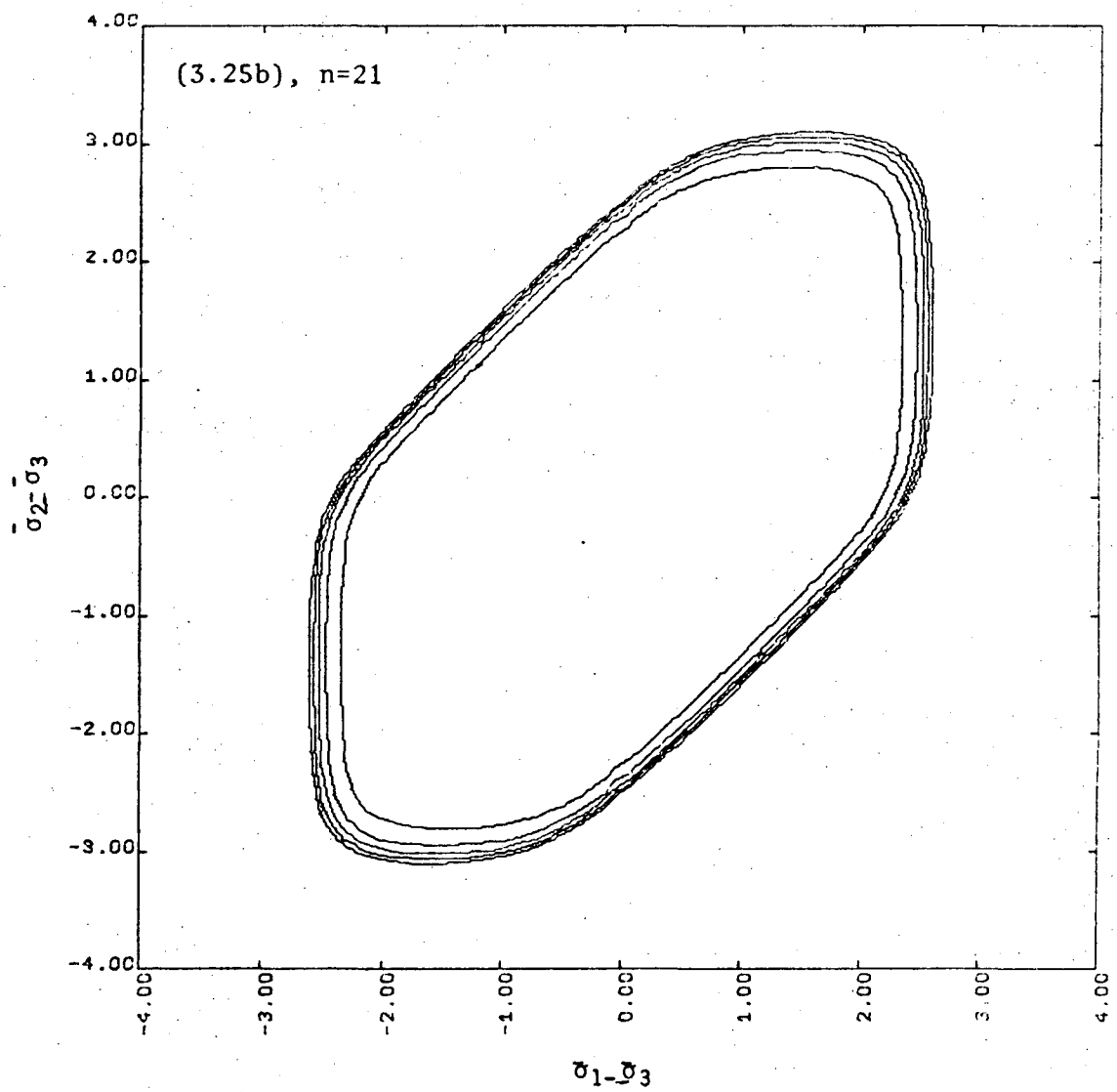
(3.25b), n=21
4.00
3.00
2.00
1.00
0.00
-1.00
-2.00
-3.00
-4.00
$\bar{\sigma}_2-\bar{\sigma}_3$
-4.00
-3.00
-2.00
-1.00
0.00
1.00
2.00
3.00
4.00
$\bar{\sigma}_1-\bar{\sigma}_3$

Fig. 19

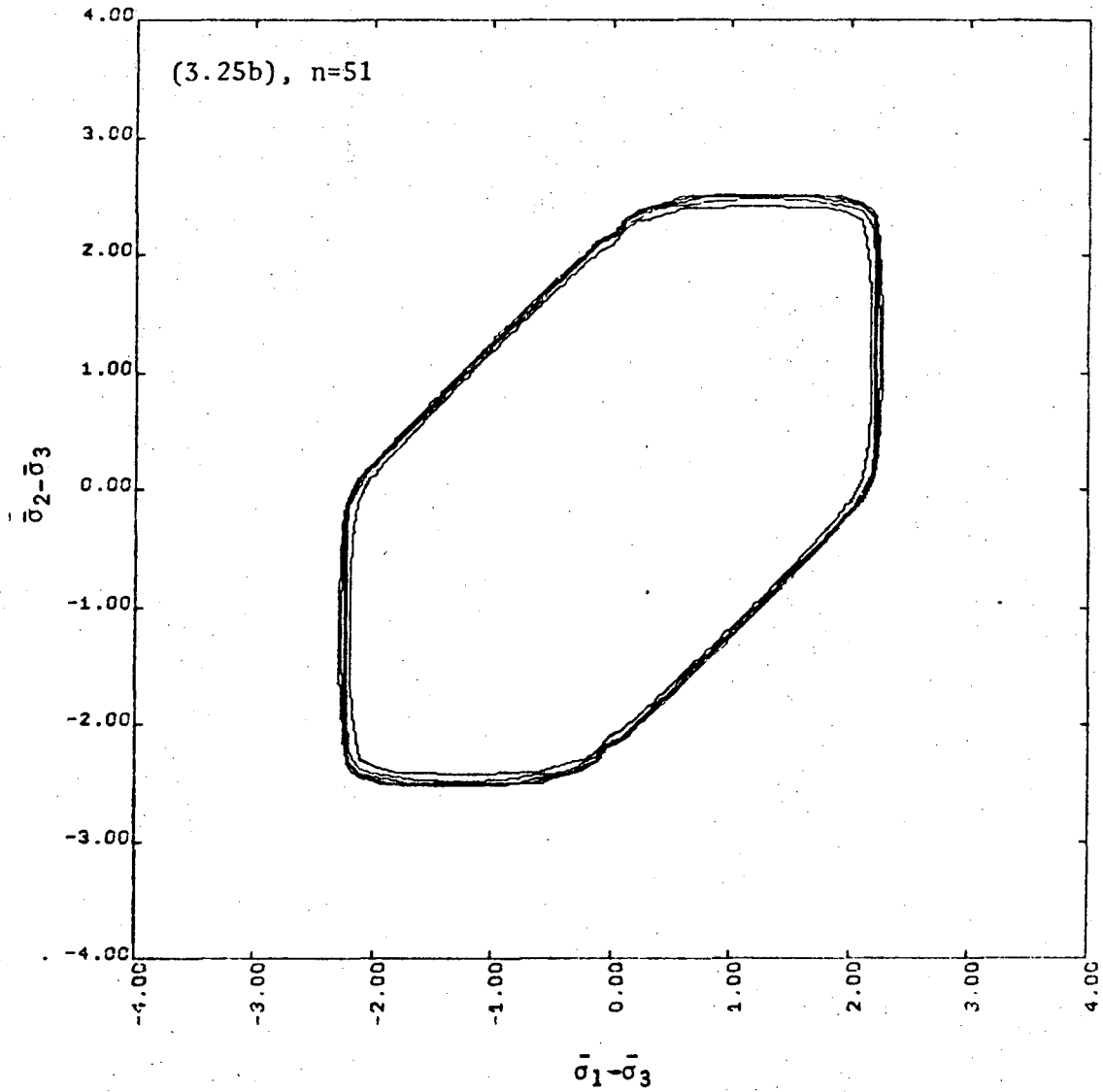
(3.25b), n=51
4.00
3.00
2.00
1.00
0.00
-1.00
-2.00
-3.00
-4.00
$\bar{\sigma}_2-\bar{\sigma}_3$
-4.00
-3.00
-2.00
-1.00
0.00
1.00
2.00
3.00
4.00
$\bar{\sigma}_1-\bar{\sigma}_3$

Fig. 20

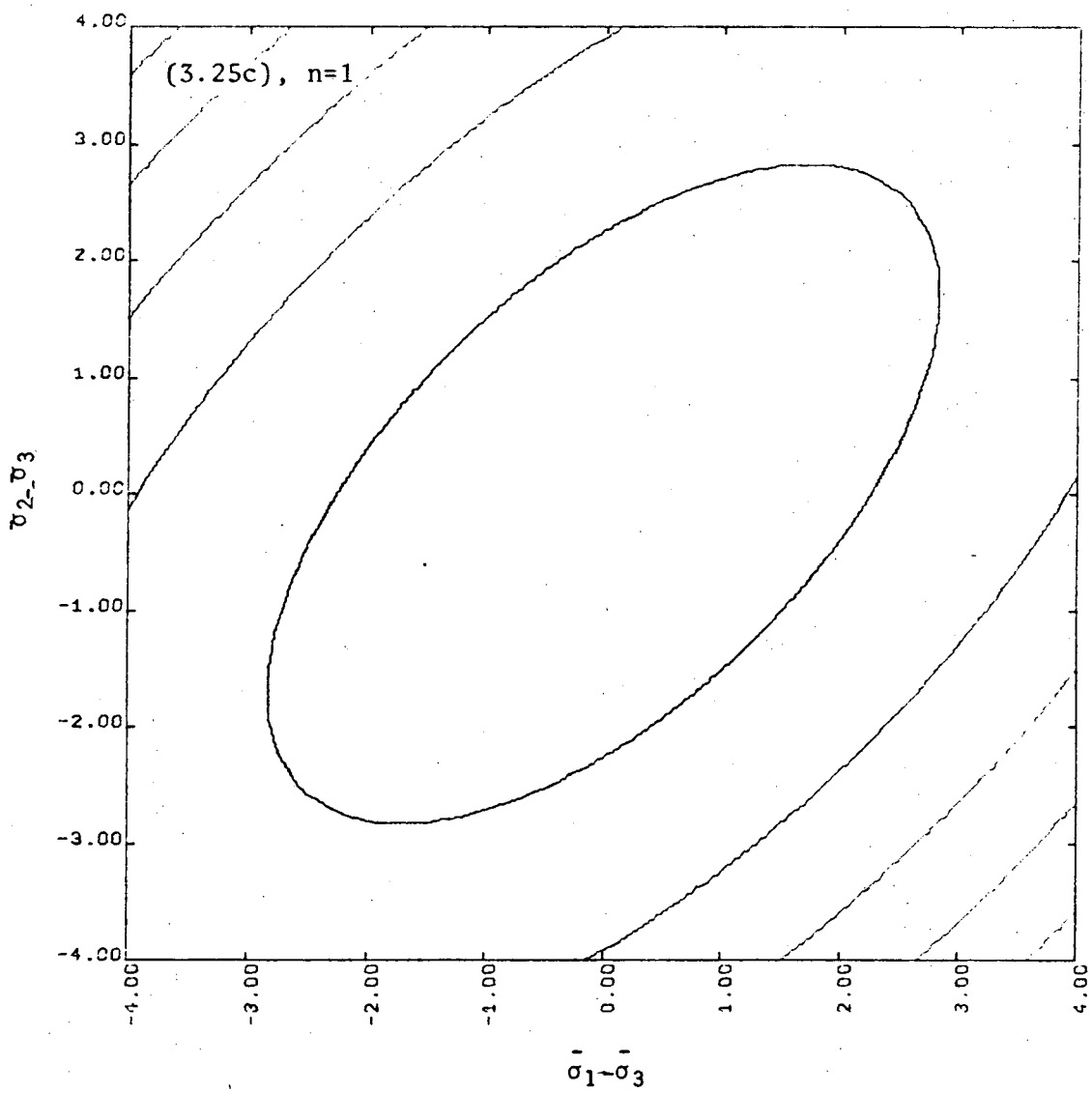
(3.25c), n=1
4.00
3.00
2.00
1.00
0.00
-1.00
-2.00
-3.00
-4.00
$\bar{\sigma}_2-\bar{\sigma}_3$
-4.00
-3.00
-2.00
-1.00
0.00
1.00
2.00
3.00
4.00
$\bar{\sigma}_1-\bar{\sigma}_3$

Fig. 21

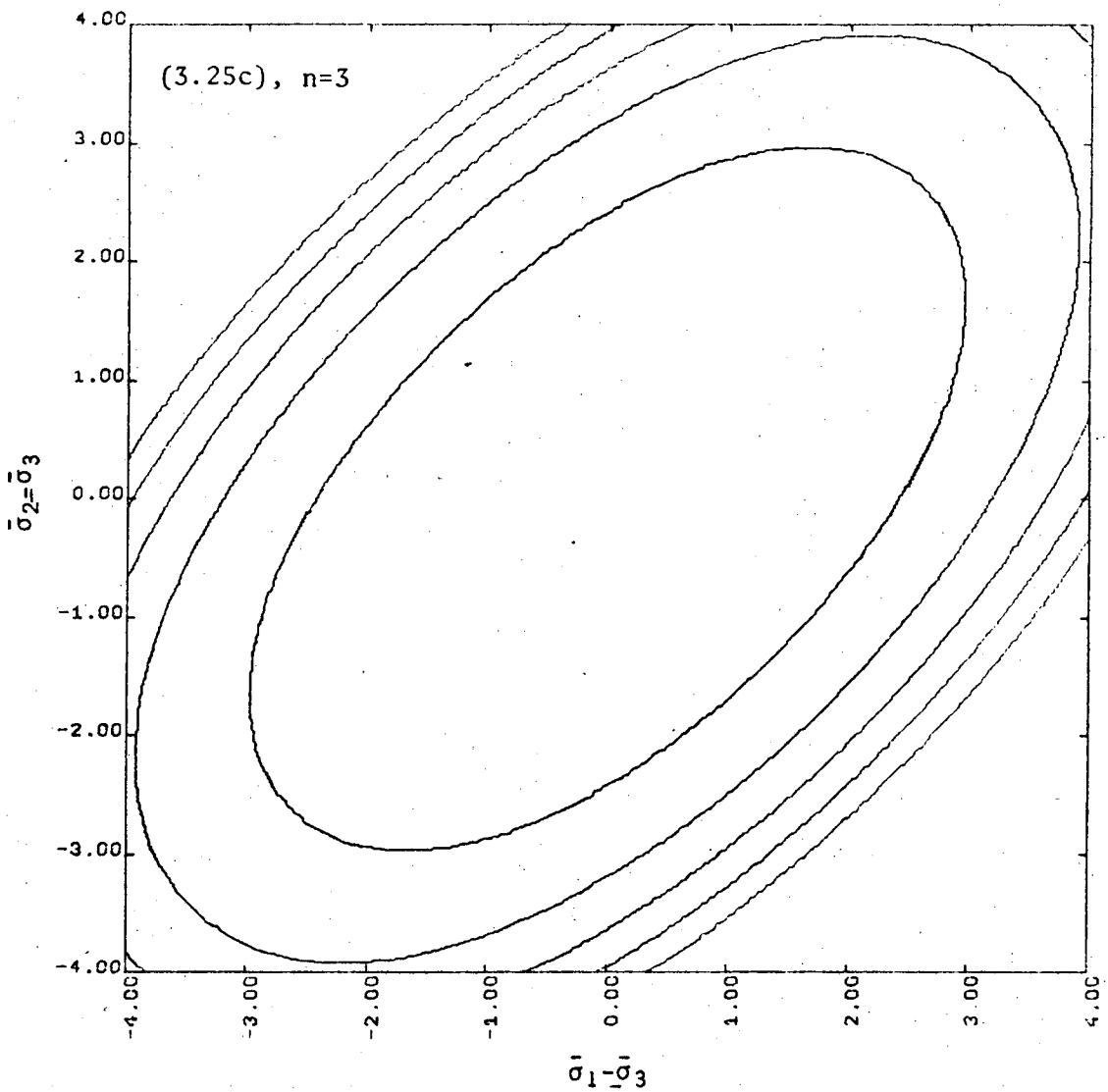
(3.25c), n=3
4.00
3.00
2.00
1.00
0.00
-1.00
-2.00
-3.00
-4.00
$\bar{\sigma}_2-\bar{\sigma}_3$
-4.00
-3.00
-2.00
-1.00
0.00
1.00
2.00
3.00
4.00
$\bar{\sigma}_1-\bar{\sigma}_3$

Fig. 22

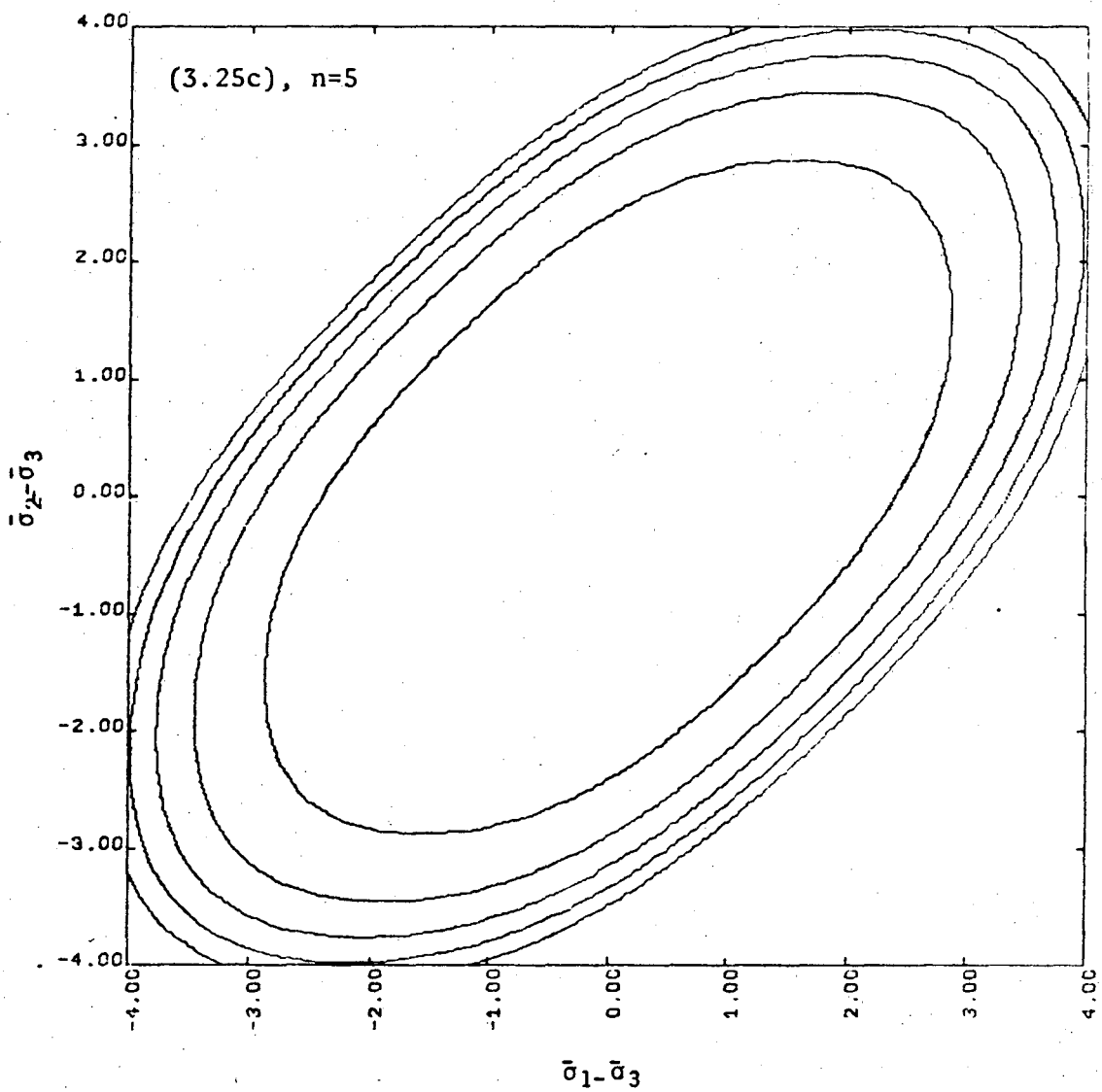
(3.25c), n=5
4.00
3.00
2.00
1.00
0.00
-1.00
-2.00
-3.00
-4.00
$\bar{\sigma}_2-\bar{\sigma}_3$
-4.00
-3.00
-2.00
-1.00
0.00
1.00
2.00
3.00
4.00
$\bar{\sigma}_1-\bar{\sigma}_3$

Fig. 23

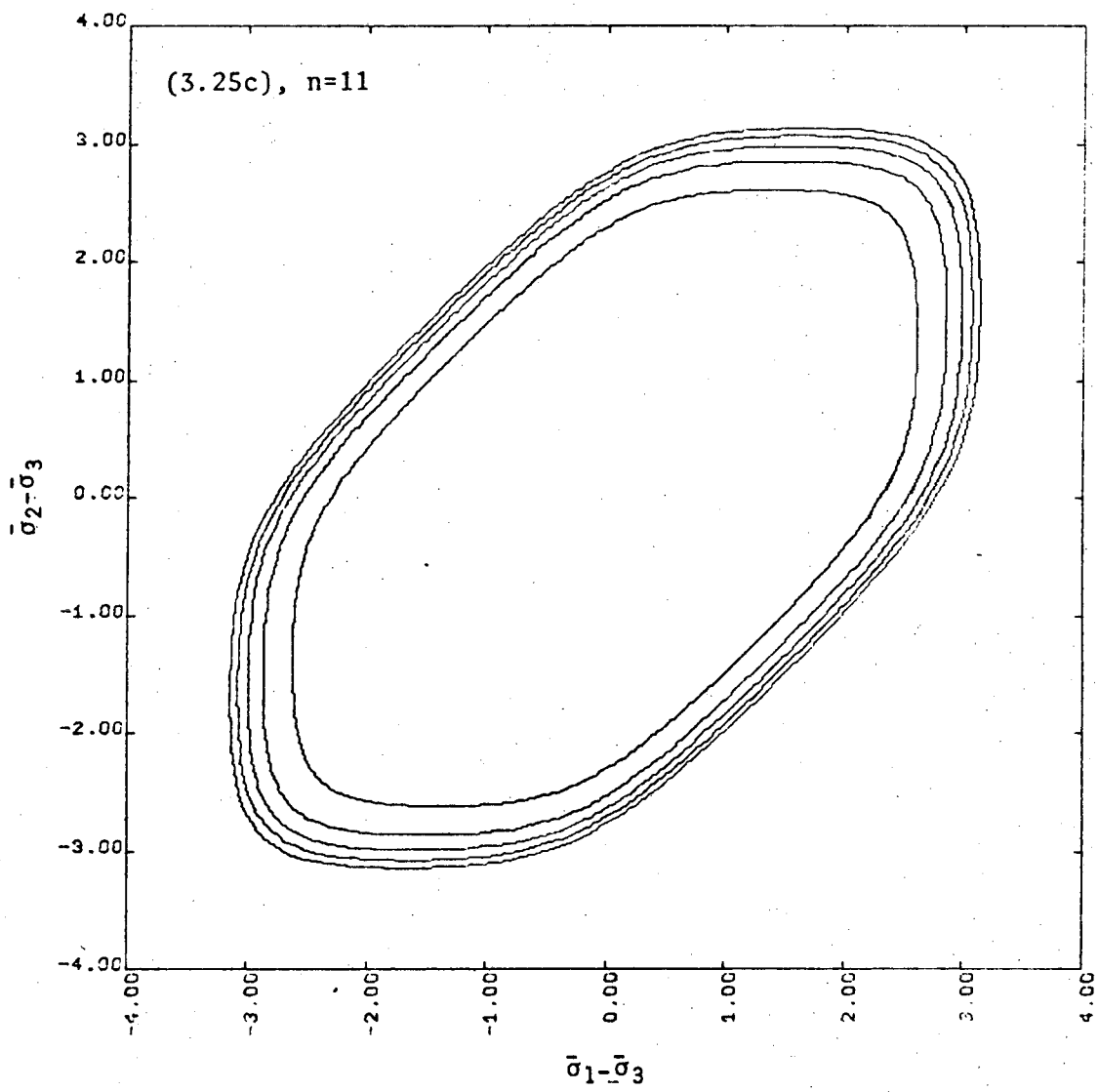
(3.25c), n=11
4.00
3.00
2.00
1.00
0.00
-1.00
-2.00
-3.00
-4.00
$\bar{\sigma}_2-\bar{\sigma}_3$
-4.00
-3.00
-2.00
-1.00
0.00
1.00
2.00
3.00
4.00
$\bar{\sigma}_1-\bar{\sigma}_3$

Fig. 24

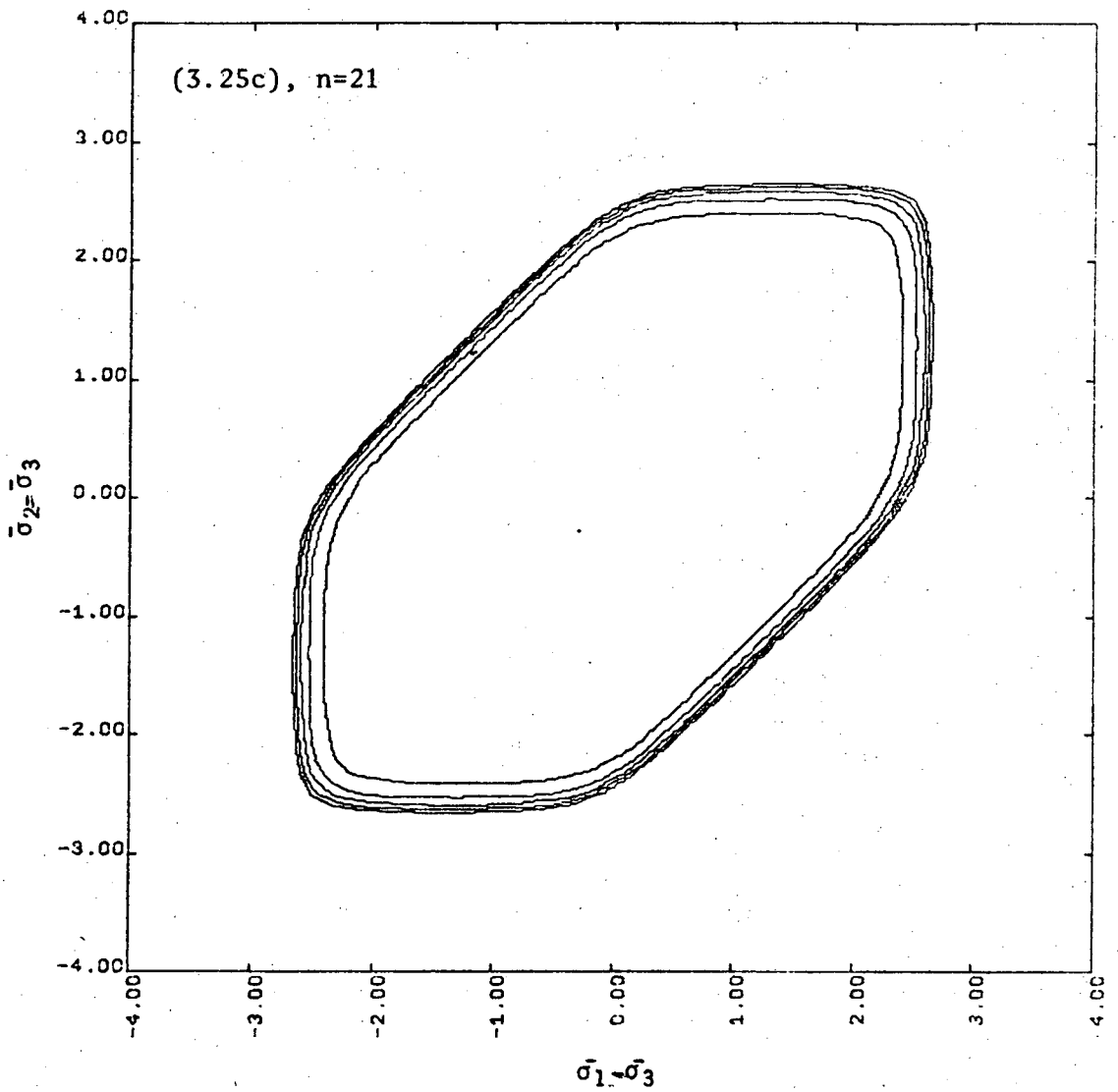
(3.25c), n=21
4.00
3.00
2.00
1.00
0.00
-1.00
-2.00
-3.00
-4.00
$\bar{\sigma}_2 = \bar{\sigma}_3$
-4.00
-3.00
-2.00
-1.00
0.00
1.00
2.00
3.00
4.00
$\bar{\sigma}_1 = \bar{\sigma}_3$

Fig. 25

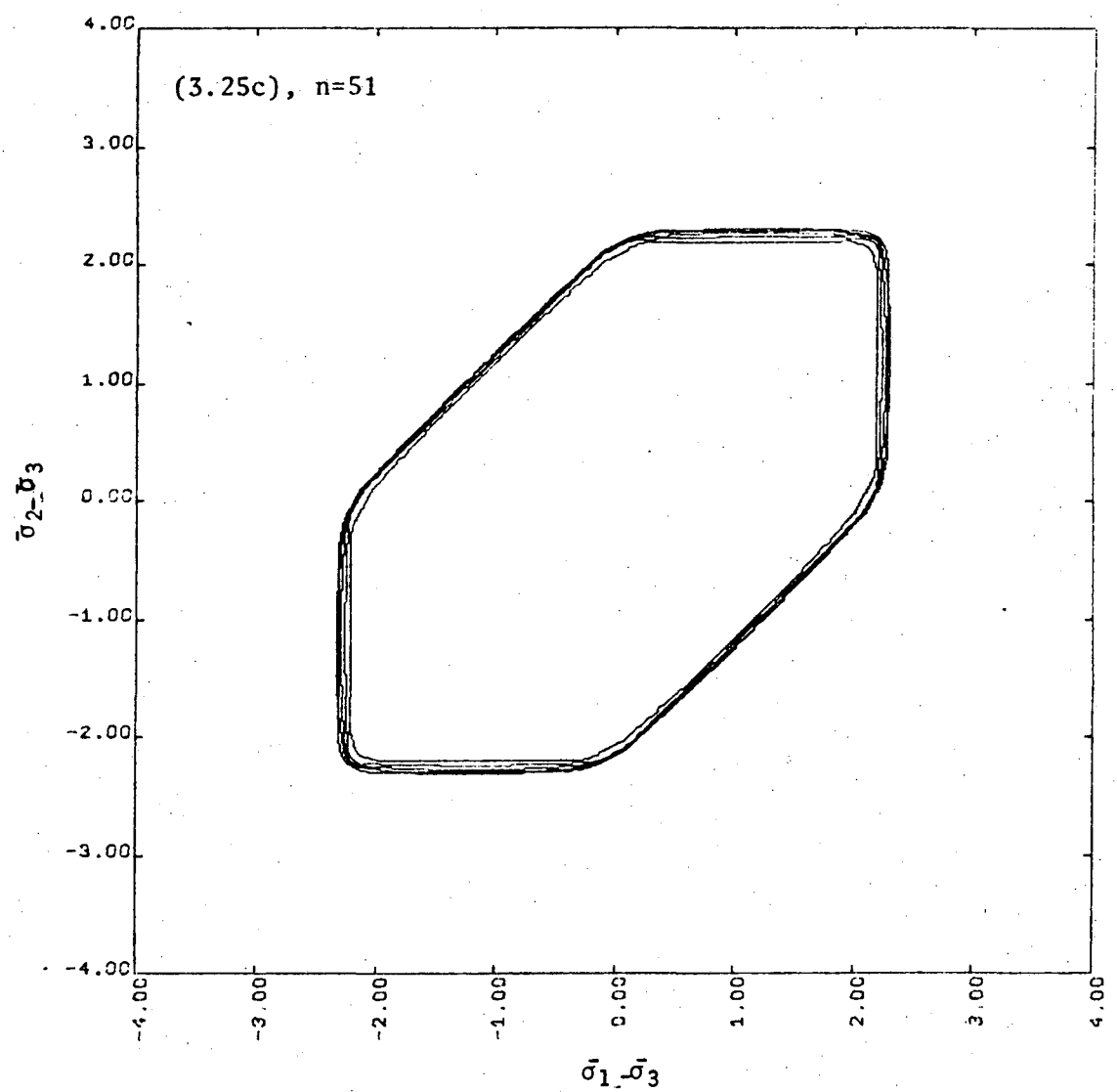
(3.25c), n=51
4.00
3.00
2.00
1.00
0.00
-1.00
-2.00
-3.00
-4.00
$\bar{\sigma}_2-\bar{\sigma}_3$
-4.00
-3.00
-2.00
-1.00
0.00
1.00
2.00
3.00
4.00
$\bar{\sigma}_1-\bar{\sigma}_3$

Fig. 26

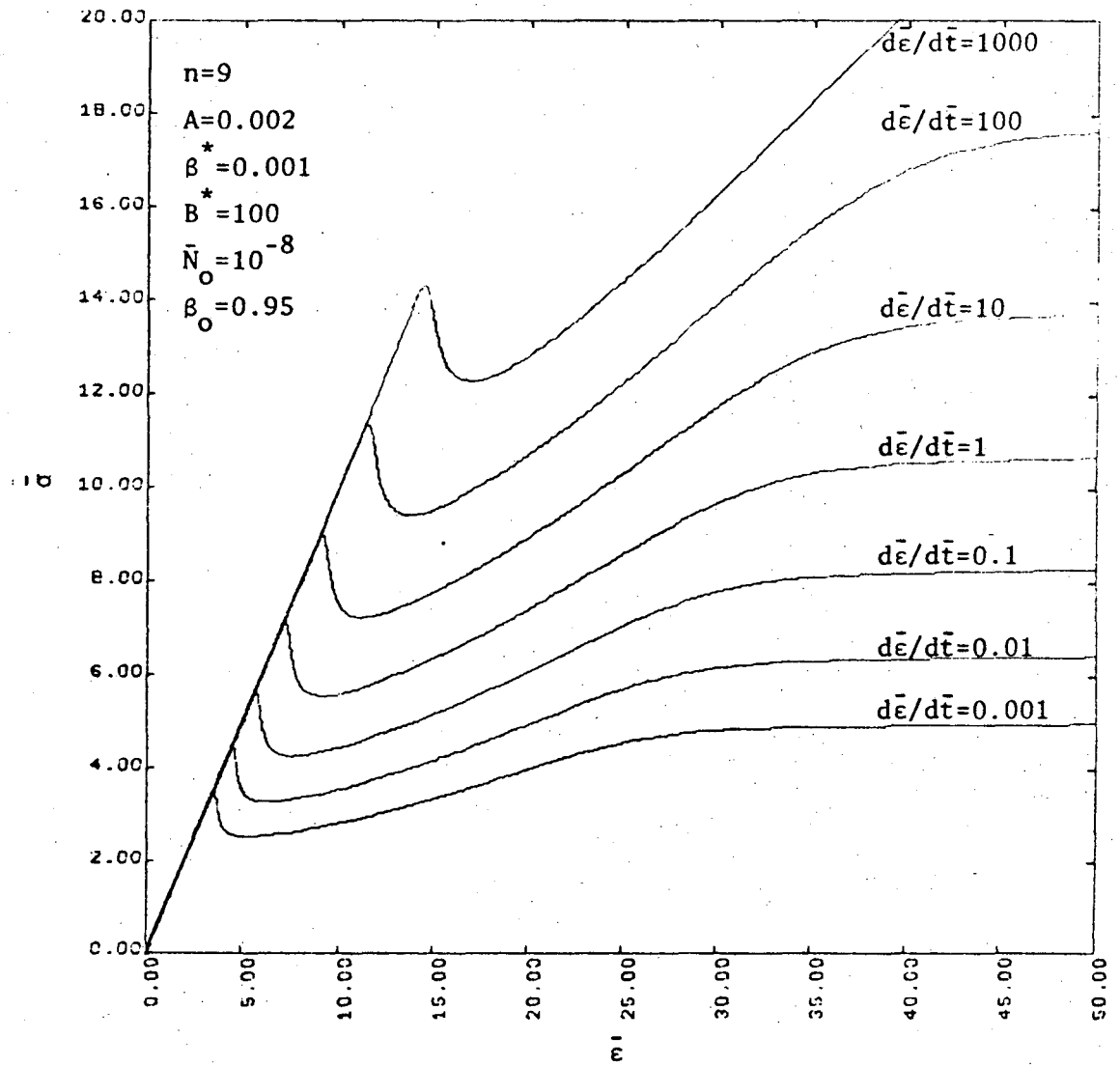
n=9
A=0.002
β*=0.001
B*=100
N̄o=10^-8
βo=0.95
dε̄/dt̄=1000
dε̄/dt̄=100
dε̄/dt̄=10
dε̄/dt̄=1
dε̄/dt̄=0.1
dε̄/dt̄=0.01
dε̄/dt̄=0.001
σ̄
ε̄
0.00
2.00
4.00
6.00
8.00
10.00
12.00
14.00
16.00
18.00
20.00
5.00
15.00
25.00
30.00
35.00
40.00
45.00
50.00

Fig. 27

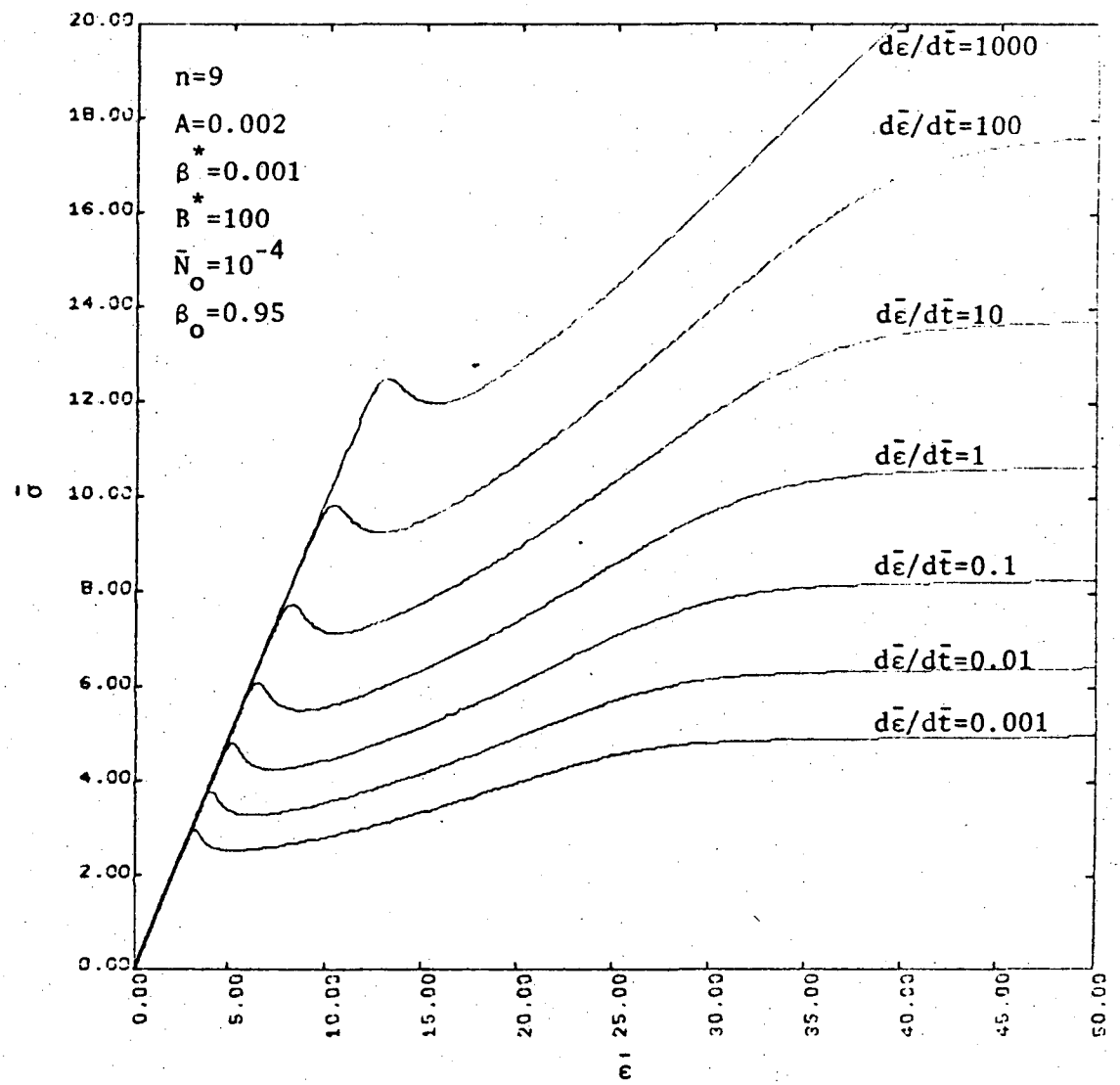
n=9
A=0.002
β*=0.001
B*=100
N̄o=10^-4
βo=0.95
dε̄/dt̄=1000
dε̄/dt̄=100
dε̄/dt̄=10
dε̄/dt̄=1
dε̄/dt̄=0.1
dε̄/dt̄=0.01
dε̄/dt̄=0.001
σ
ε
0.00
2.00
4.00
6.00
8.00
10.00
12.00
14.00
16.00
18.00
20.00
5.00
15.00
25.00
30.00
35.00
40.00
45.00
50.00

Fig. 28

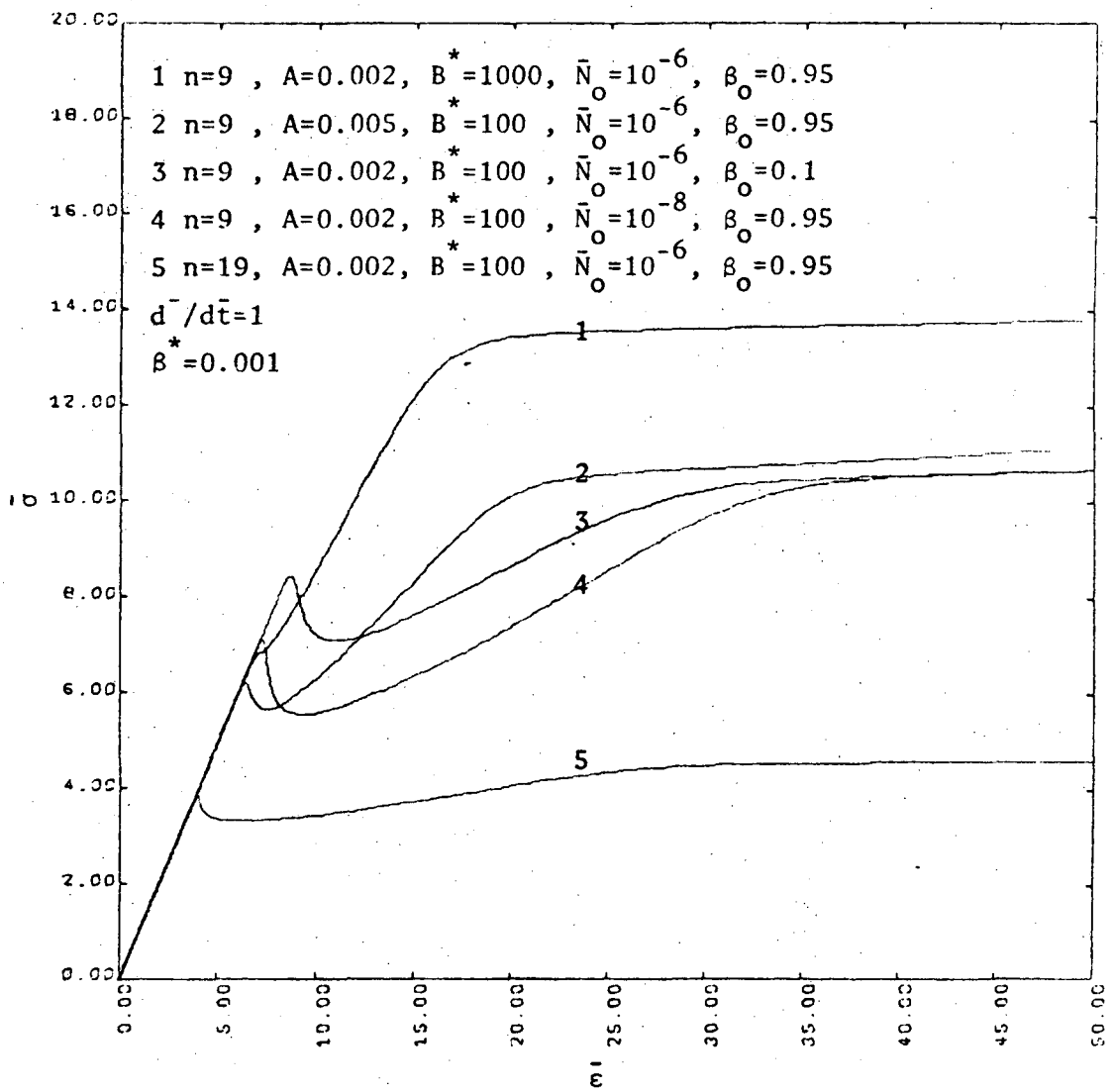
1 n=9 , A=0.002, B*=1000, N̄o=10^-6, βo=0.95
2 n=9 , A=0.005, B*=100 , N̄o=10^-6, βo=0.95
3 n=9 , A=0.002, B*=100 , N̄o=10^-6, βo=0.1
4 n=9 , A=0.002, B*=100 , N̄o=10^-8, βo=0.95
5 n=19, A=0.002, B*=100 , N̄o=10^-6, βo=0.95
d⁻/dt̄=1
β*=0.001
1
2
3
4
5
20.00
18.00
16.00
14.00
12.00
10.00
8.00
6.00
4.00
2.00
0.00
0.00
5.00
10.00
15.00
20.00
25.00
30.00
35.00
40.00
45.00
50.00

Fig. 29

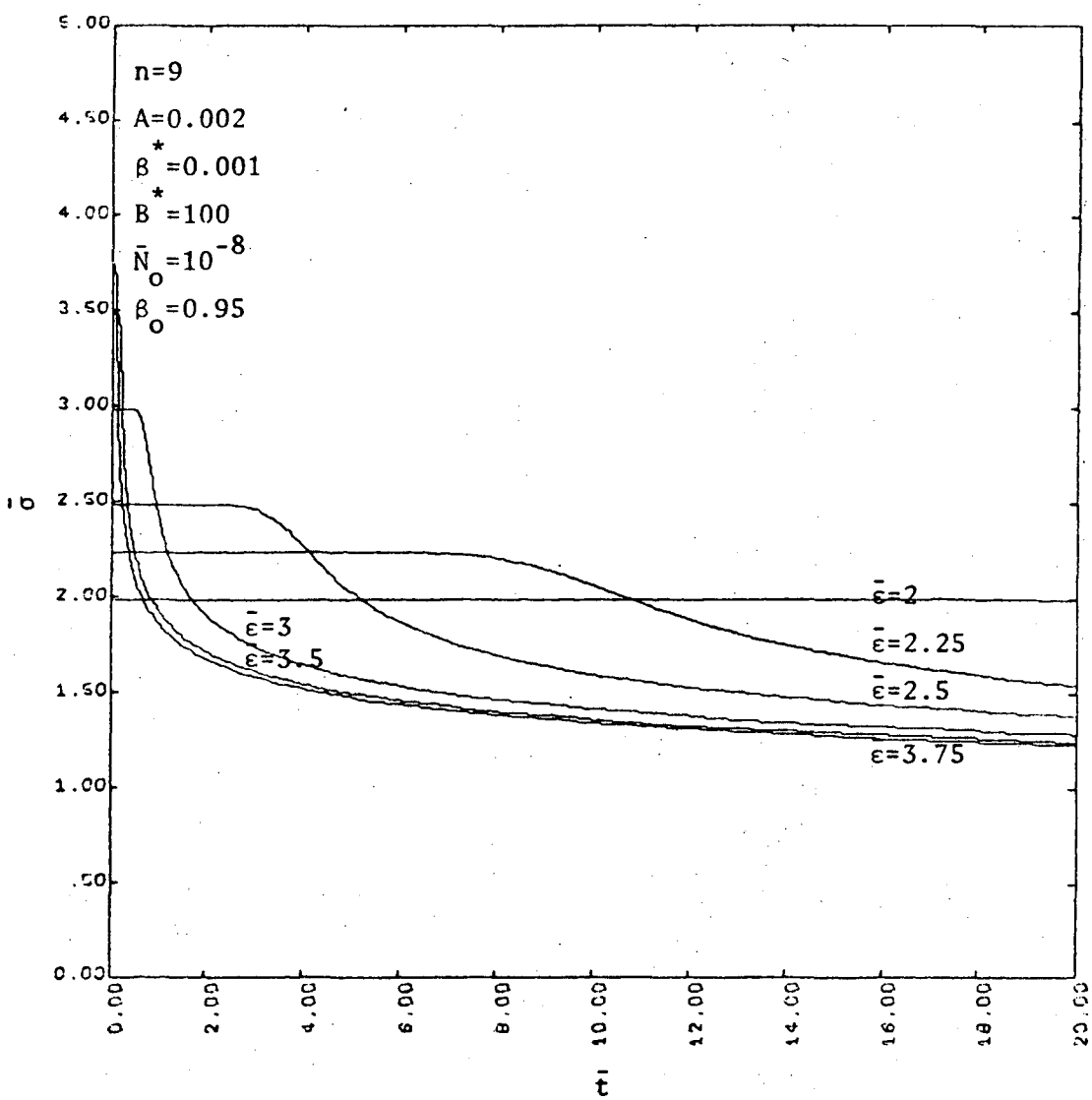
n=9
A=0.002
β*=0.001
B*=100
N̄o=10^-8
βo=0.95
ε̄=2
ε̄=2.25
ε̄=2.5
ε̄=3.75
ε̄=3
ε̄=3.5
σ̄
t̄
5.00
4.50
4.00
3.50
3.00
2.50
2.00
1.50
1.00
.50
0.00
0.00
2.00
4.00
6.00
8.00
10.00
12.00
14.00
16.00
18.00
20.00

Fig. 30

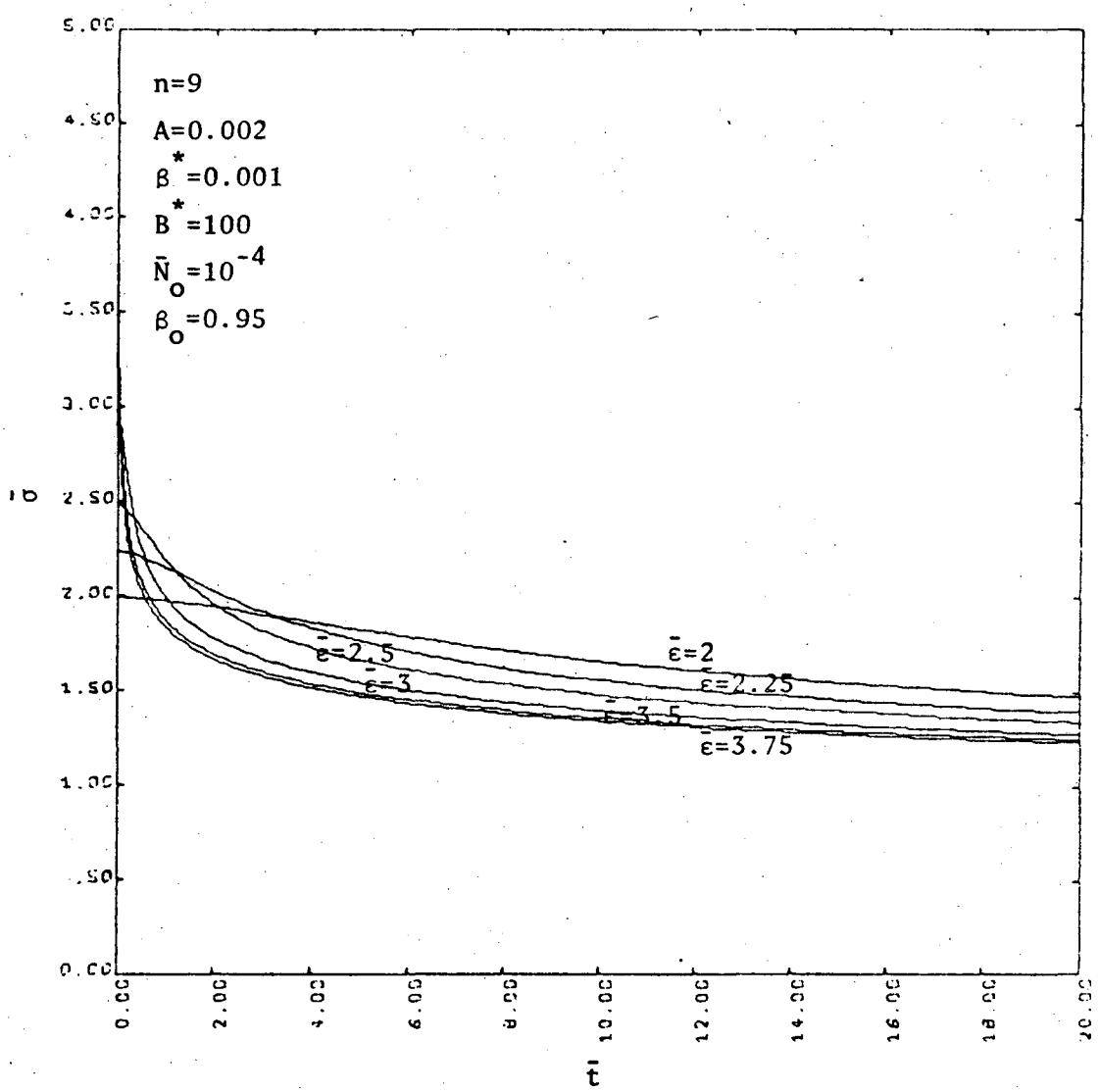
n=9
A=0.002
β*=0.001
B*=100
N̄o=10^-4
βo=0.95
ε̄=2
ε̄=2.25
ε̄=2.5
ε̄=3
ε̄=3.5
ε̄=3.75
t̄
0.00
2.00
4.00
6.00
8.00
10.00
12.00
14.00
16.00
18.00
20.00
0.00
.50
1.00
1.50
2.00
2.50
3.00
3.50
4.00
4.50
5.00

Fig. 31

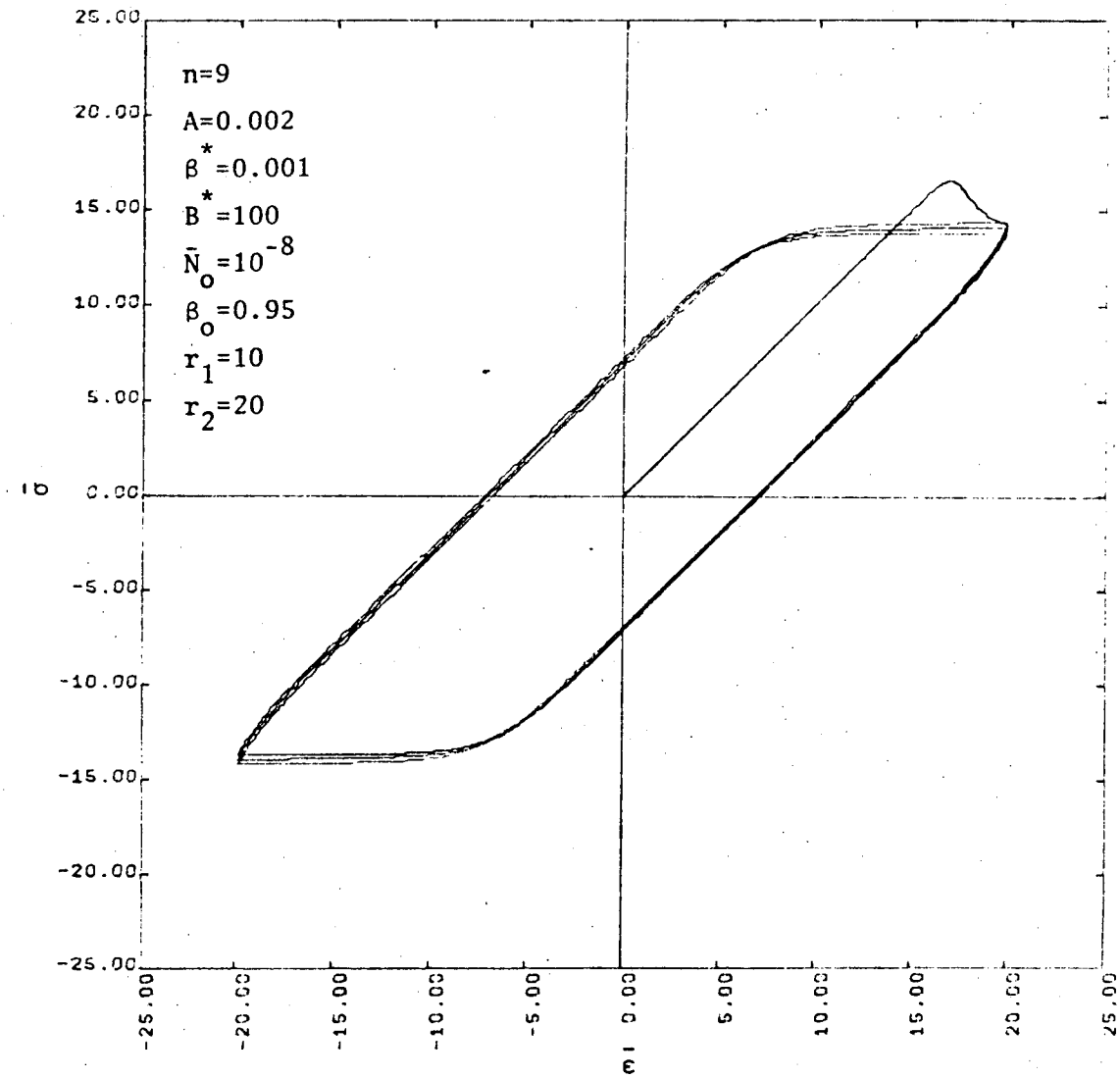
n=9
A=0.002
β*=0.001
B*=100
Ño=10^-8
βo=0.95
r1=10
r2=20
25.00
20.00
15.00
10.00
5.00
0.00
-5.00
-10.00
-15.00
-20.00
-25.00
σ
-25.00
-20.00
-15.00
-10.00
-5.00
0.00
5.00
10.00
15.00
20.00
25.00
ε

Fig. 32

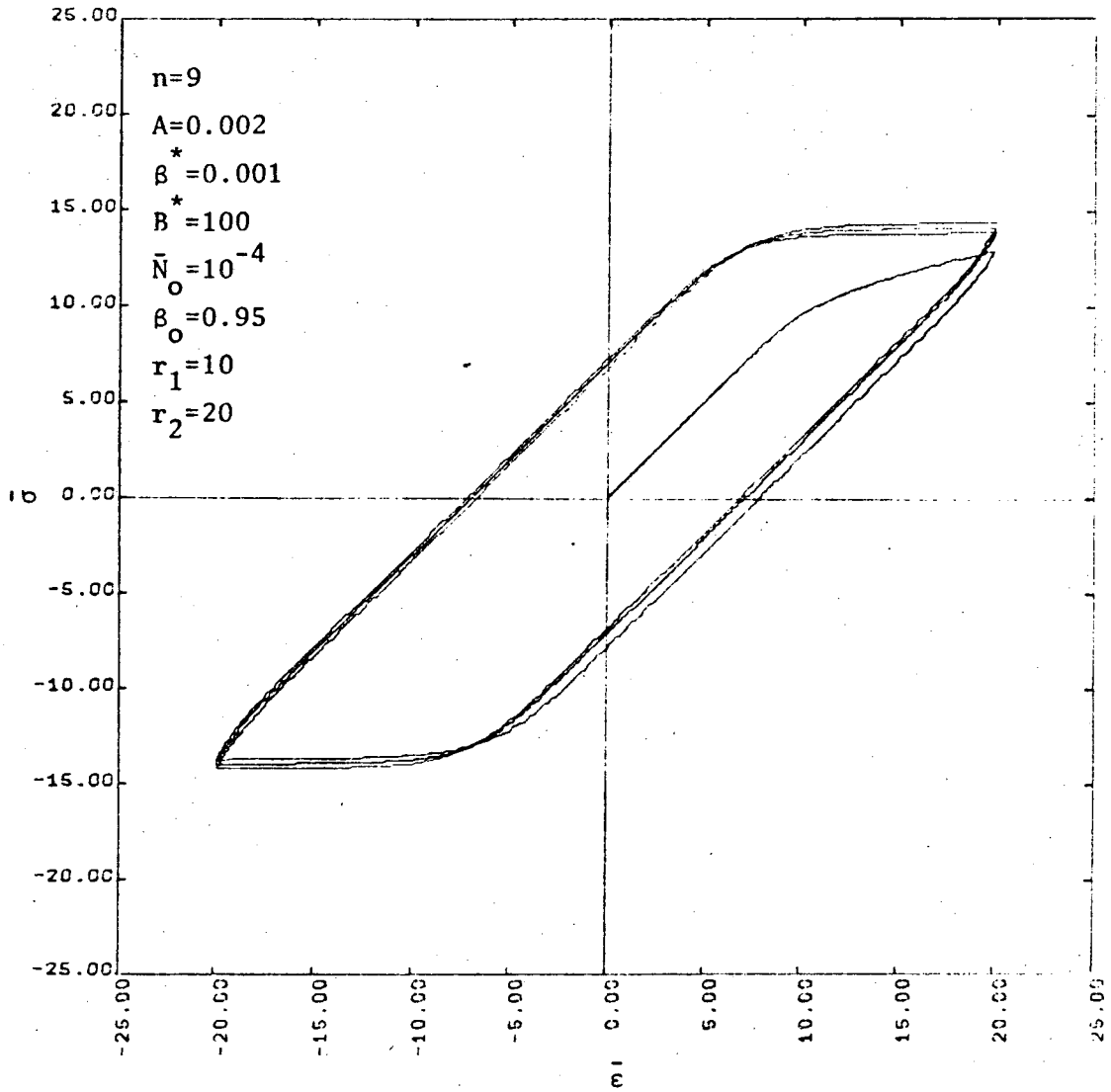
n=9
A=0.002
β*=0.001
B*=100
N̄o=10^-4
βo=0.95
r1=10
r2=20
25.00
20.00
15.00
10.00
5.00
0.00
-5.00
-10.00
-15.00
-20.00
-25.00
-25.00
-20.00
-15.00
-10.00
-5.00
0.00
5.00
10.00
15.00
20.00
25.00

Fig. 33

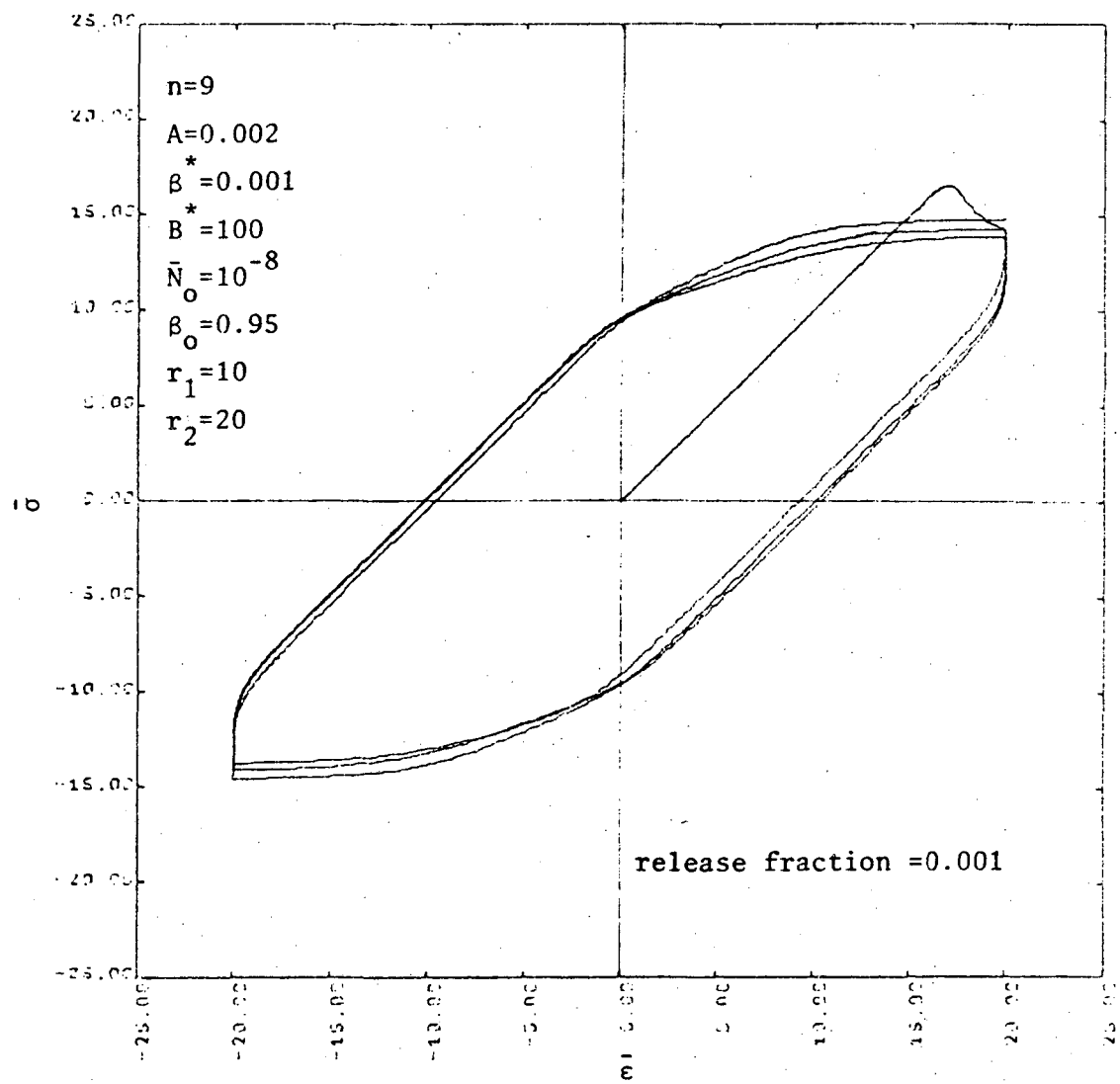
n=9
A=0.002
β*=0.001
B*=100
N̄o=10^-8
βo=0.95
r1=10
r2=20
release fraction =0.001
σ
ε

Fig. 34

LEGAL NOTICE

This report was prepared as an account of work sponsored by the United States Government. Neither the United States nor the United States Atomic Energy Commission, nor any of their employees, nor any of their contractors, subcontractors, or their employees, makes any warranty, express or implied, or assumes any legal liability or responsibility for the accuracy, completeness or usefulness of any information, apparatus, product or process disclosed, or represents that its use would not infringe privately owned rights.

TECHNICAL INFORMATION DIVISION
LAWRENCE BERKELEY LABORATORY
UNIVERSITY OF CALIFORNIA
BERKELEY, CALIFORNIA 94720